Petrology of Sedimentary Rocks

G421P13, summer semester, 2/1 hours, 3-4th year

2. Carbonates - II. diagenesis, dolomitization

Karel Martínek

Institute of Geology and Palaeontology

overview

diagenesis of grains – mikrobial micritization, borings, recrystalization; argonite (A), high-Mg calcite (HMC) → low-Mg calcite (LMC)

cementation – pore fluids supersaturated CaCO3, mineralogy of cements depends on PCO2, Mg/Ca ratio

neomorphism – recrystalization – change of mineralogy and/or structure

dissolution – carstification, pressure dissolution, stylolites

compaction

dolomitization, dedolomitization

diagenetic environments – meteoric vadose, meteoric phreatic, marine phreatic, burial

diagenetic environments
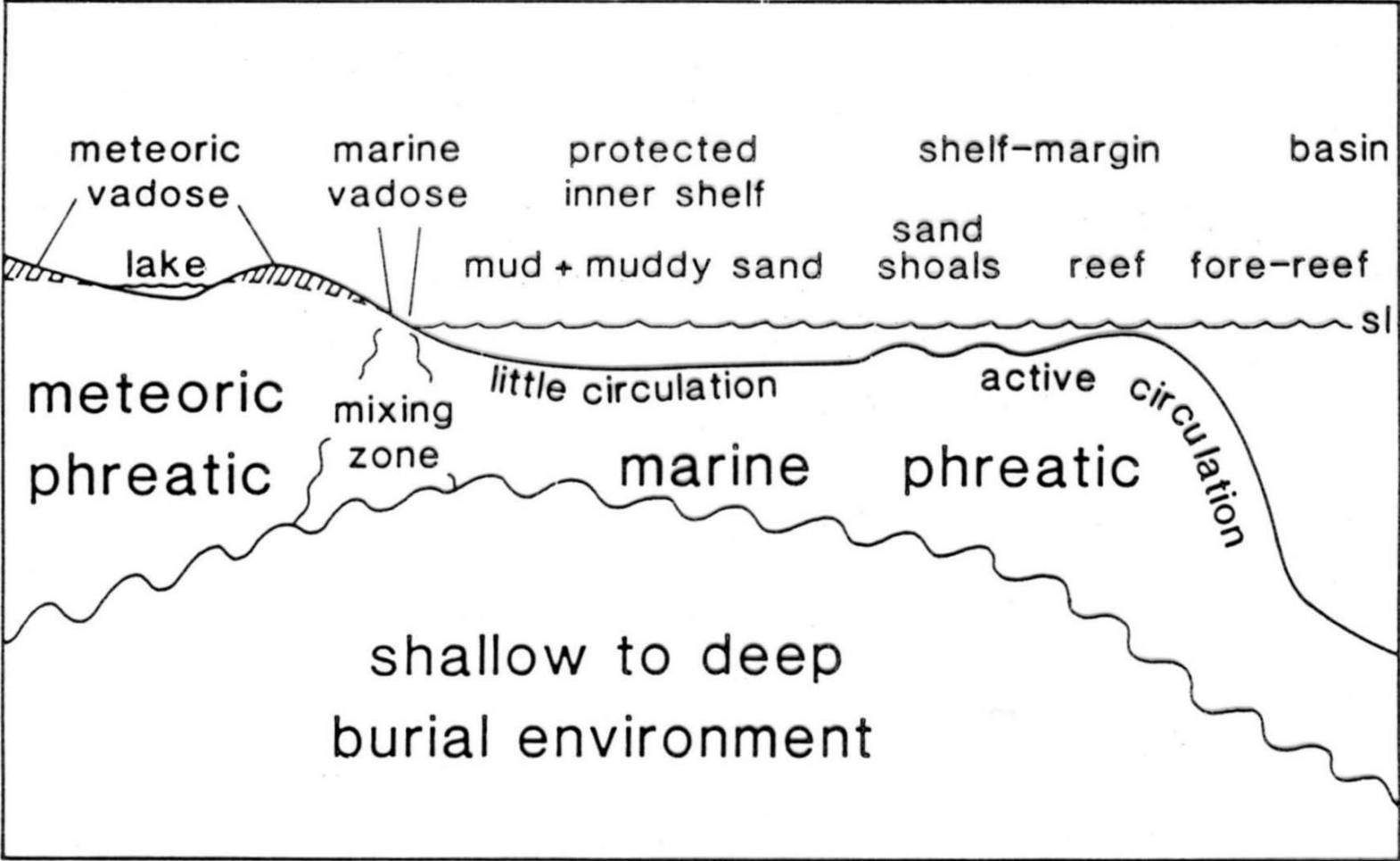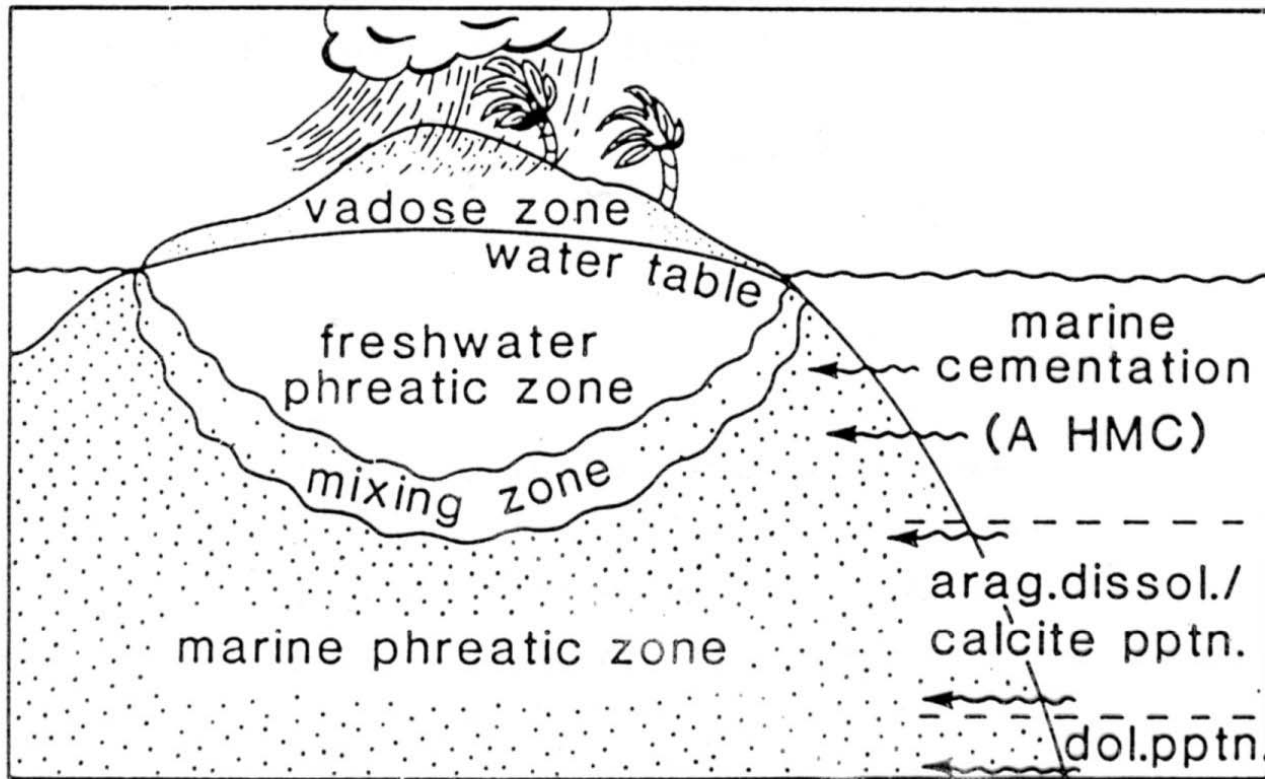
Fig. 7.2 *Diagenetic environments fo· an isolated platform, atoll or shelf margin, where an island is present with a freshwater lens. With increasing depth, seawater will become less saturated with respect to $CaCO_3$ so that aragonite may be dissolved and calcite precipitated, and eventually dolomite may be precipitated. This part of the model could apply to any platform or shelf margin. Depths will depend on the saturation state of seawater at the time.*

marine diagenesis - overview

present-day cements

intertidal-subtidal – beachrock; A, HMC tmely – **needle/accicular fringe surrounding grains**, perpendicular to grain surface; phreatic – **isopachous**; HMC dark mikritic grain coatings, pore fillings; grain micritization; cement sources: a) phys.-chem. precipitation during evaporation on tidal flat, b) biochem. microbial precipitation (algal photosynthesis, bacterial calcification, decay of organic matter)

shallow subtidal – lagoons – **microbial micritization**; higher energy – cementation, **hardgrounds**; cements: **needle/accicular A**, **micritic HMC** – **grain coatings, peloidal structures**, surface crusts; reefs – high variability of cement types

deep water cementation – up to 3,5 km depth, impregnation by phosphates and Fe,Mg oxides; Bahamas - cements: micritic LMC, deeper water - nodularization; warm undercurrents: thin crusts, nodules of lithified pelagic material, needle A and mikritic A cement; cementation – low sedimentation rates, water-sediment interaction (but not with pore fluids)

present-day marine dissolution – higher lattitudes – low CaCO3 saturation – dissolution of bioclasts in first 100s m depth
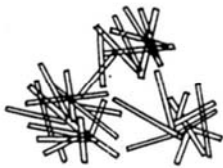
modern marin cements and their geometries
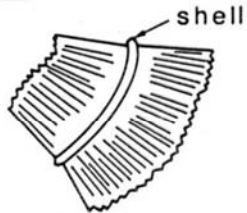
ARAGONITE CEMENTS
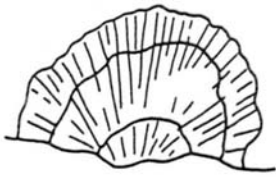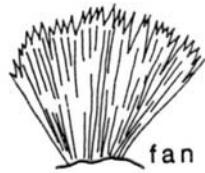
botryoids   fan
10mm

mesh of needles   acicular fringe   shell

HIGH Mg CALCITE CEMENTS
100µm

bladed   equant   peloidal

CEMENT GEOMETRY
1mm
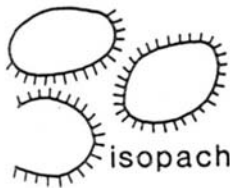
isopachous
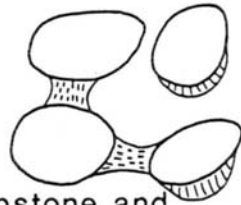
dripstone and meniscus

polygonal boundary
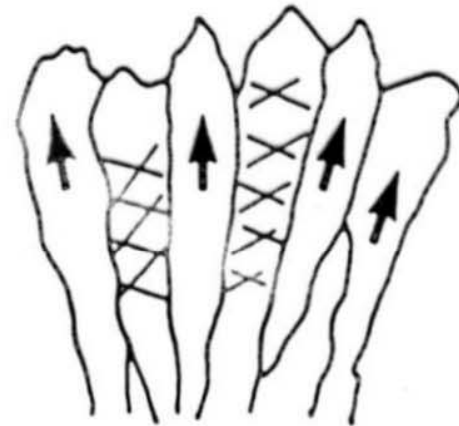
6

undulose extinction
curved twin planes
subcrystals

unit extinction
straight twin planes

fascular–optic

radiaxial

radial-fibrous

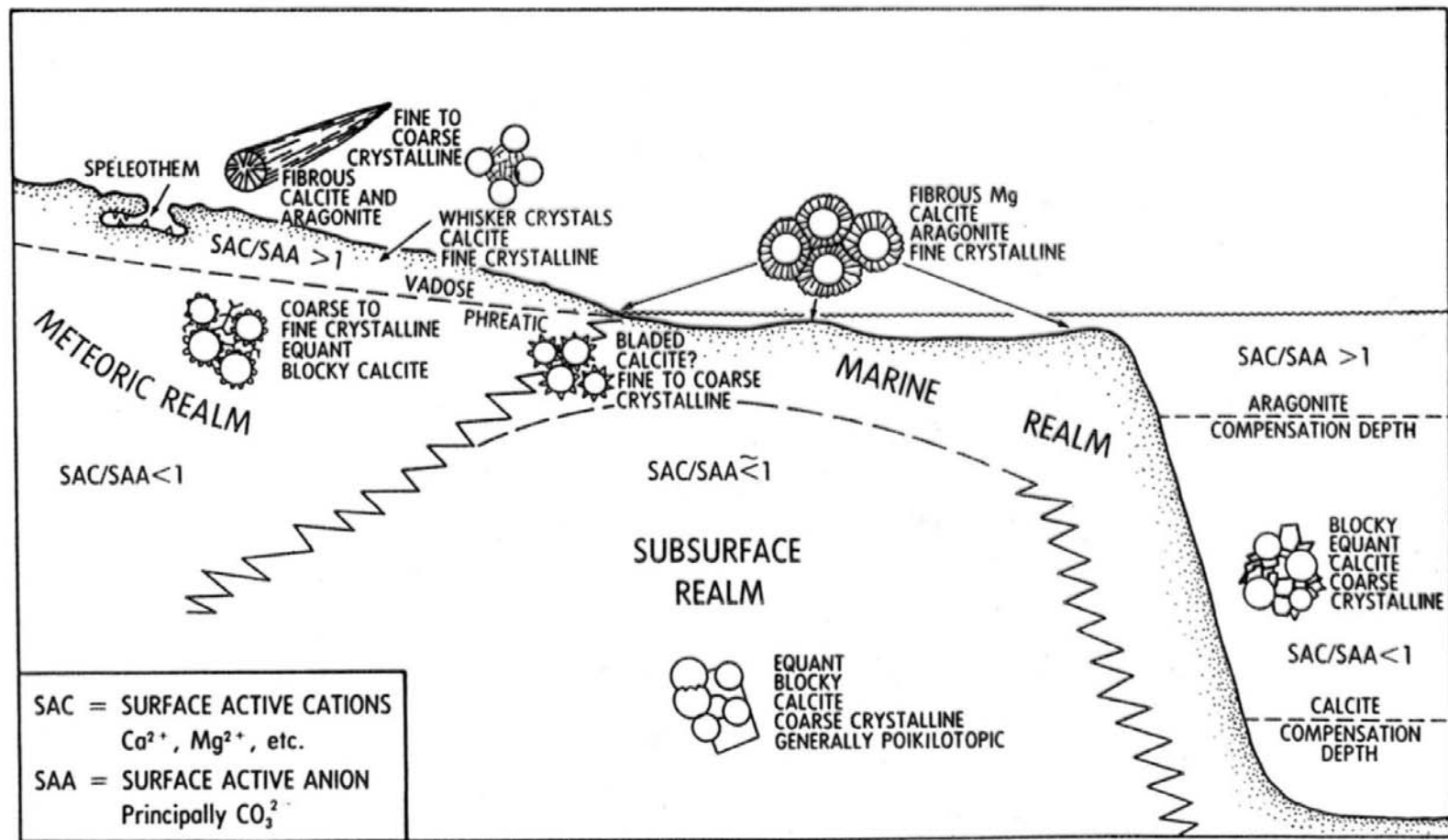Fig. 4.50 Common types of fibrous calcite. After Kendall (1985).

Fig. 3.5 Schematic diagram showing anticipated growth habits of pore-fill calcite cement in the principal diagenetic environments, as controlled by the ratio of surface active cations (SAC) to surface active anions (SAA).

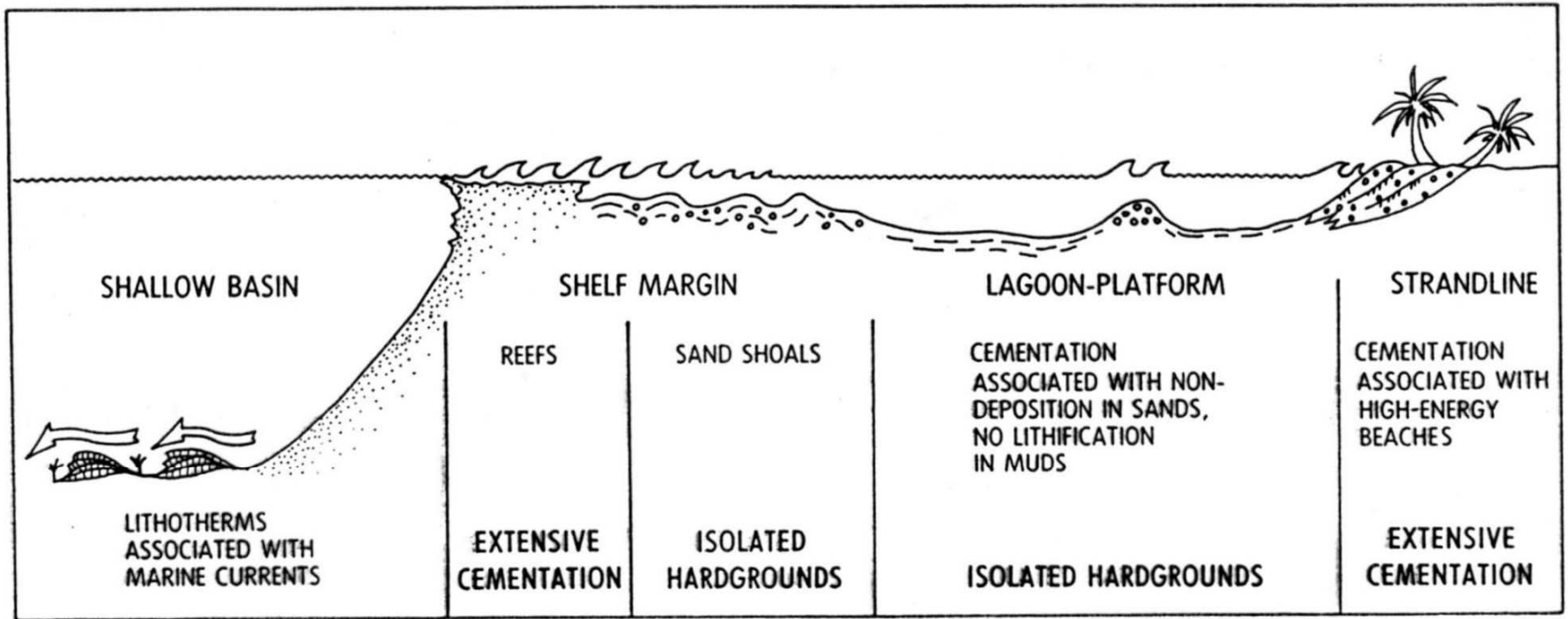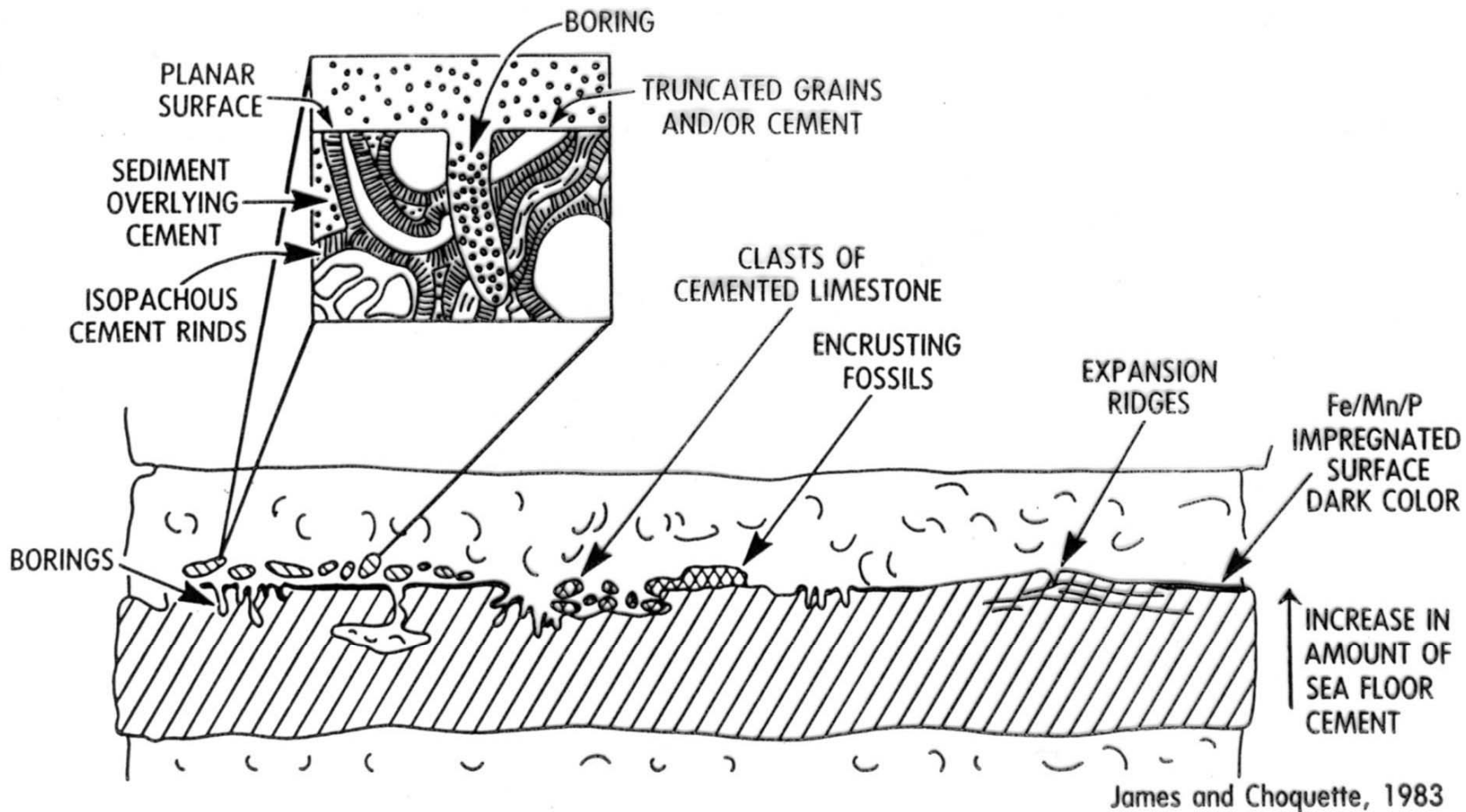| SHALLOW BASIN	SHELF MARGIN		LAGOON-PLATFORM	STRANDLINE
	REEFS	SAND SHOALS	CEMENTATION ASSOCIATED WITH NON-DEPOSITION IN SANDS, NO LITHIFICATION IN MUDS	CEMENTATION ASSOCIATED WITH HIGH-ENERGY BEACHES
LITHOTHERMS ASSOCIATED WITH MARINE CURRENTS	EXTENSIVE CEMENTATION	ISOLATED HARDGROUNDS	ISOLATED HARDGROUNDS	EXTENSIVE CEMENTATION

Fig. 4.5. Diagenetic processes associated with shallow marine depositional environments.

9

Fig. 4.10. Criteria for the recognition of marine hardgrounds. Reprinted with permission of the Geological Association of Canada.
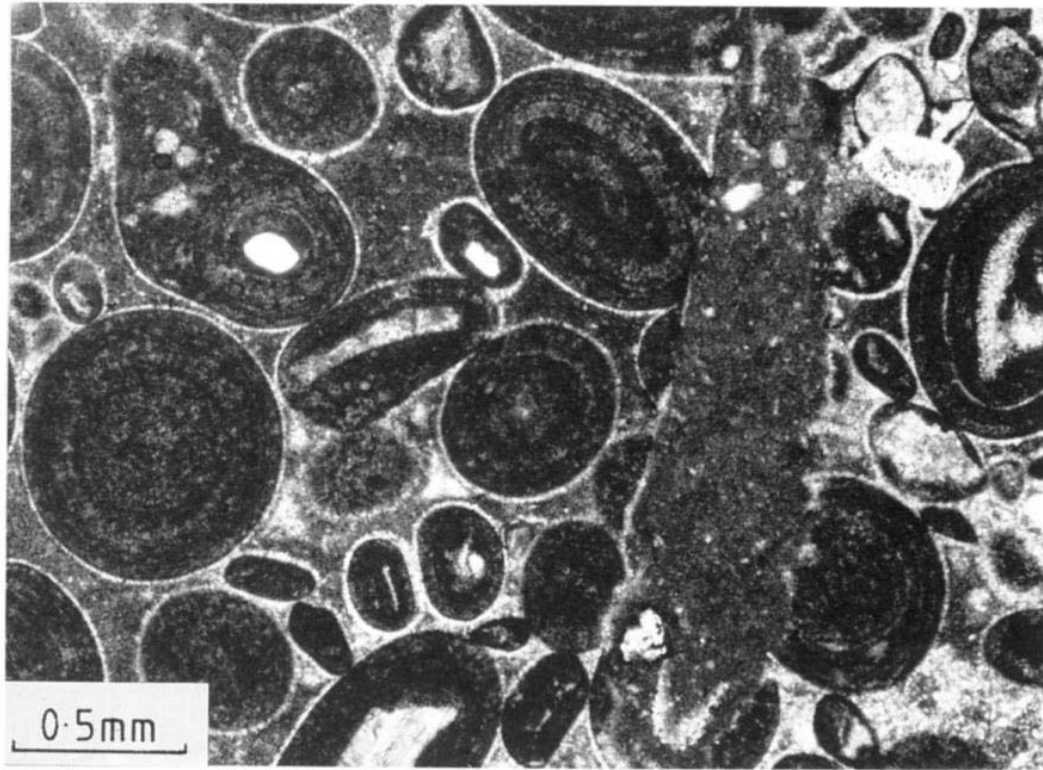
Fig. 7.9 *Oolitic sand cemented in the submarine environment to form a hardground which was then bored. Photomicrograph shows thin isopachous fringe of fibrous calcite around ooids and then micrite partly filling the intergranular porosity. The micrite may be an internal sediment or in part a cement. The ooids, micrite and fibrous calcite are cut by a boring which is itself filled with micrite. The early cementation prevented any compaction of this oolite which has grains in point contact. Middle Jurassic, Cotswolds, UK.*
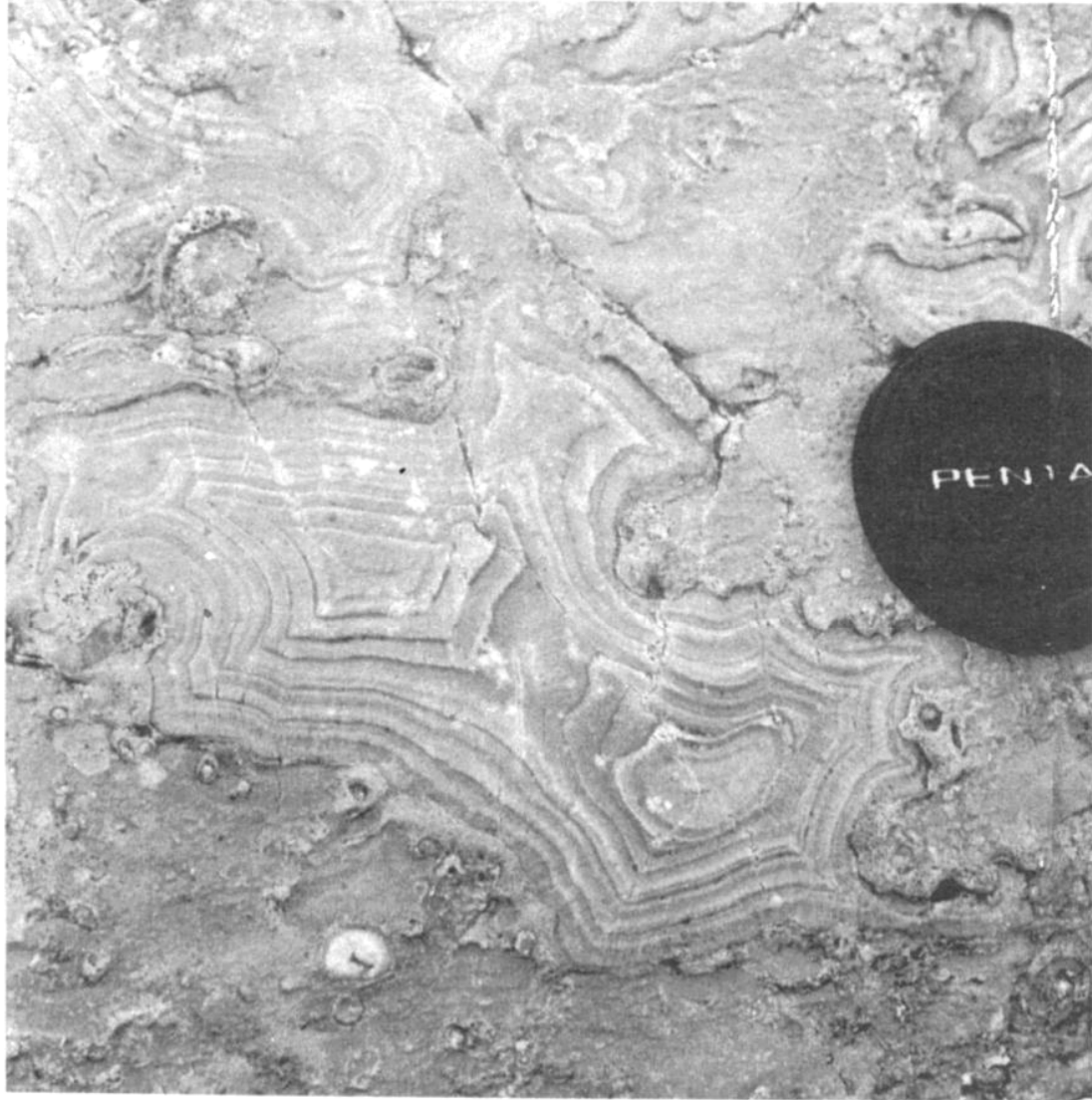
Fig. 7.8 *Marine cement in a Triassic reef, Hafelekar, Austria. Isopachous layers of fibrous calcite cementing fore-reef debris and known locally as 'Grossoolith'. Lens cap 6 cm diameter.*

12

A

0·5mm

B

0·2mm

C

50 μm

13

B
25 μm

D
0.5 mm

C
0.5 mm

F
20 μm

A

0·5mm

C

10 µm

B

15
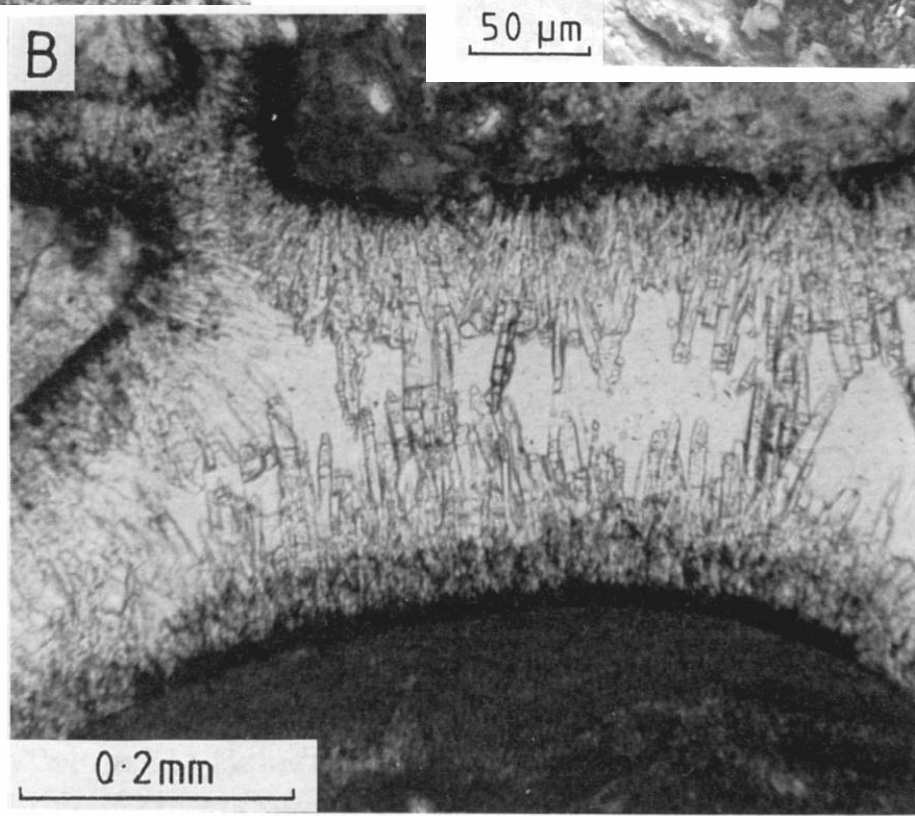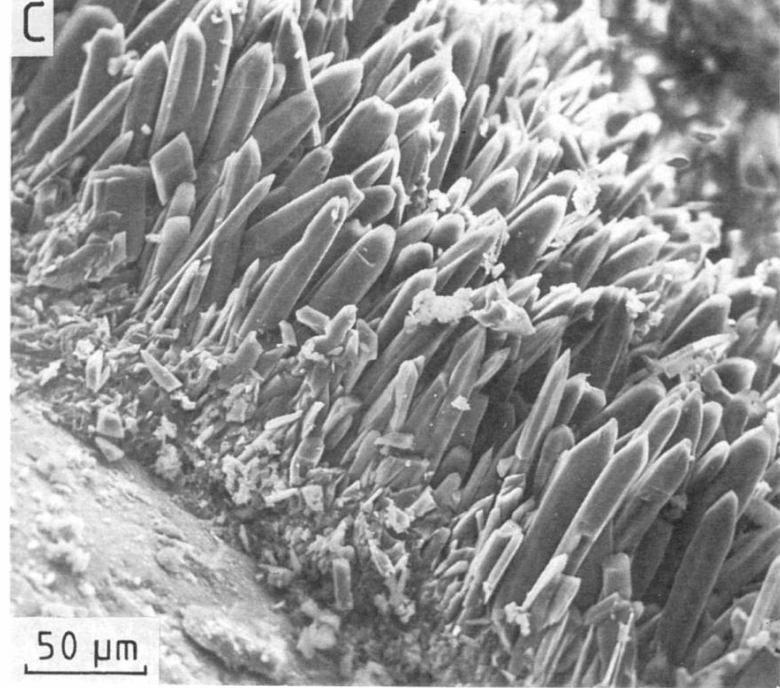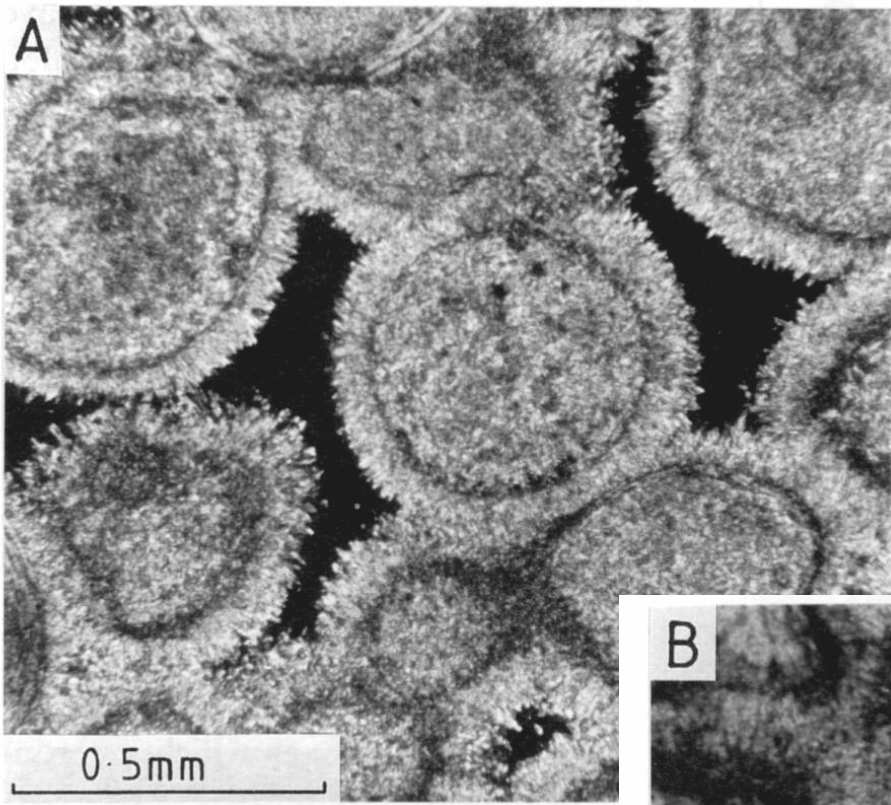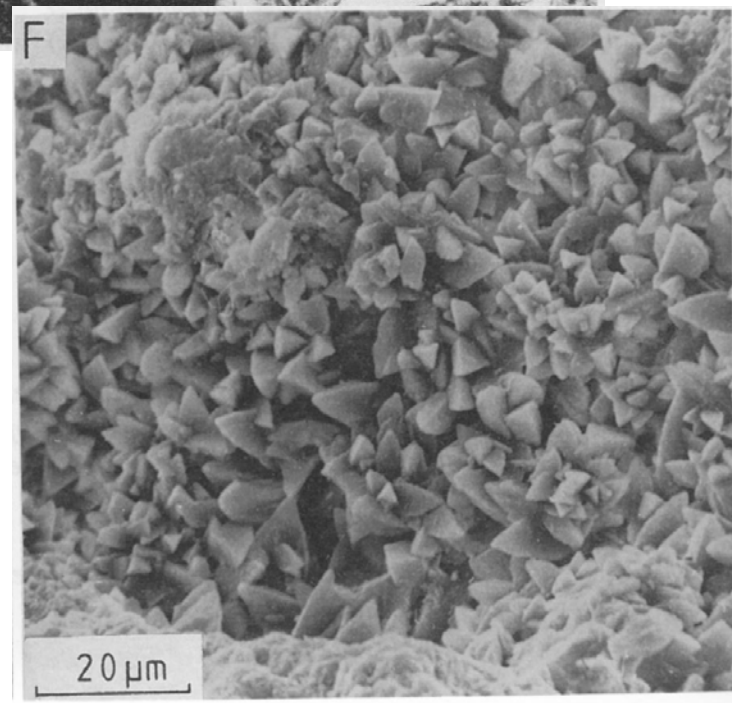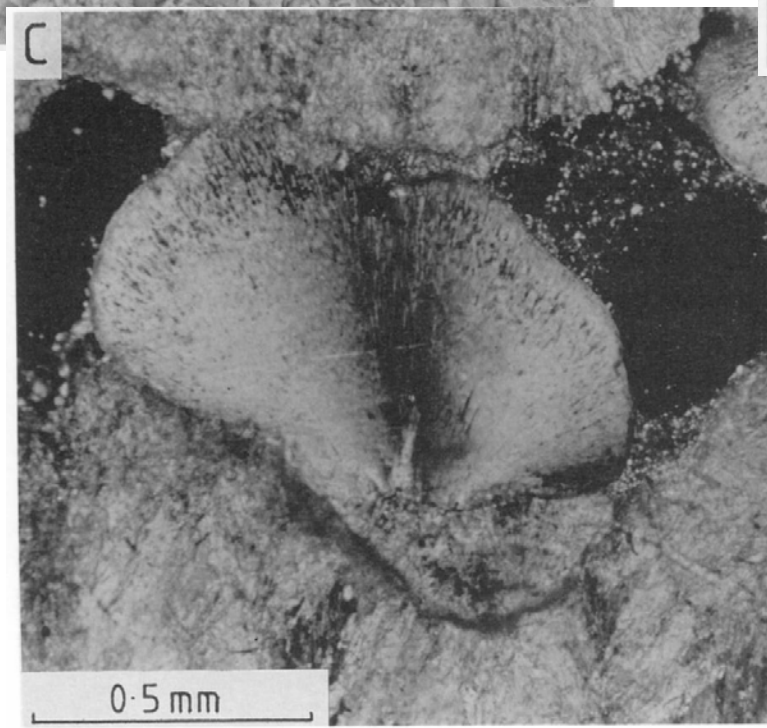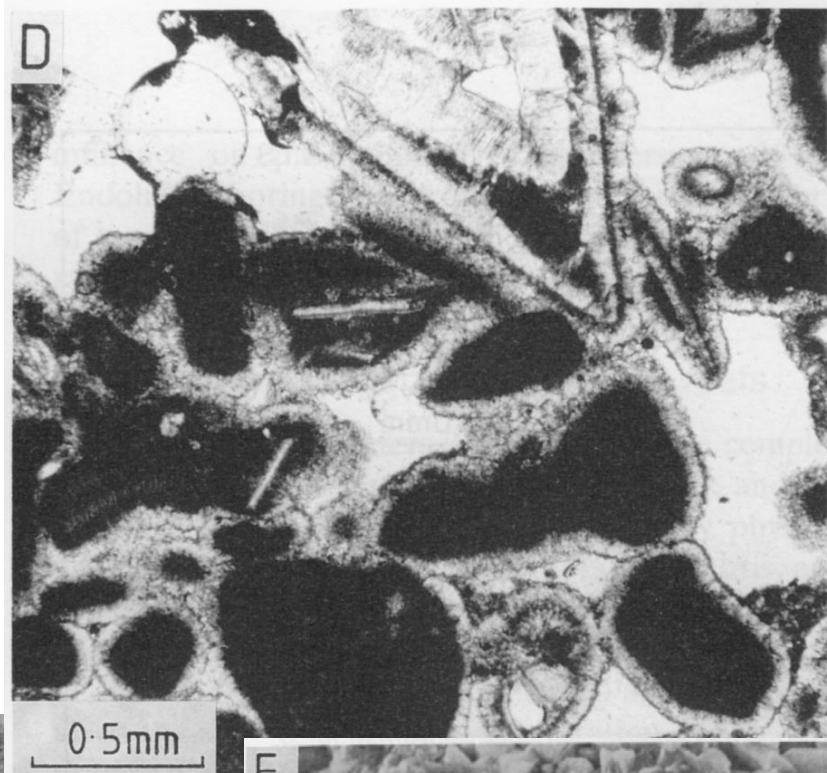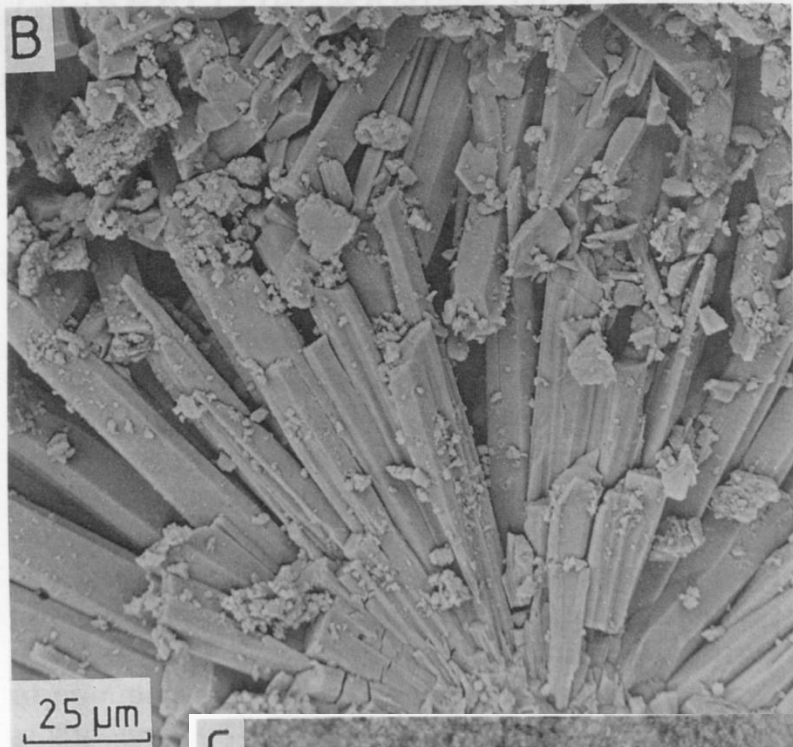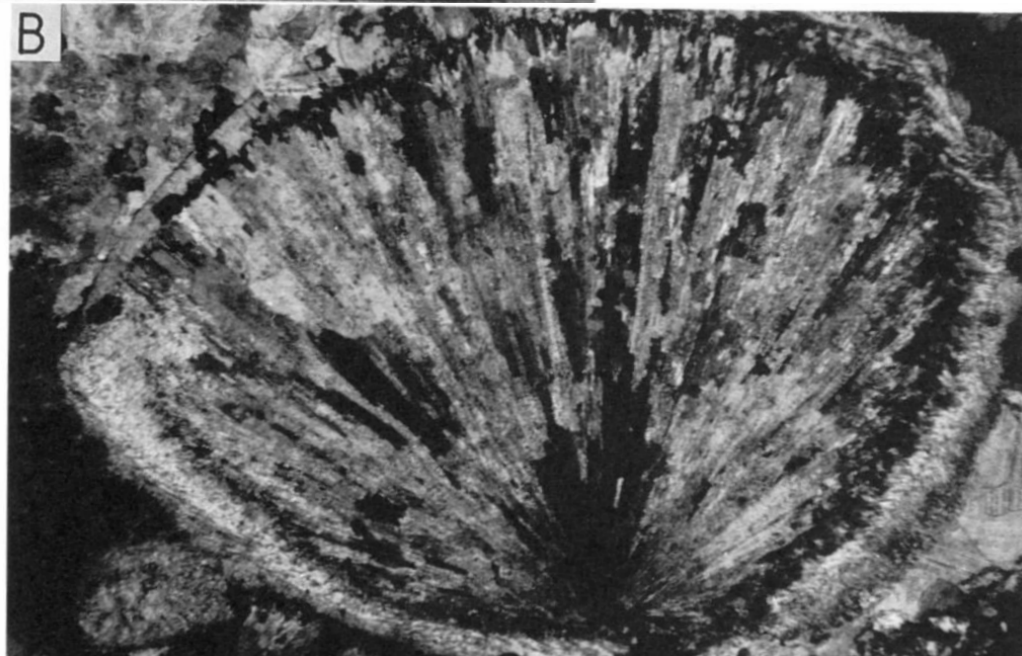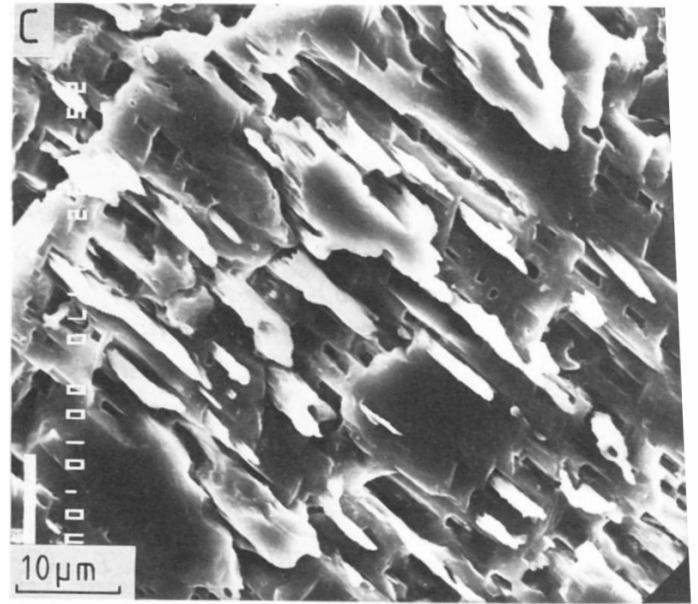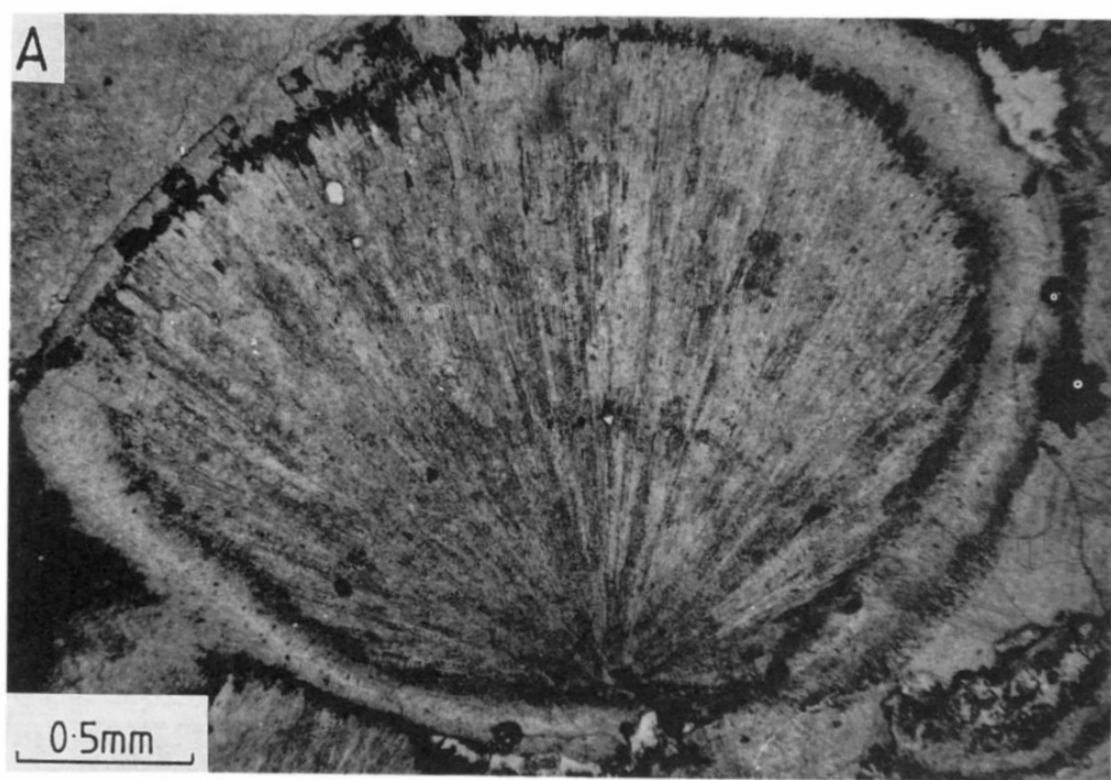
cement mineralogy
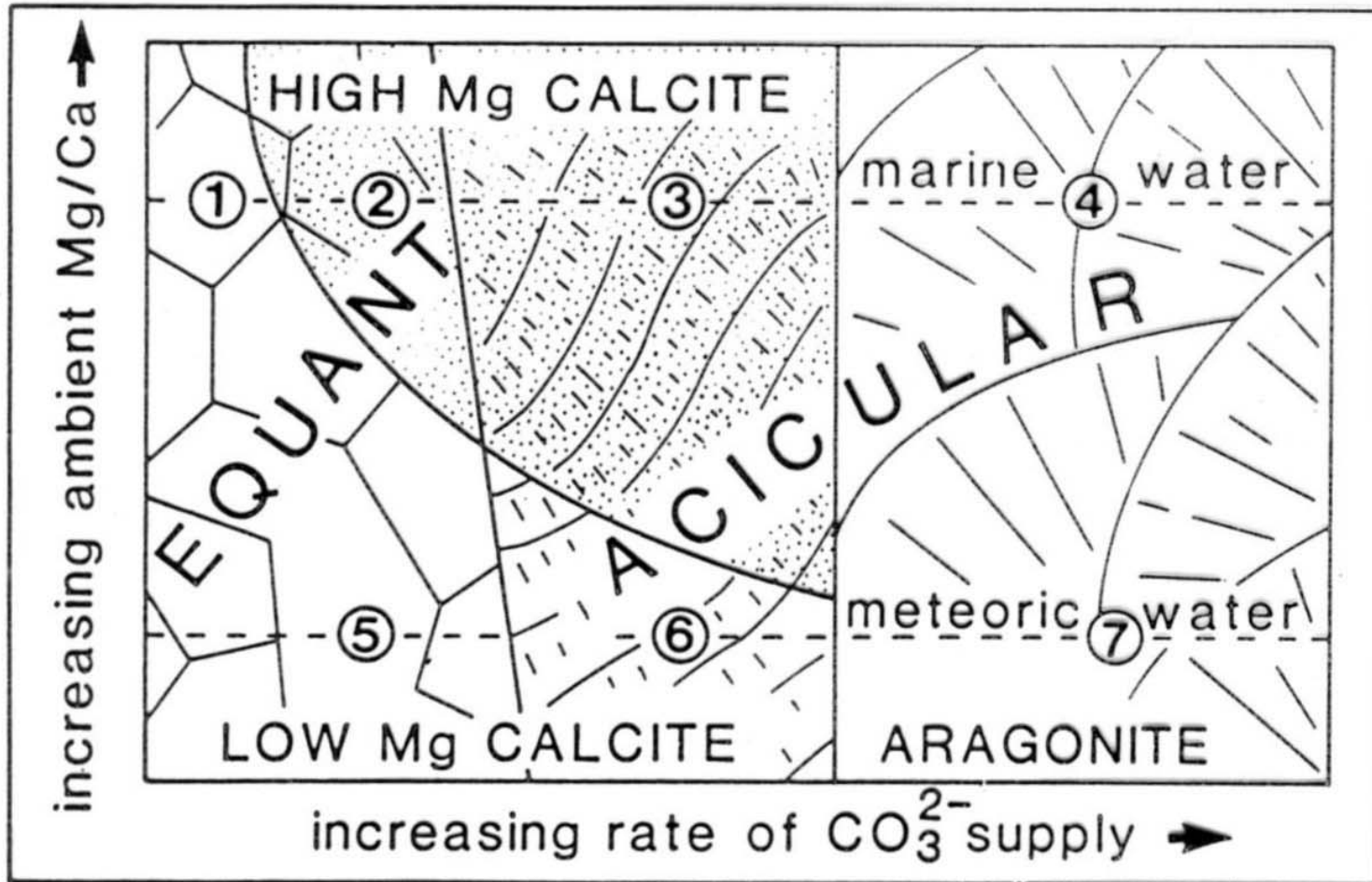
dissolution
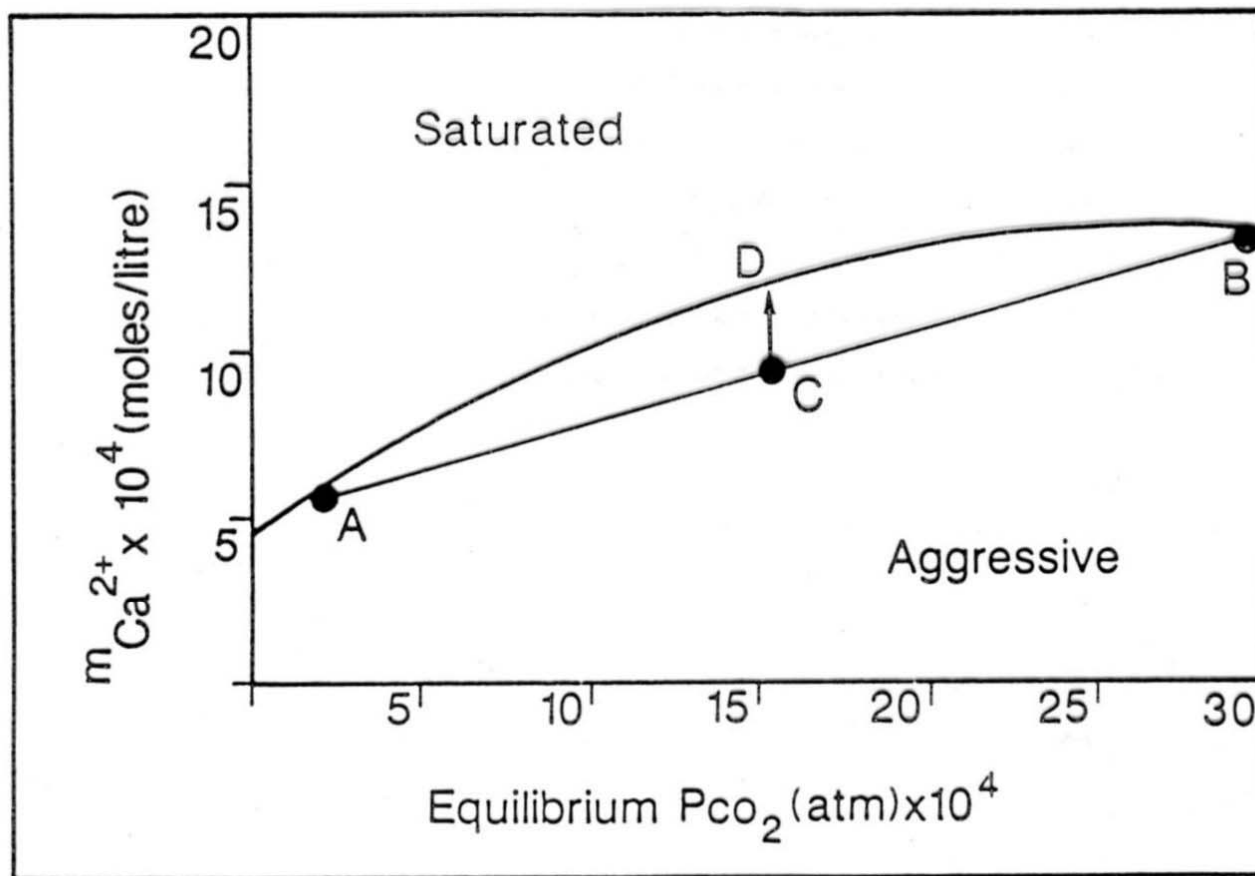
Fig. 7.20 *Mixing corrosion effect. The solid curve shows the solubility of CaCO₃ with respect to the total CO₂ in solution. If two liquids, A and B are mixed, an undersaturated solution results, C. It evolves by dissolution of calcite to equilibrium at D. From various sources.*
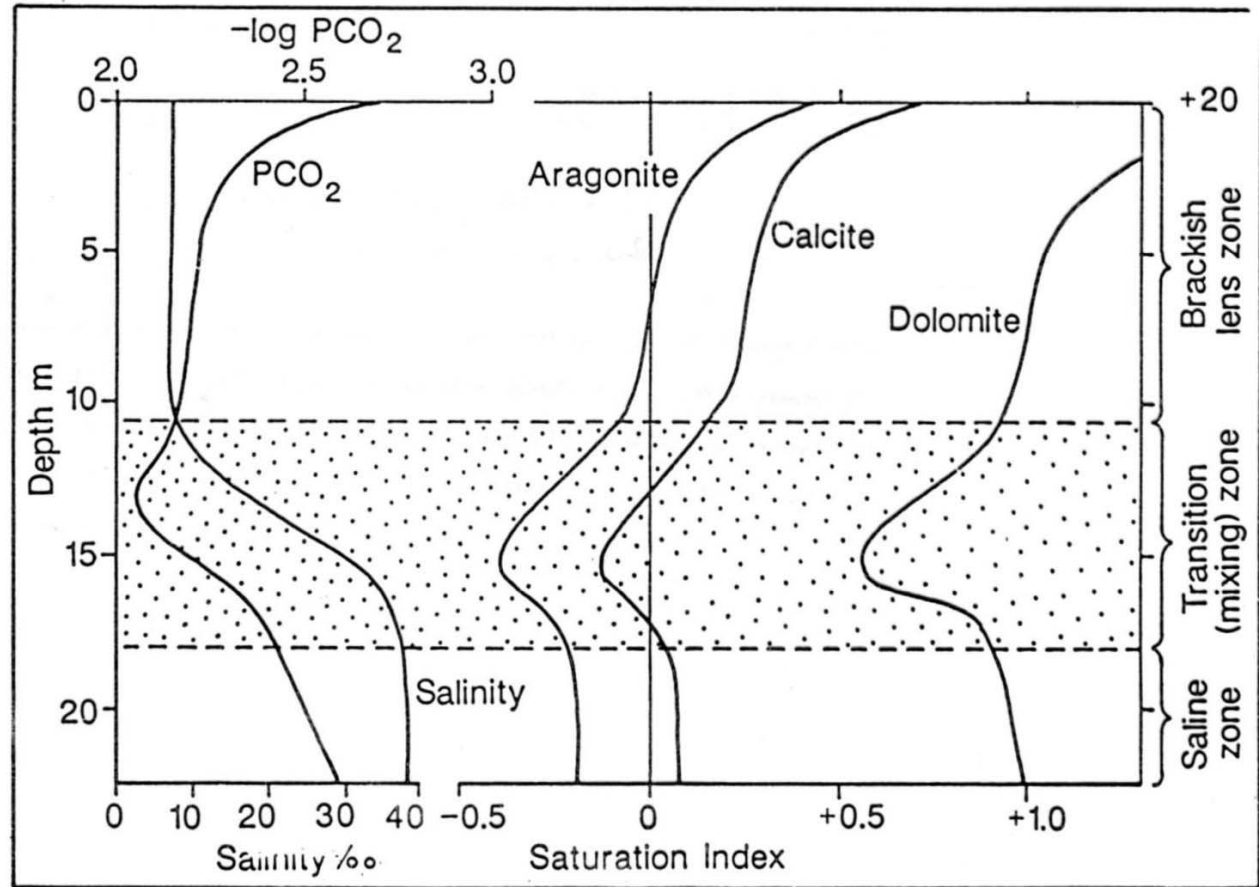
Fig. 7.21 *Vertical variation of salinity, P_{CO_2}, and the saturation indices of aragonite, calcite and dolomite through the meteoric–marine mixing zones within a 'blue hole', Andros Island. After Smart et al. (1988).*

18
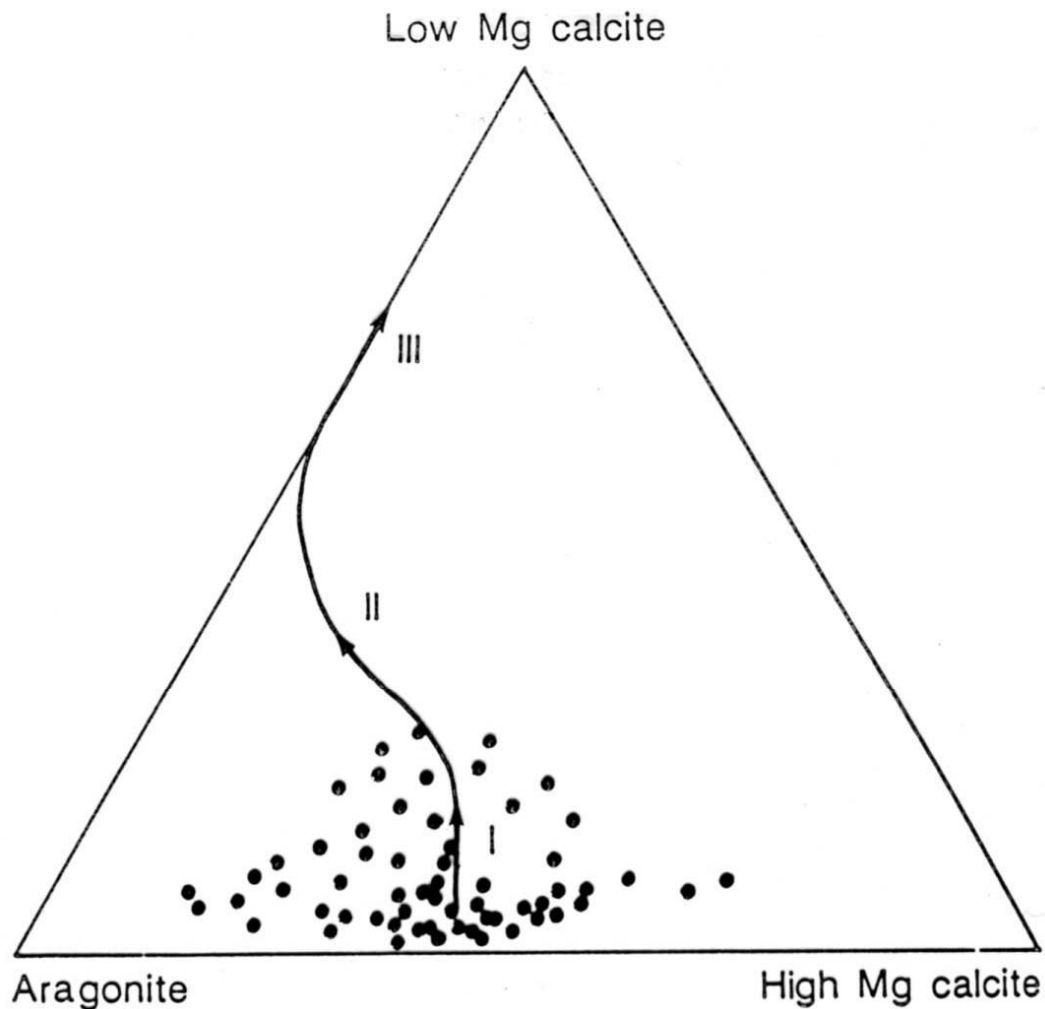
Fig. 7.22 *Triangular diagram showing the typical mineralogical evolution of Quaternary marine sediments during prolonged meteoric diagenesis. Stippled area represents range of marine sediments. I, initial cementation by low-Mg calcite. II, loss of Mg from high-Mg calcites. III, dissolution of aragonites and cementation by low-Mg calcite. Modified from Tucker (1981).*

19

marine diagenesis

diagenesis in sedimentary record

early d. – on the seafloor or close to sediment surface; late d. – burial
diagnostic features of marine cements: 1) early (1st generation), 2)
isopachous fringes surrounding grains, 3) needle/accicular/prismatic
structure, 4) following generatin is typically sparite
aragonite cements – usually calcitised, **isopachous** fringes
calcite cements – accicular (**needle, prismatic**) calcite, perpendicular
to substrate; reefs – **micritic and peloidal HMC**; hardgounds –
syntaxial overgrowths, equant sparite – both also typical for meteoric
diagenesis and burial

processes: mikritic cement – rapid nucleation, slow accretion;
needle/prismatic – faster accretion perpendicular to substrate; equant
sparite – very slow nucleation

250 μm (a)
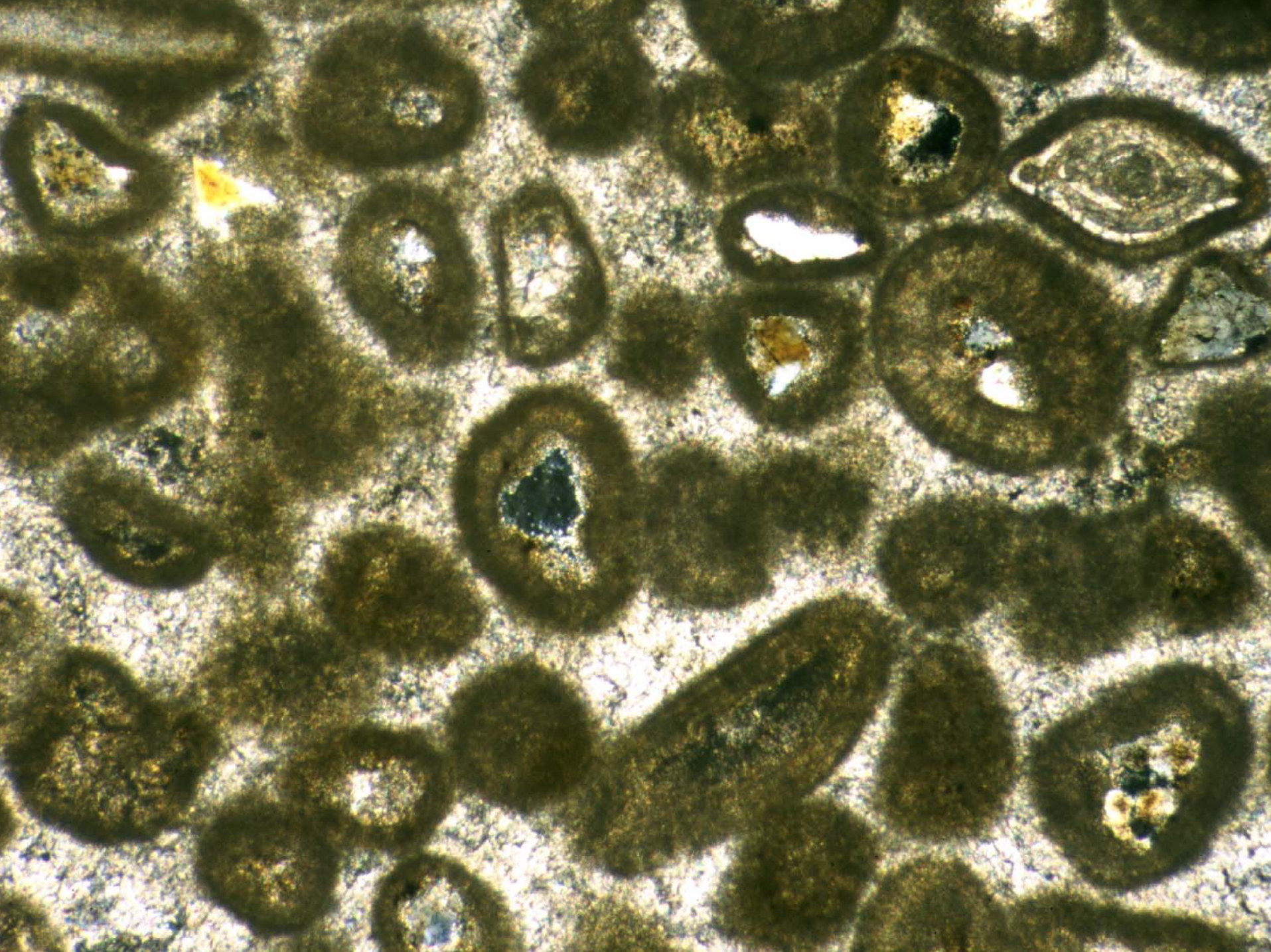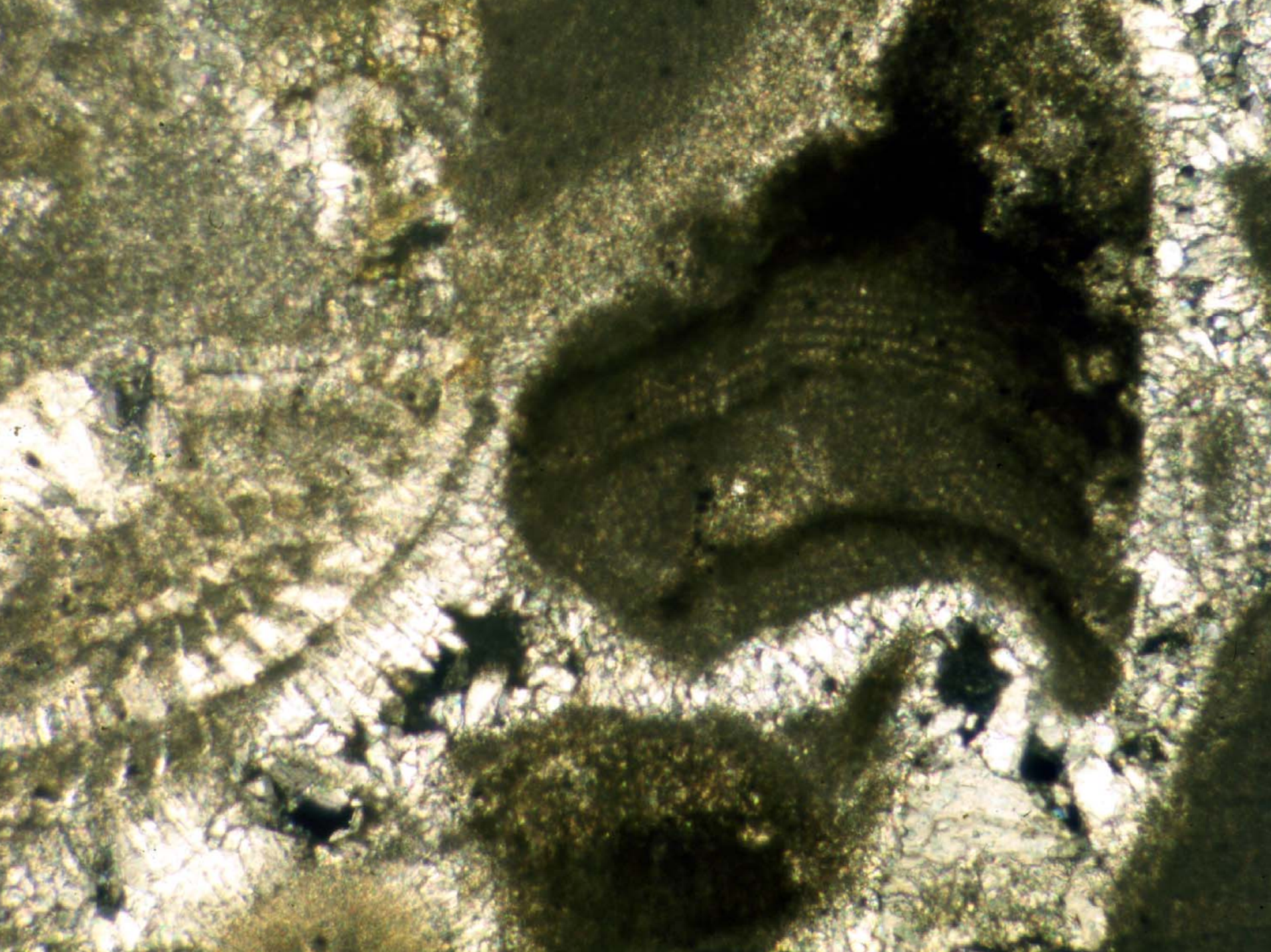
burial diagenesis
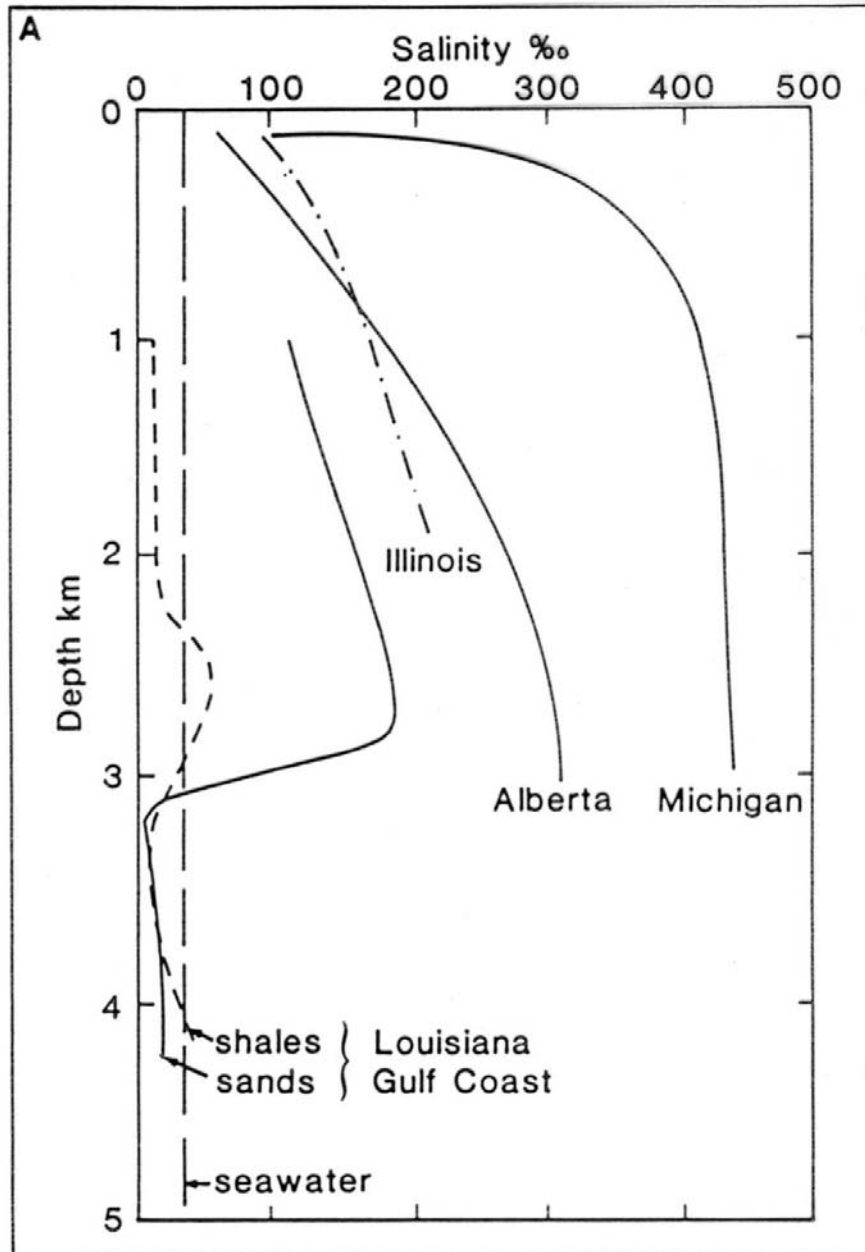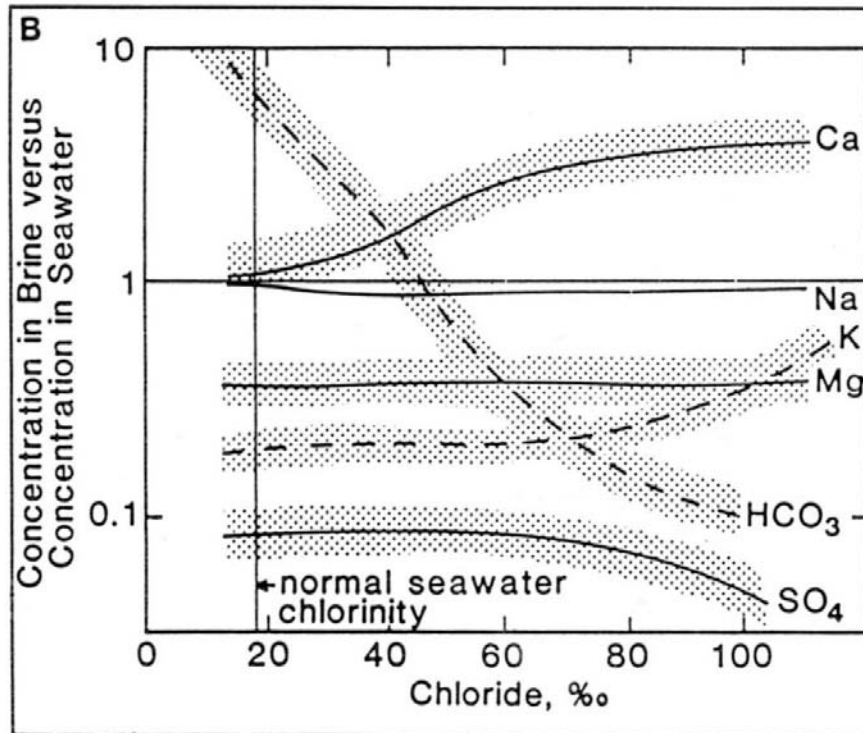
Fig. 7.30 (A) Generalized salinity variations with depth for formation waters from the Alberta, Illinois, Louisiana Gulf Coast and Michigan Basins (B) Generalized variations in chemical composition of subsurface brines in the Illinois Basin with increasing chlorinity. Values are normalized with respect to seawater of the same chloride content. From Hanor (1983).

geothermal gradient
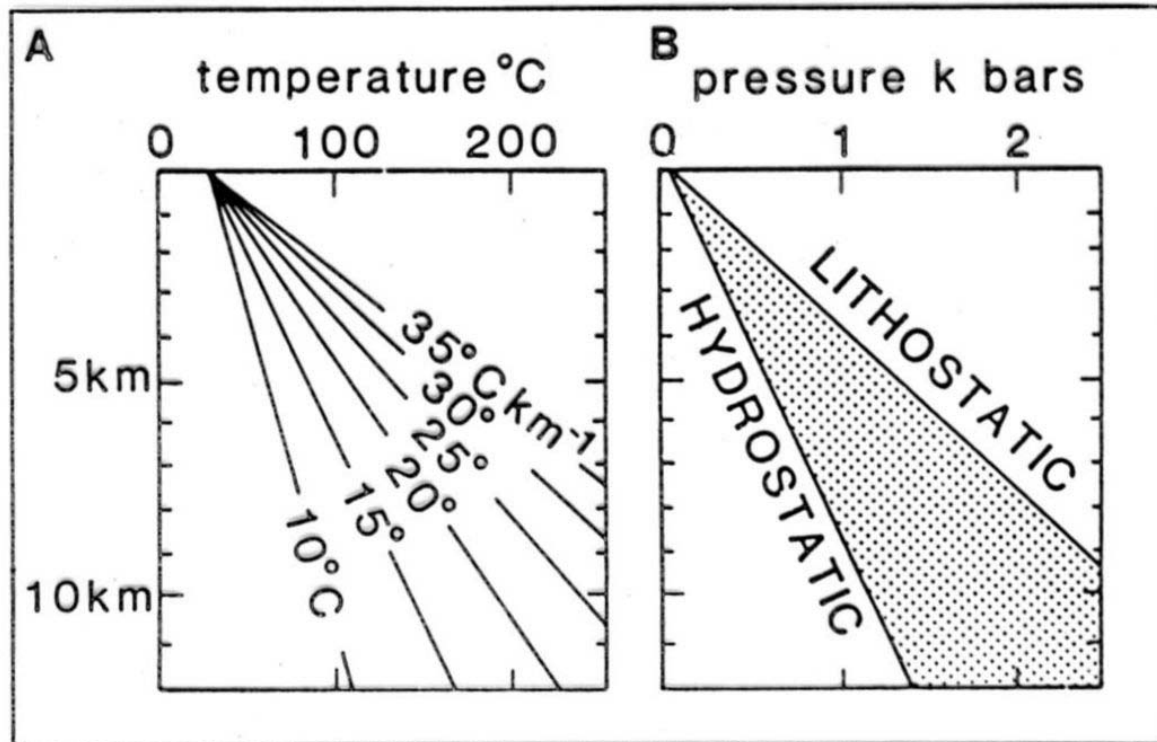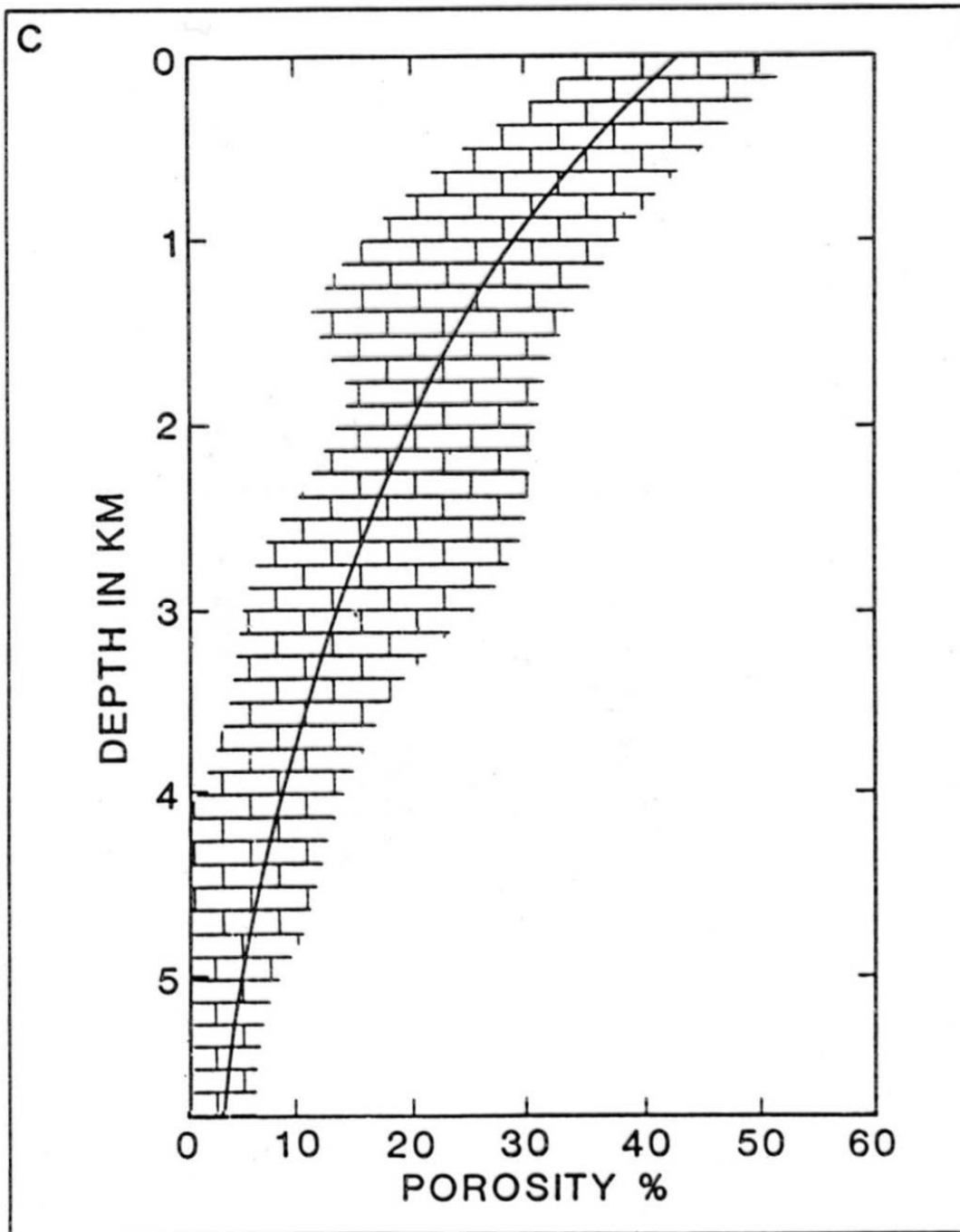
meteoric diagenesis

dissolution (secondary porosity, carstification), cementation, pedogenesis
vadose zone – upper – infiltration, lower – percolation
phreatic **- syntaxial overgrowths, equant spar cements**
vadose – asymmetric: **meniscus, gravity cements**

isopachous cement – phreatic   early stage
asymmetrical – vadose
syntaxial overgrowths
calcite replacing aragonite – sparry cements
LMC infilling pores   late stage
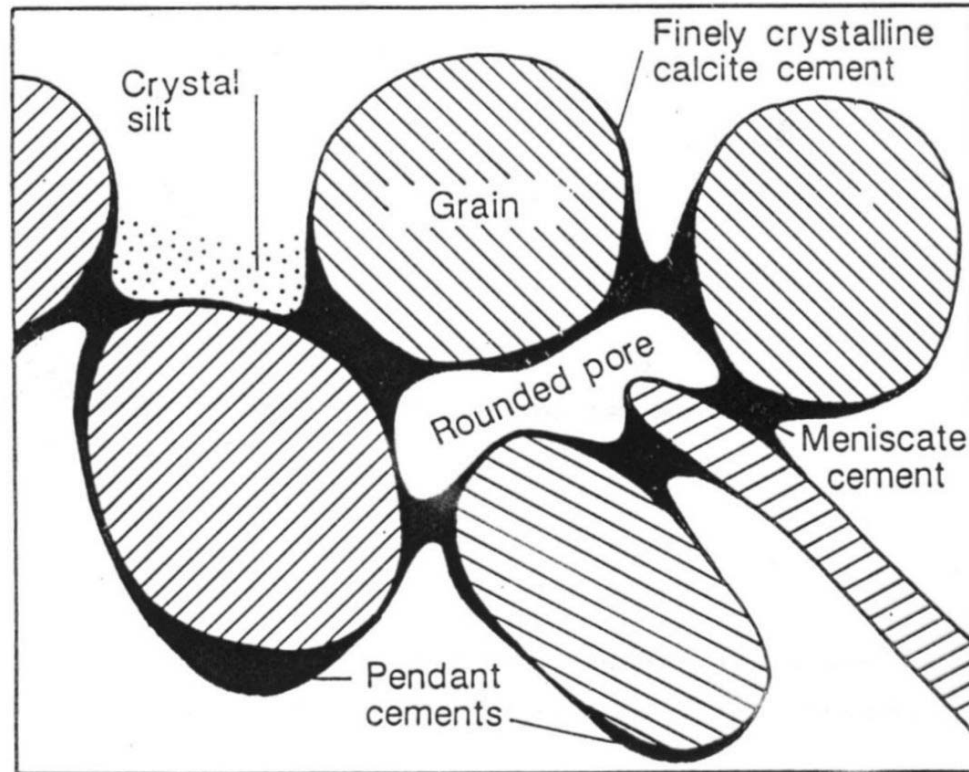
Fig. 7.27 *Common cement geometries in vadose zones (see text).*
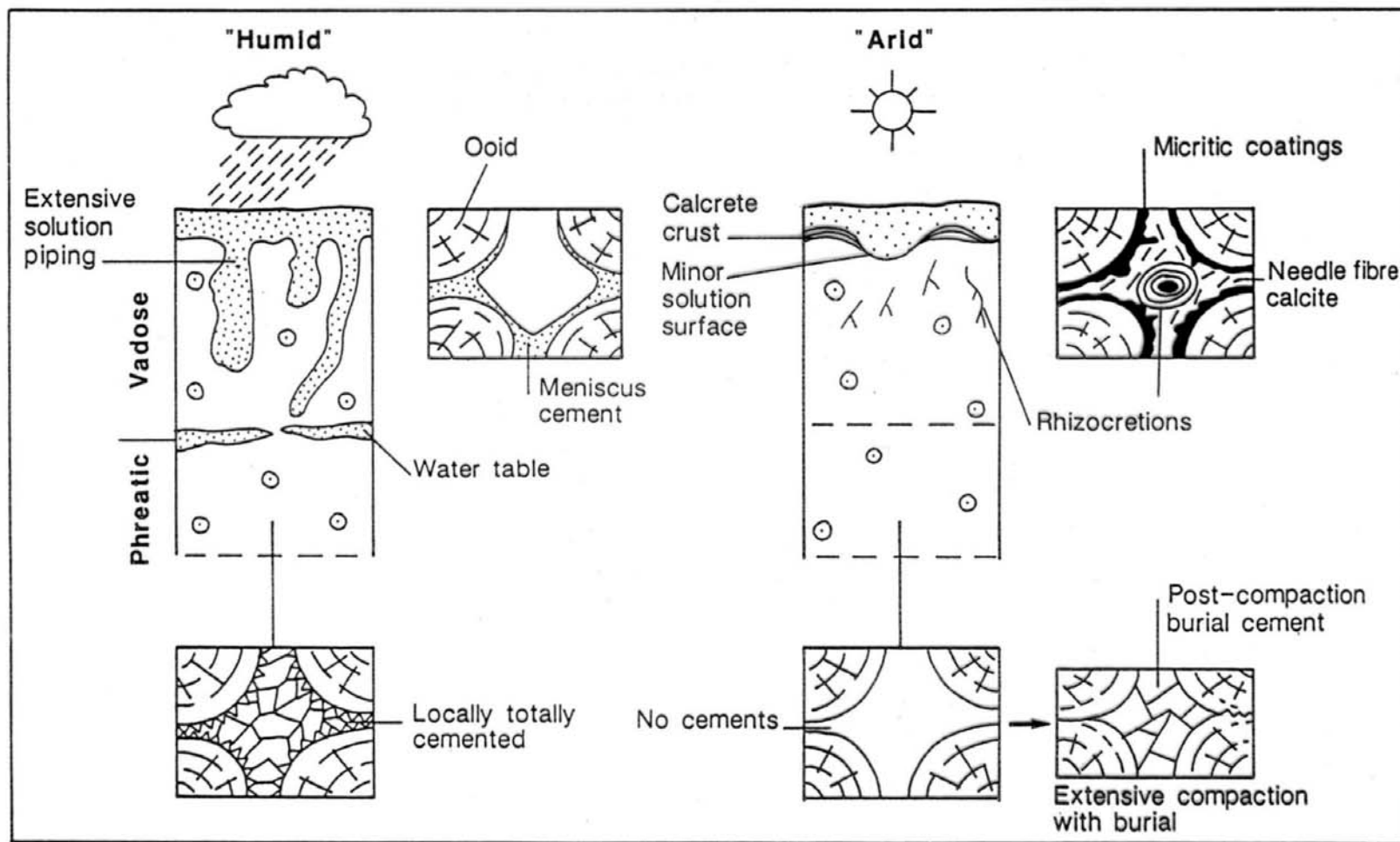
Fig. 7.24 *Contrasting styles of karstification, meteoric cementation and porosity evolution in Early Carboniferous oolitic limestones from south Wales. Based on Hird & Tucker (1988) and Wright (1988).*
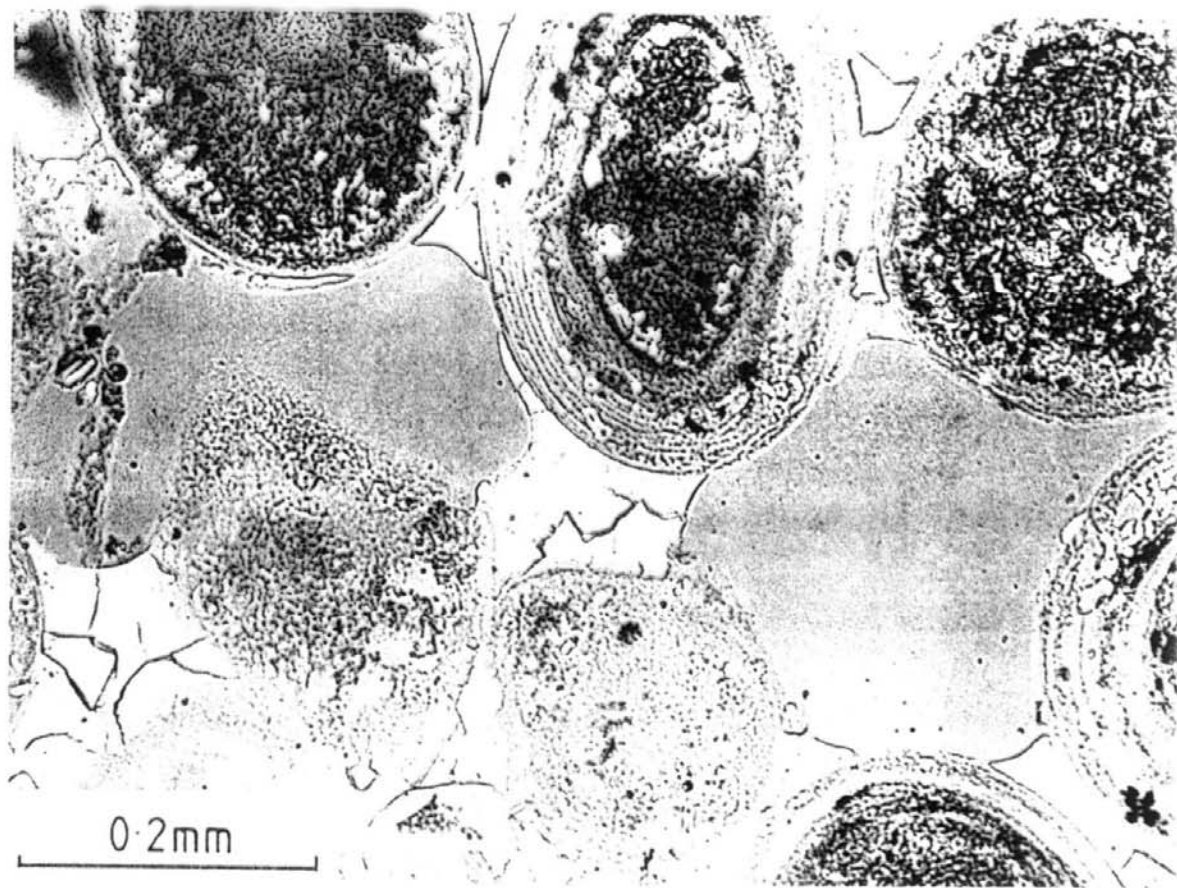
Fig. 7.28 *Meniscus cement, vadose zone, Joulter's Cay, Bahamas.*

0·2mm

31

kalcite spar

equigranular mosaic, syntaxial overgrowths, poikilotopic spar
-meteoric phreatic zone, sourc of $CaCO_3$ – pore fluids
-burial, source of $CaCO_3$ – pressure solution
cement stratigrafphy, catode luminiscence, stable isotopes, fluid inclusions

A equant spar drusy mosaic

B compromise boundaries in drusy mosaics

C syntaxial overgrowth

D poikilotopic spar

33

E prismatic spar

marine cement

F equant spar equicrystalline mosaic
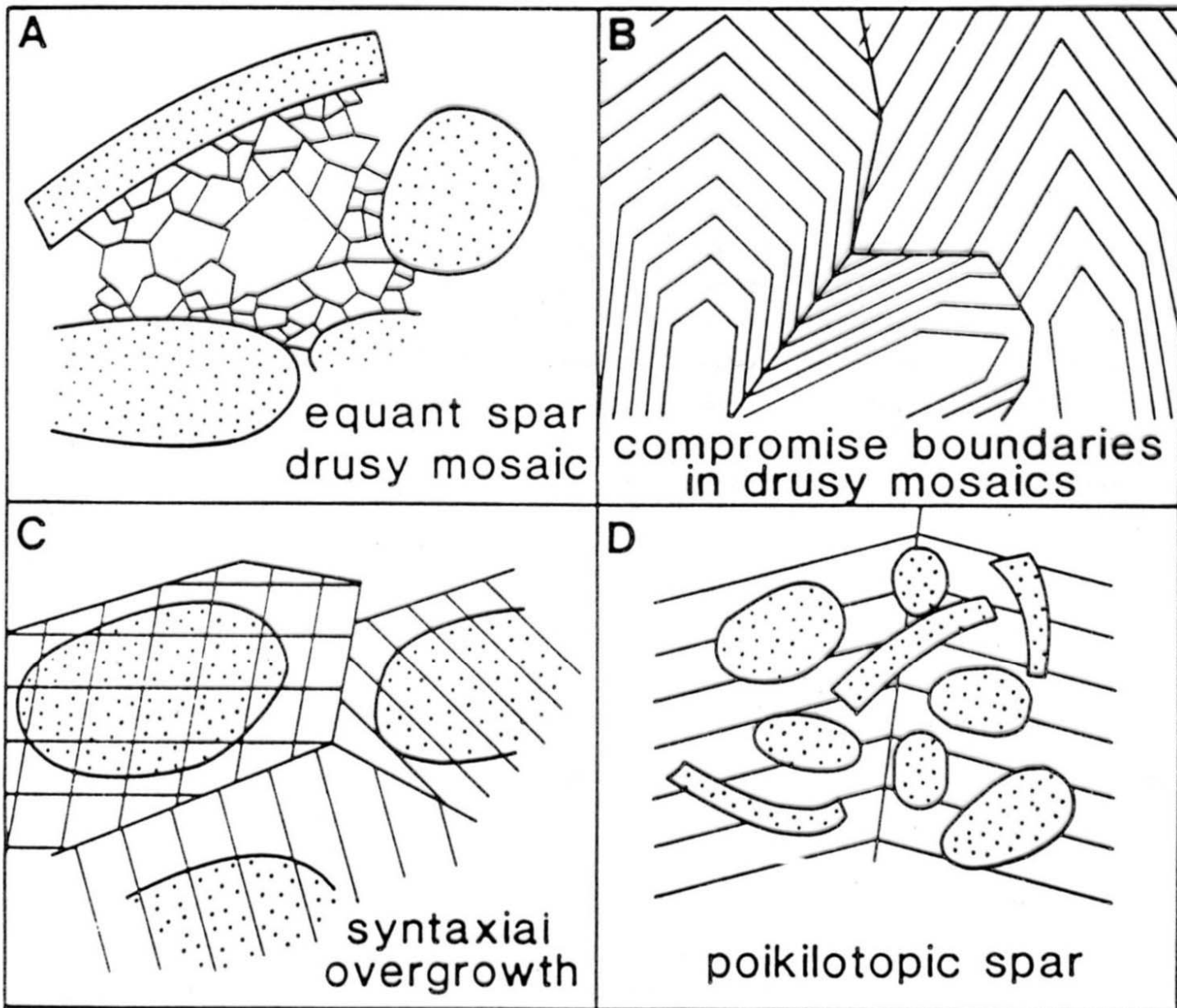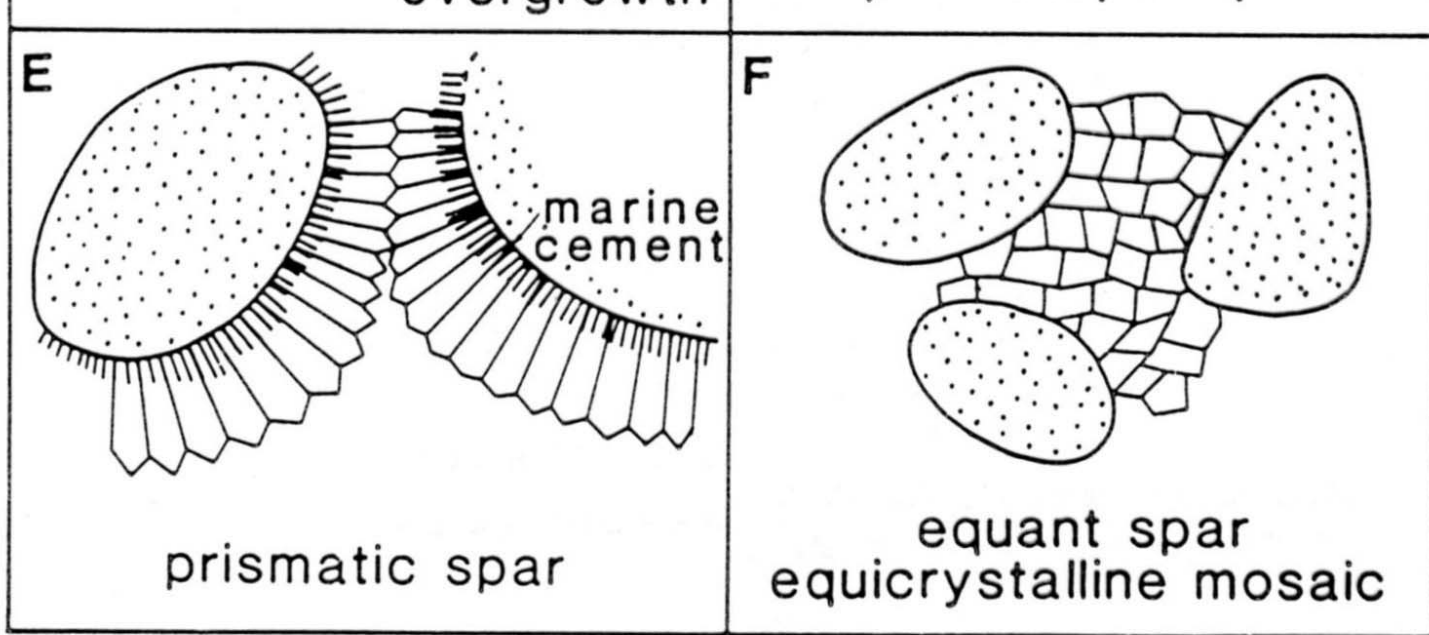
Fig. 7.32 *Calcite spar: sketches illustrating the common types.*
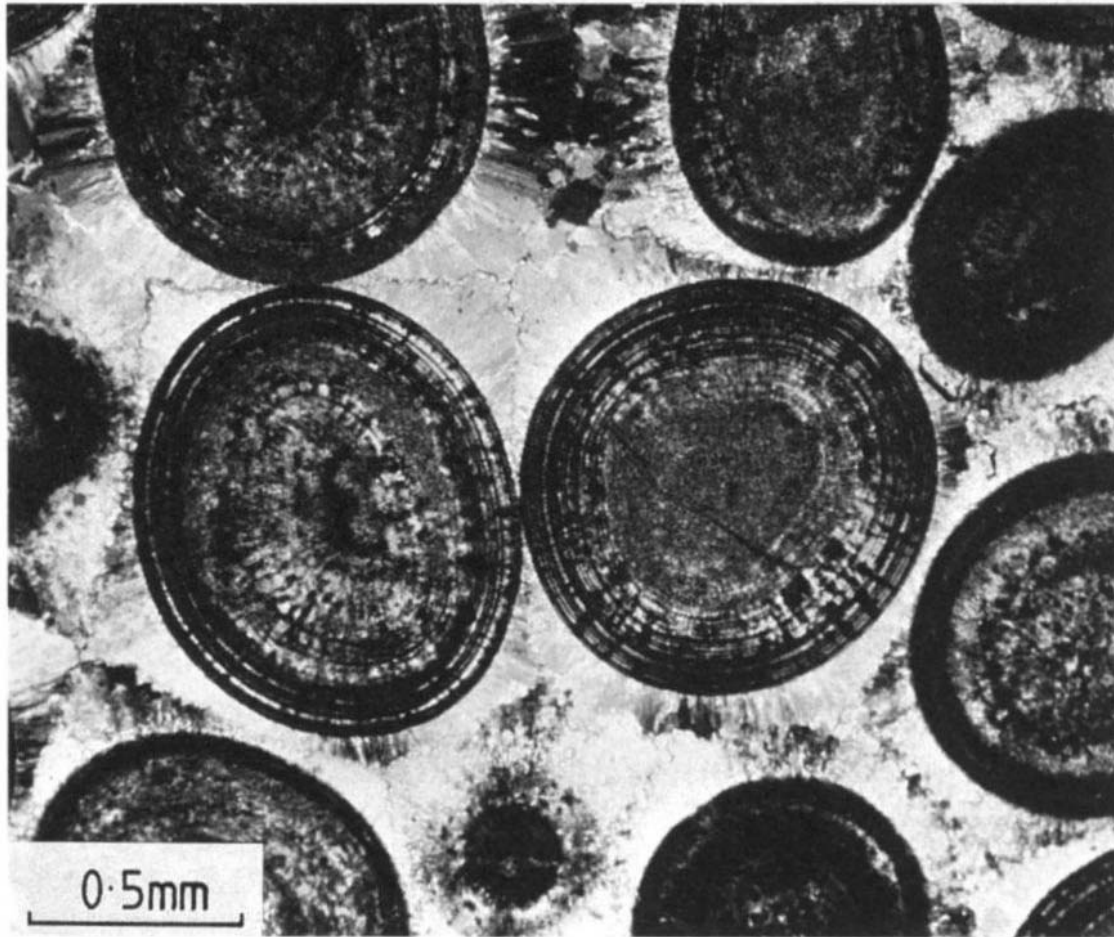
Fig. 7.14 *Fibrous calcite marine cement (primary) around ooids (also primary calcite) with prominent polygonal compromise boundary between fringes. These more acicular crystals are in optical continuity with radial-fibrous crystallities of the ooids. Jurassic Smackover Formation, subsurface Arkansas. Crossed polars.*

35

neomorphism

A→C, C→C, dissolution + reprecipitation

aggradational neomorphism – following crystal phase is coarser-grained; a) micrite → microspar, pseudospar, b) calcitization of aragonite

calcilutites: **microspar** (4-10 mm), **pseudospar** (10-50 mm); irregular uneven grain boundaries, irregular grainsize, clastic grains floating in spar; pseudobrecciation

calcitization of A grains and cements – **druse spar**; a) relics of original bioclast structures, b) irregular mosaics of greins with different sizes, c) brownish coloring of neomorphic spar (relics of org. matter) - pseudopleochroism

degradational neomorphism – grain size is decreasing; rare; usually during metamorphism or deformation
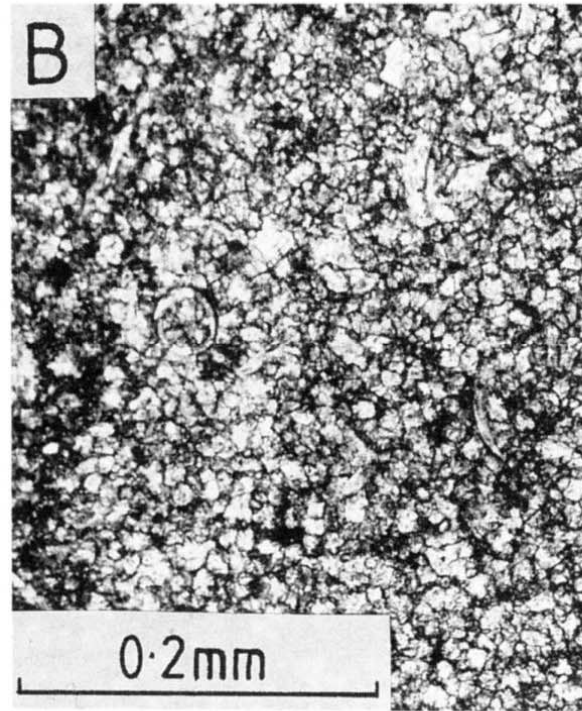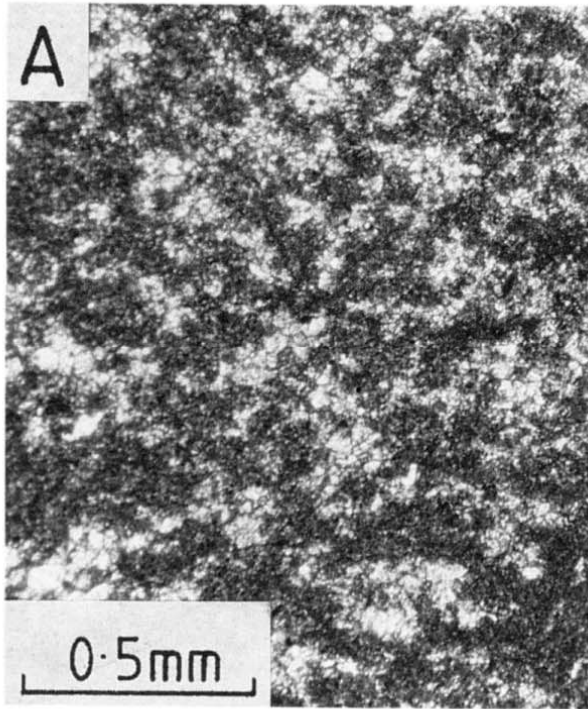
Fig. 7.41 *Neomorphic spar. (A) Patches of microspar in a micritic pelagic limestone resulting from aggrading neomorphism. Upper Devonian, West Germany. (B) Coarse microspar mosaic of equant crystals with floating skeletal debris. Pseudobreccia, Lower Carboniferous, northwest England.*

37

compaction

mechanical c. – early stages of diagenesis; reorganizing particles to more fitted/stable fabric; deformation of large clasts, cements, mikritic overgowths; bioklastic wackestone → b. packstone
chemical c. – deeper burial (hundreds of m); matrix dissolution → fitted fabric; stylolites, dissolution seams

a. cubic packing (48% porosity) b. rhombohedral packing (26% porosity) c. point contacts in thin section

d. concavo-convex contacts e. mechanical fracture of grains f. plastic deformation of grains

g. sutured contacts between grains h. late stylolites cutting grains and spar i. dissolution seams
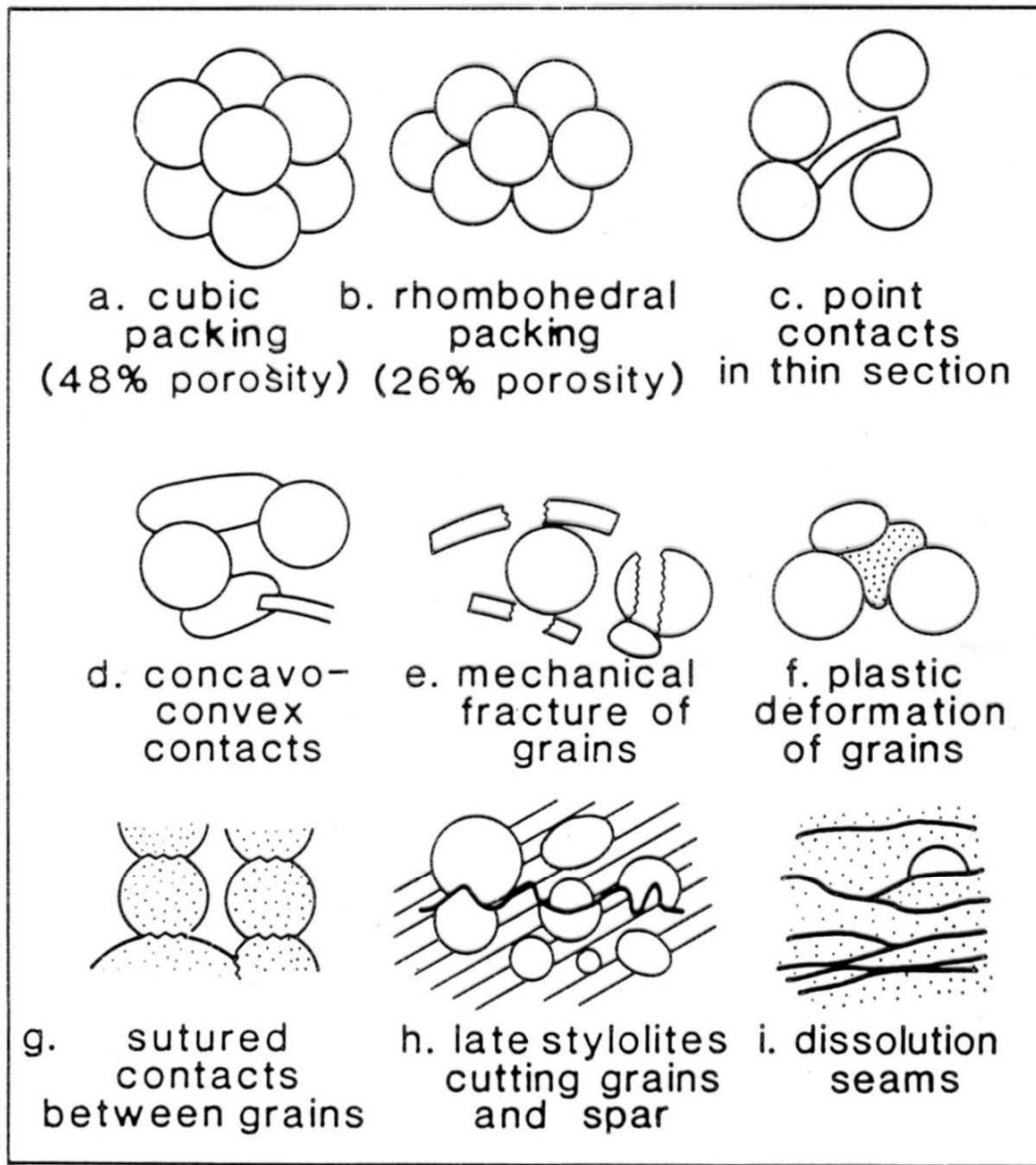
Fig. 7.37 *Grain packing, grain contacts and mechanical and chemical compaction textures in limestones.*

39

Within the figure:
- Bedding plane
- Hard limestone
- Fissile limestone
- uncompacted
- Grainstones
- Wackestones
- compacted
- fitted fabric
- dissolution seams
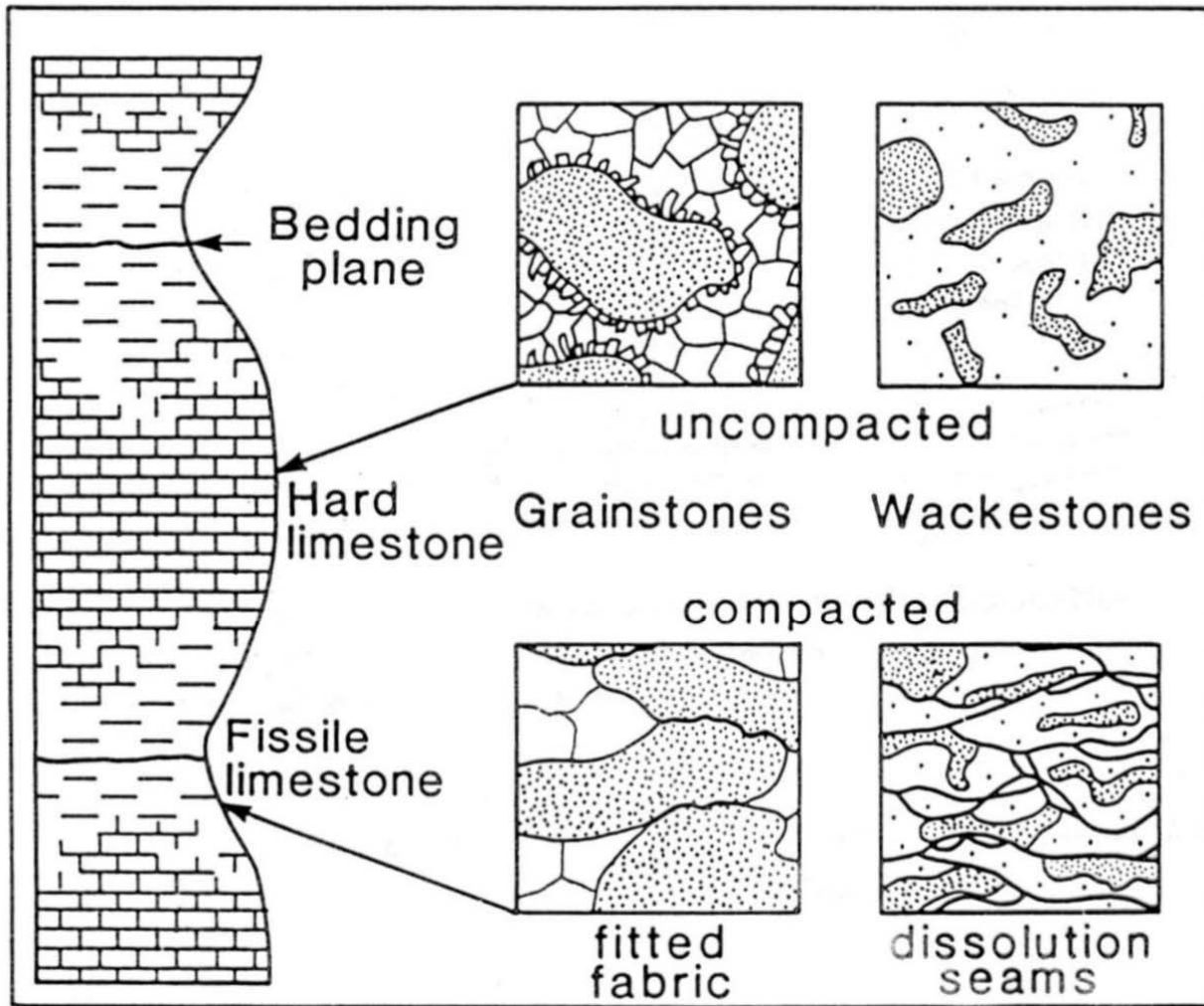
Fig. 7.40 *Uncompacted, hard limestones alternating with fissile limestones showing fitted fabrics and dissolution seams. This is the result of episodic subseafloor cementation. After Bathurst (1987).*

41

500 μm   (a)

500 μm   (d)

42
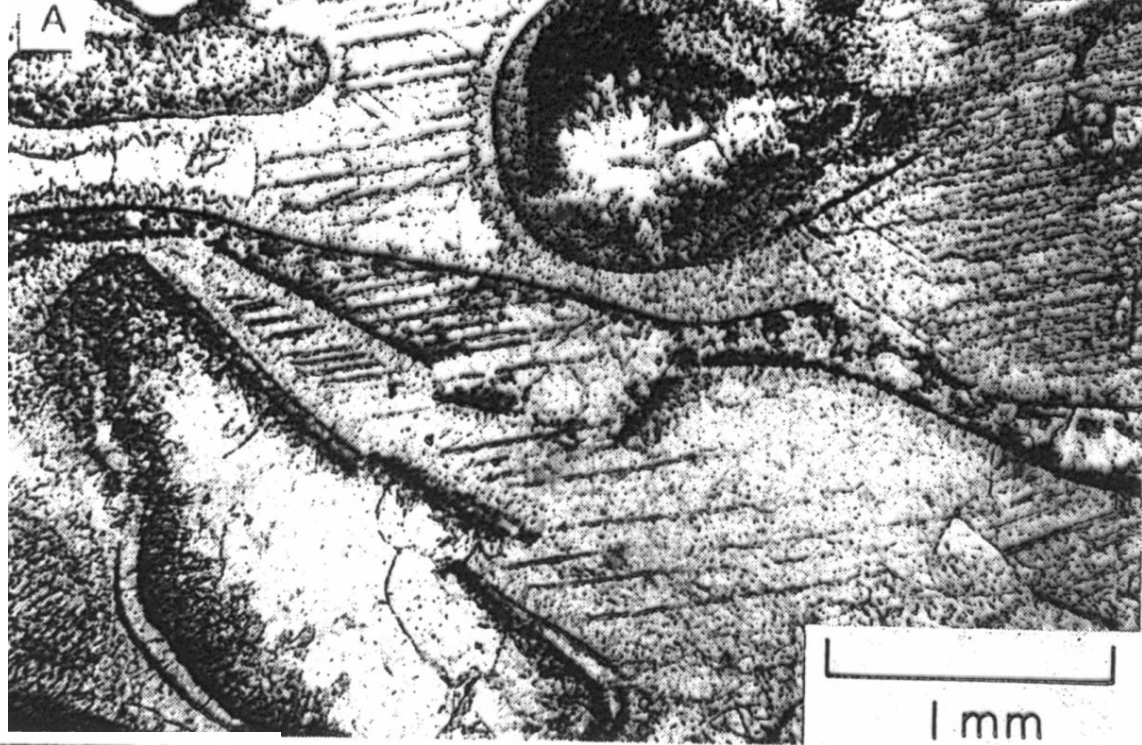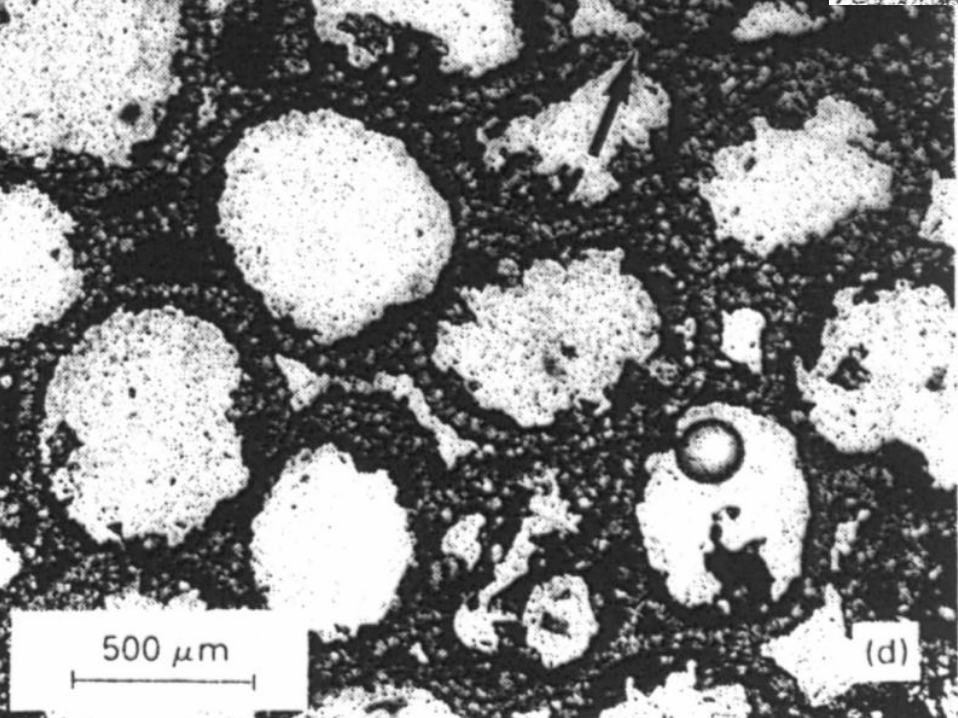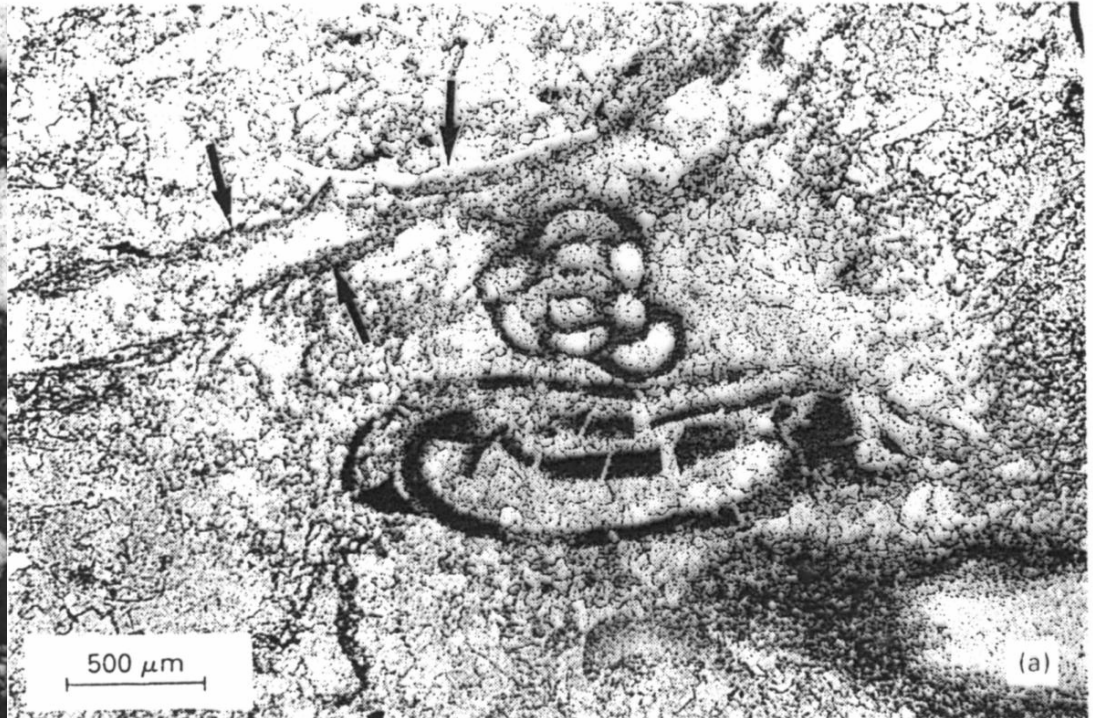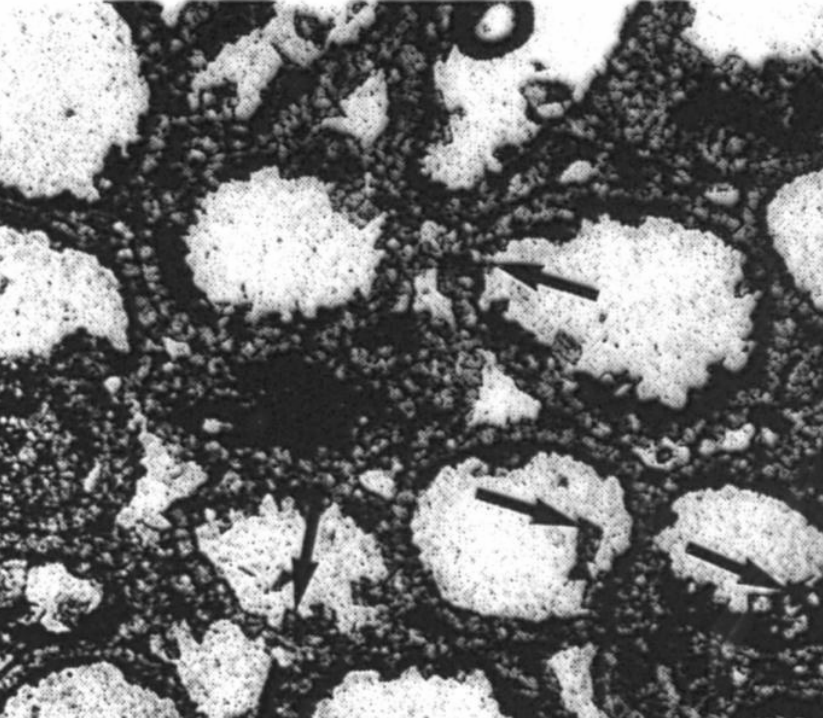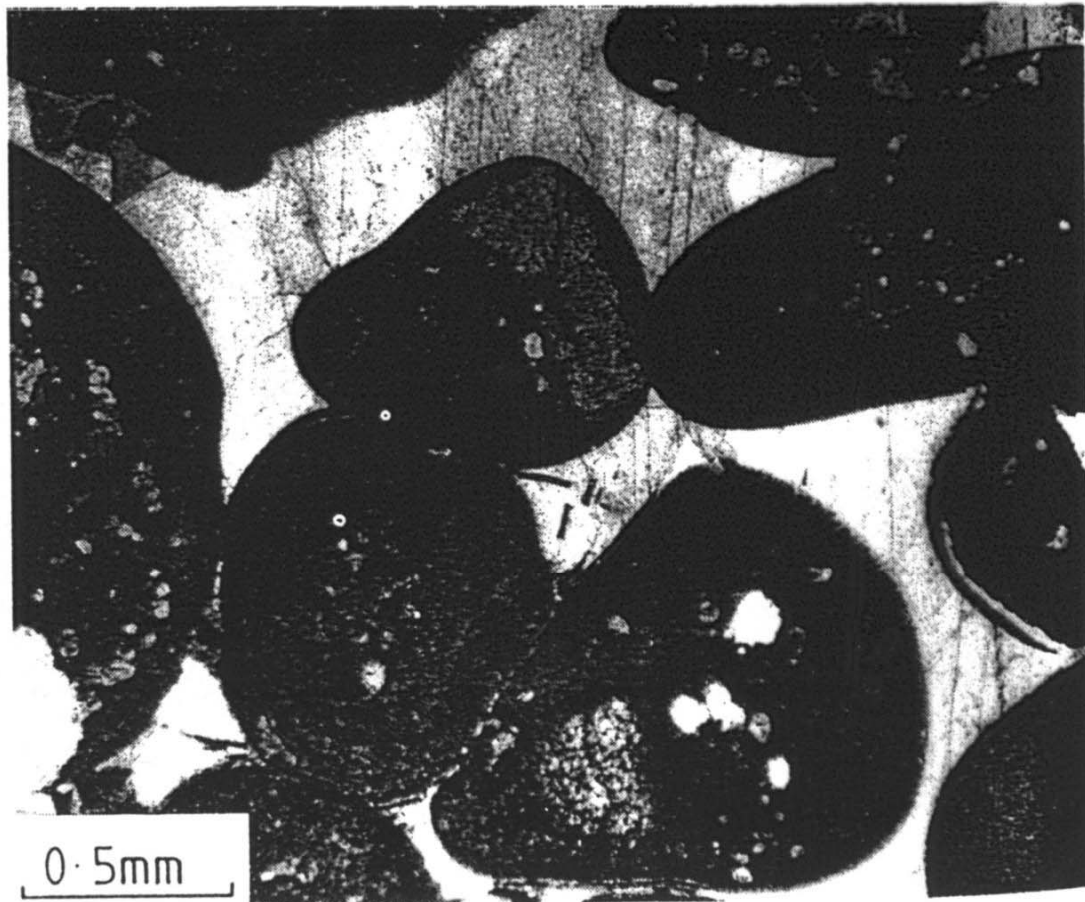
Fig. 7.38 *Concavo-convex and microstylolitic contacts in Smackover Oolite, Jurassic, Louisiana subsurface. Notice also the spalling and fracture of thin oolitic coating off the central grain. Intergranular porosity later filled by very coarse, poikilotopic calcite spar (white).*

43
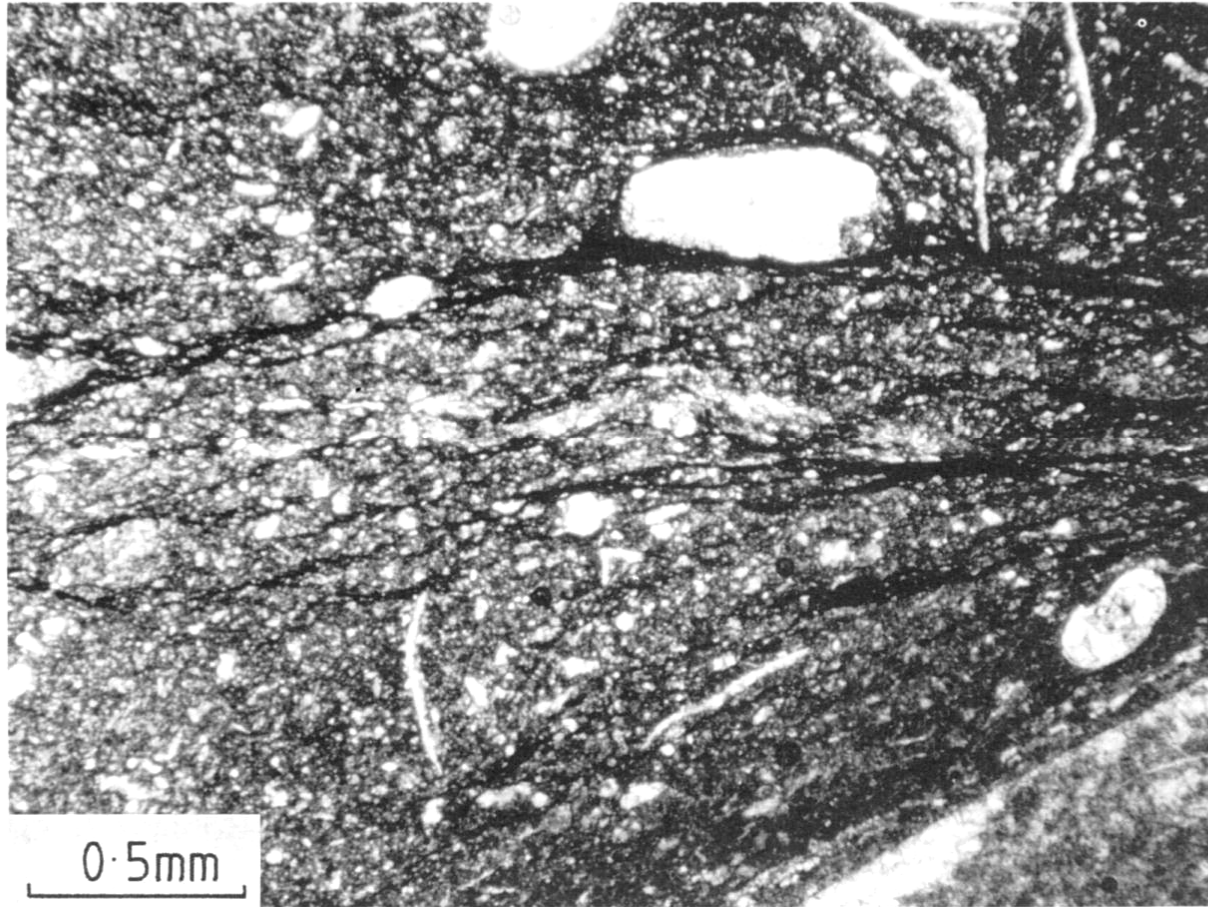
Fig. 7.39 *Dissolution seams with insoluble residue (clay) concentrated along them. Upper Devonian, Griotte (pelagic limestone), southern France.*

0·5mm

44

Meniscus Cement
(Vadose)

A

Microstalactitic Cement
(Vadose)

B

Circumgranular Crust Cement (Phreatic)

PORE SPACE   CEMENT   GRAINS
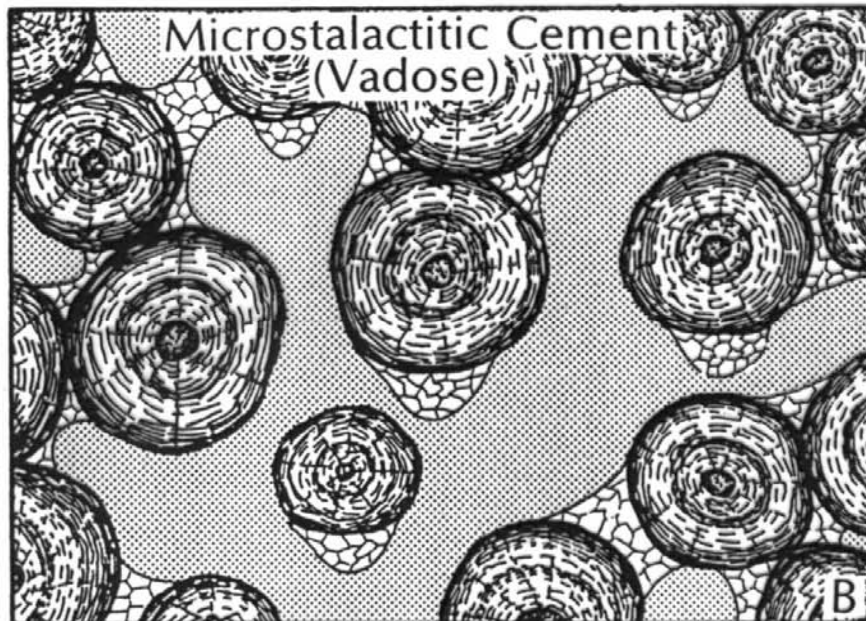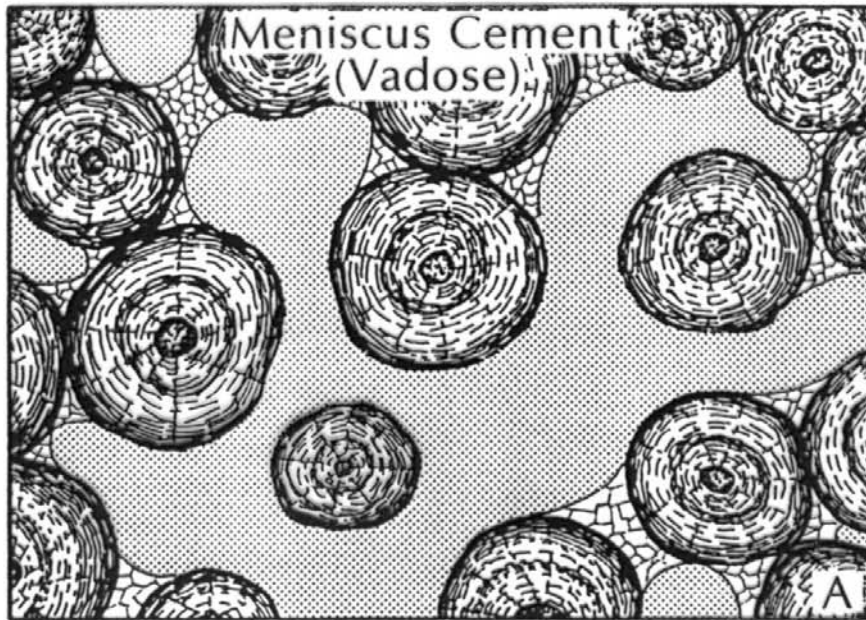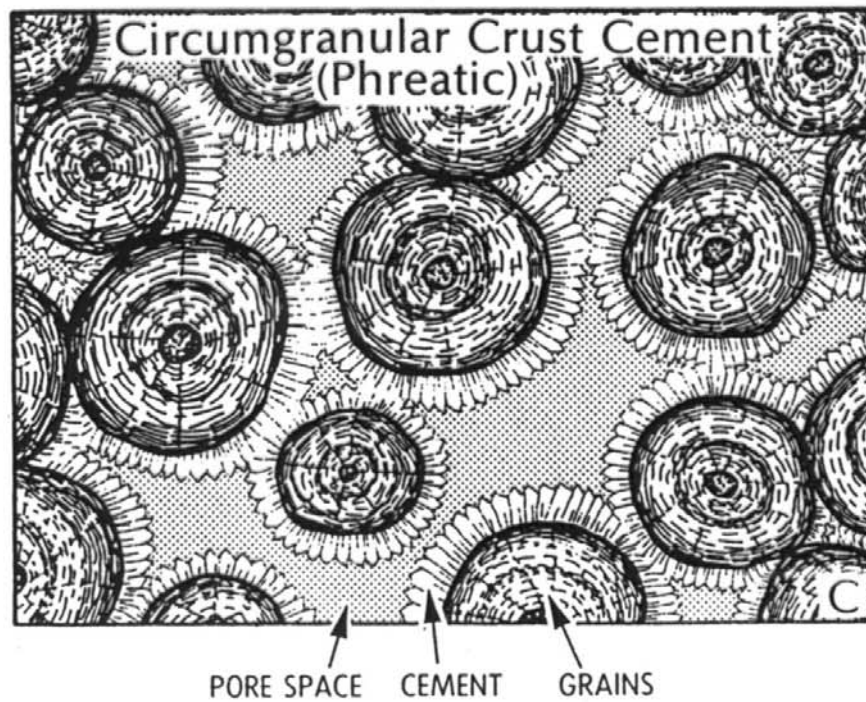
Fig. 3.6. Cement distributional patterns as a function of diagenetic environment. A. In the vadose zone, cements are concentrated at grain contacts and the resulting pores have a distinct rounded appearance due to the meniscus effect . The resulting cement pattern is termed meniscus cement. B. In the vadose zone immediately above the water table there is often an excess of water that accumulates at the base of grains as droplets. These cements are termed microstalactitic cements. C. In the phreatic zone, where pores are saturated with water, cements are precipitated as circumgranular crusts.

47

48
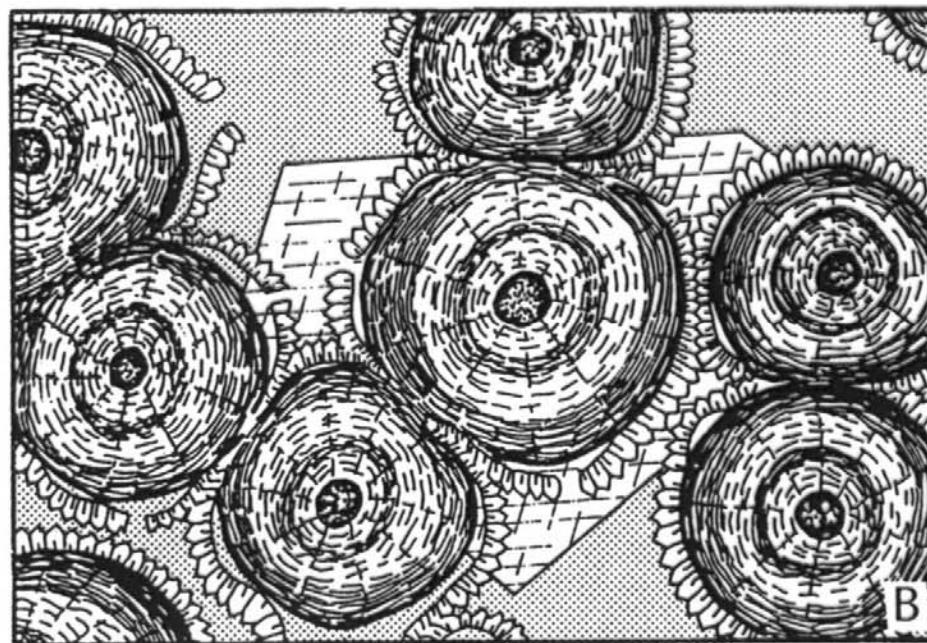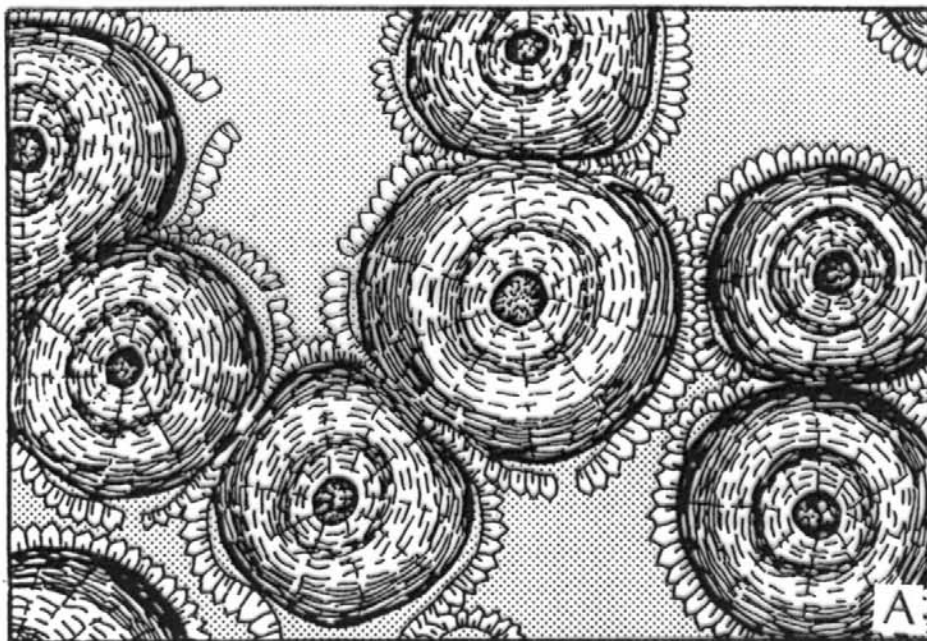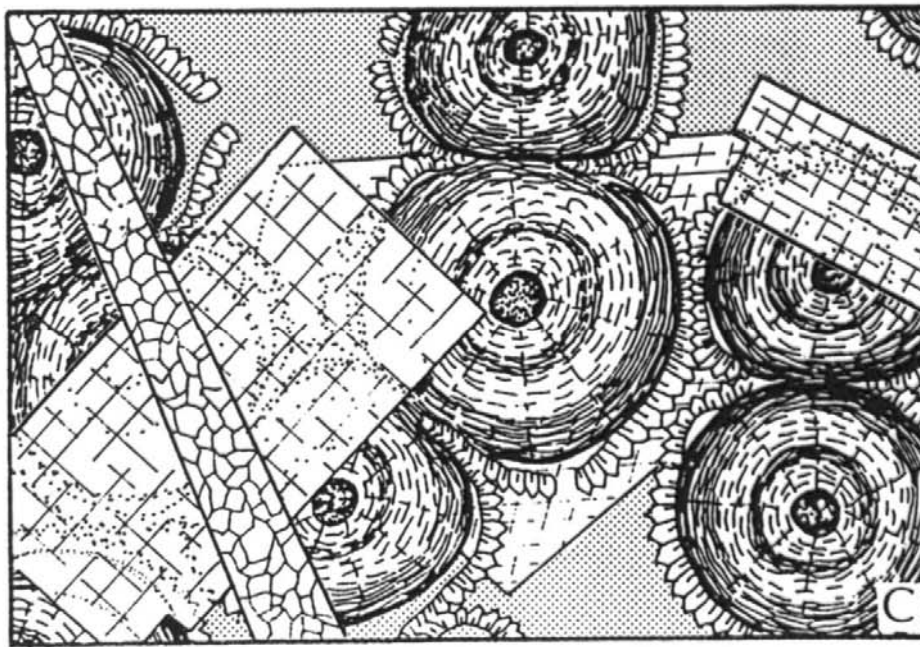
Fig. 3.8. Timing of diagenetic events by petrographic relationships. A. Involvement of isopachous cement in compaction indicates that cement was early. B.Cement that encases compacted grains and spalled isopachous cement is relatively late. C. Cross cutting relationships of features such as fractures and mineral replacements are useful. Calcite filling fracture is latest event, replacement anhydrite came after the late poikilotopic cement, but before the fracture, while the isopachous cement was the earliest diagenetic event.

ORIGINAL SEDIMENT

- a aragonite
- c calcite
- HMC high Mg calcite
- LMC low Mg calcite
- v void
- m micrite envelope
- d drusy calcite spar
- p poikilotopic calcite

MARINE

A B

METEORIC

C D
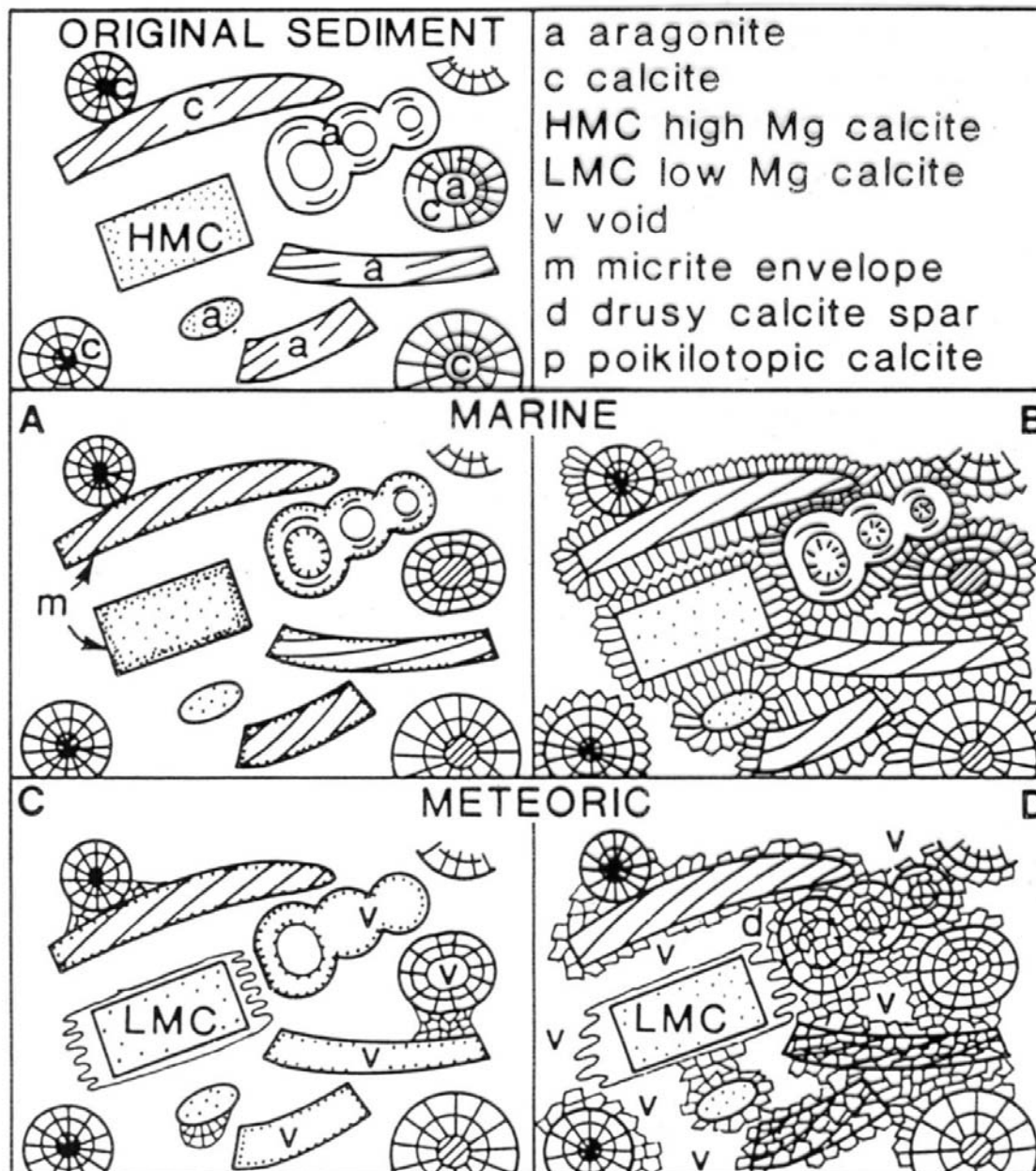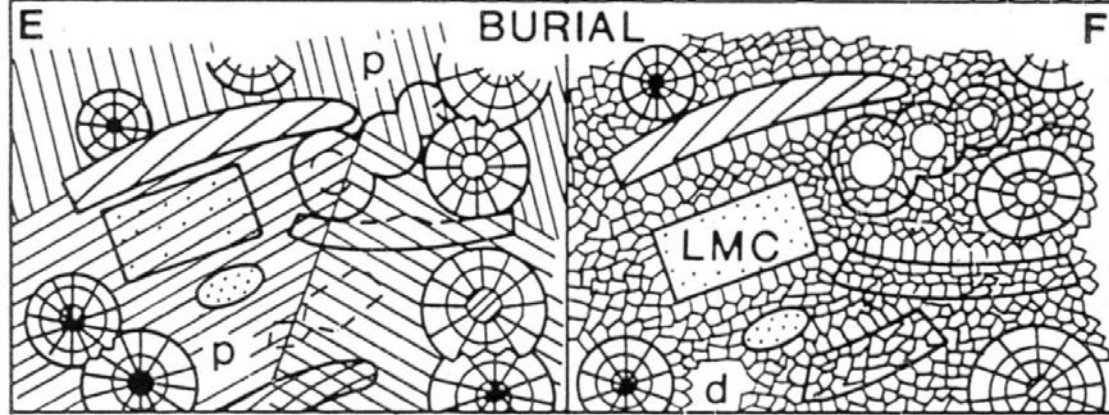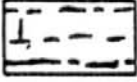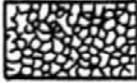
Fig. 7.42 *End-member diagenetic models for marine, meteoric and burial environments. Model A is for marine diagenesis in a poorly agitated or stagnant location where grain micritization is dominant. Model B is for marine diagenesis in a high-energy location where there is much cementation through seawater pumping. Model C is for meteoric diagenesis in an active zone of much dissolution, whereas model D applies to a zone of more $CaCO_3$-saturated meteoric water where cementation and grain replacement are features. Model E applies to the burial diagenesis of sediments which have little near-surface cement and so compaction is extensive, whereas model F is appropriate for sediments which have been well lithified before any significant compaction. See text for further discussion.*
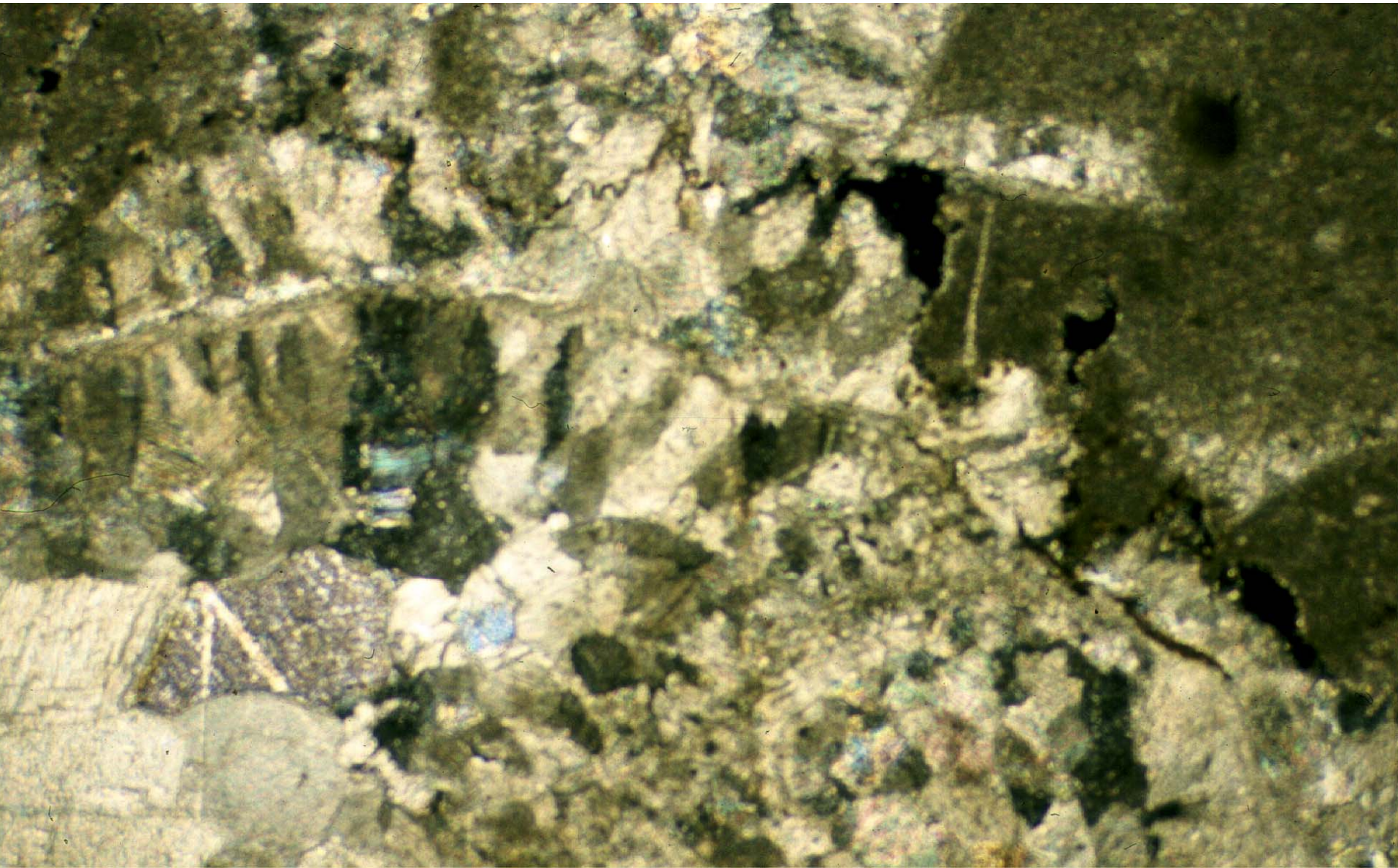
BASIC POROSITY TYPES

FABRIC SELECTIVE

PRIMARY

	INTERPARTICLE	BP
	INTRAPARTICLE	WP
	FENESTRAL	FE
	SHELTER	SH
	GROWTH-FRAMEWORK	GF

SECONDARY

	INTERCRYSTAL	BC
	MOLDIC	MO

NOT FABRIC SELECTIVE

	FRACTURE	FR
	CHANNEL*	CH
	VUG*	VUG
	CAVERN*	CV

*Cavern applies to man-sized or larger pores of channel or vug shapes.

FABRIC SELECTIVE OR NOT
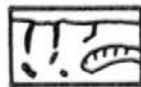
BRECCIA BR   BORING BO   BURROW BU   SHRINKAGE SK

53

Fig. 2.1. Classification of carbonate porosity. Classification consists of basic porosity types, such as moldic. Each type is represented by an abbreviation (MO). Modifying terms include genetic modifiers, size modifiers and abundance modifiers. Each modifier also has an abbreviation. Reprinted by permission of the American Association of Petroleum Geologists.
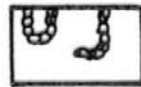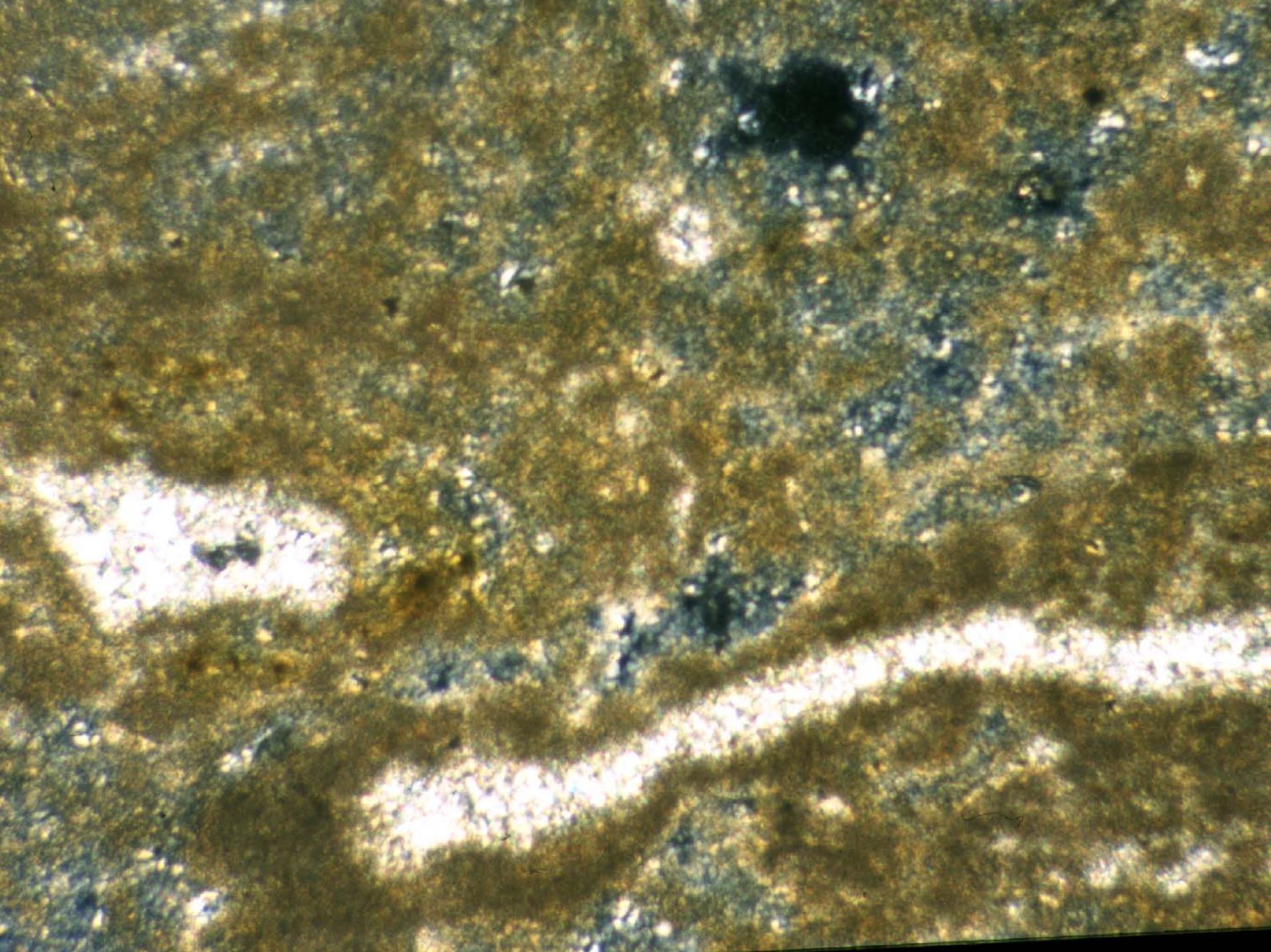
Dolomitization

limestone → dolomitization → dolostone → dedolomitization → limestone
dolomite, protodolomite, Fe-dolomite
dolomitization   - very early - penekontemporaneous dolomite
                    - late – after cementation, burial (epigenetic d.)
strukturaly selective d., eg. focused on matrix or bioclasts
dolomitization HMC – preserving original structures; dol. A - recrystalization,
destruction of original structures
barroque/saddle dolomite – large crystals, barroque/saddle shaped crystals
and shistosity, undulose extinction → burial (HT, hydrocarbons, sulphide
mineralization)
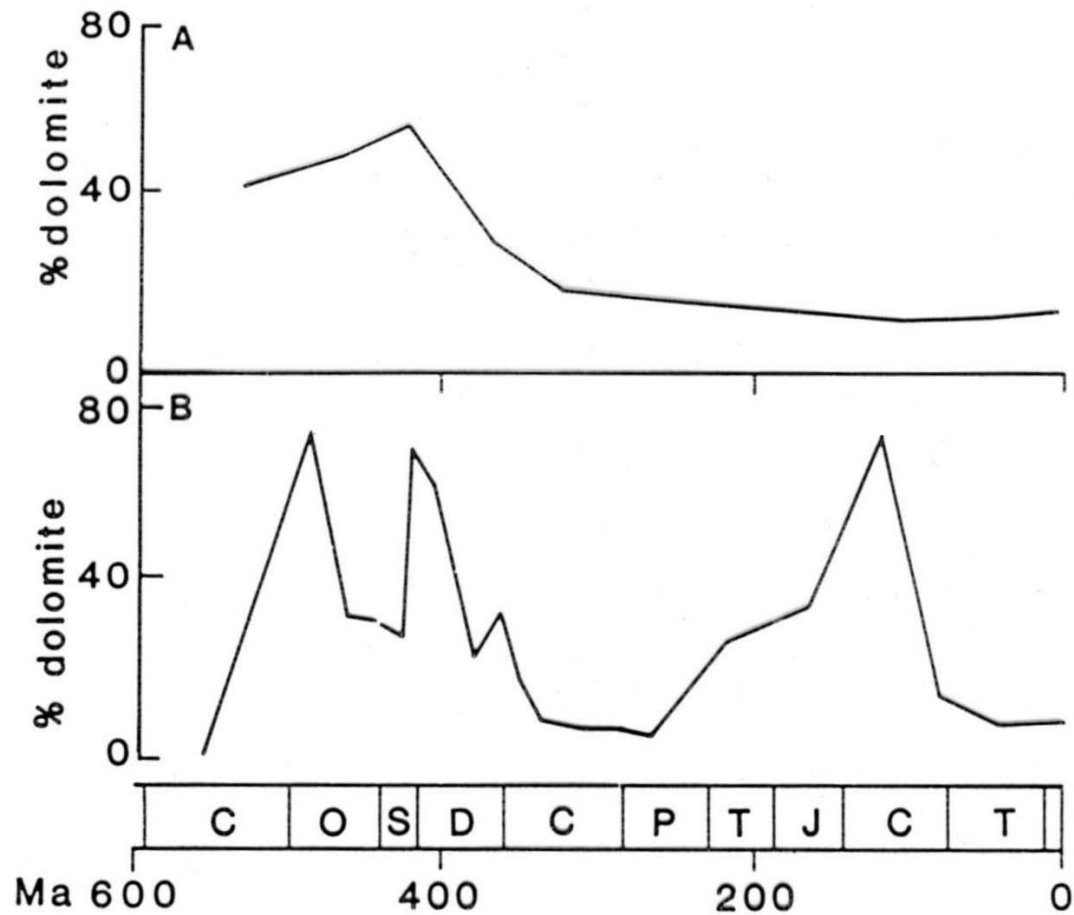
Fig. 4.65 Geological record of dolomites through the Phanerozoic. A, Increasing dolomite occurrence back in time as suggested by many earlier workers. B, A recent compilation showing a more variable trend, which broadly corresponds with the global sea-level curve (greater abundance of dolomite coinciding with higher sea-level stand). The global sea-level curve is given in Fig. 4.4. After Given & Wilkinson (1987).

57
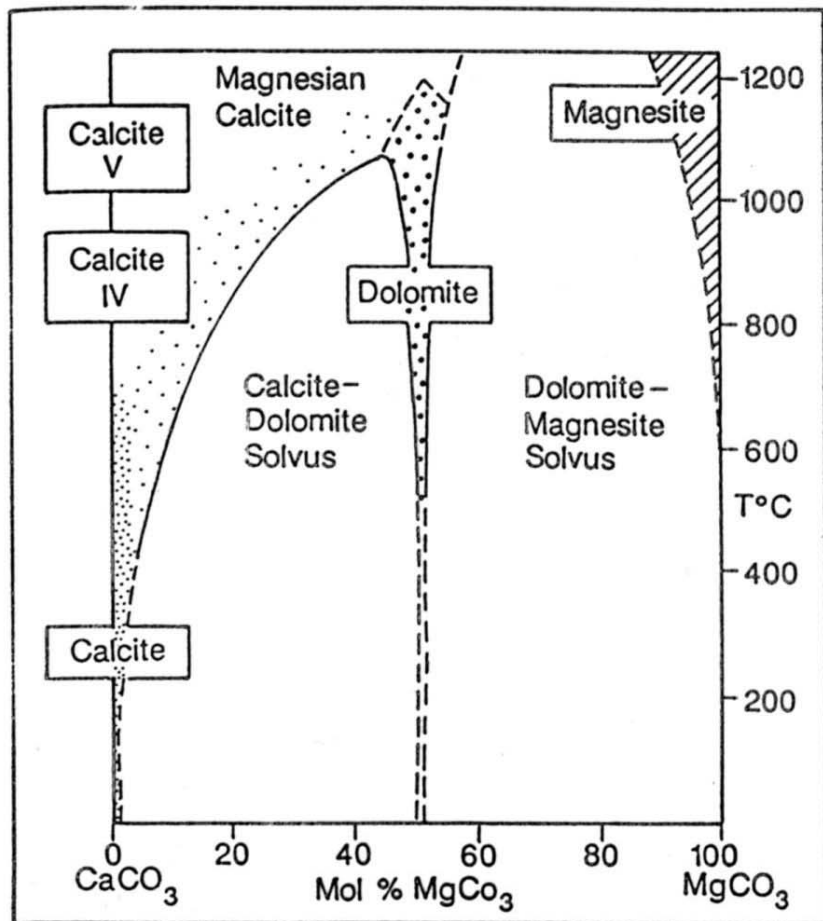
Fig. 6.7 *Phase relations of the CaCO₃–MgCO₃ system. High temperature margin to dolomite field conjectural. After Goldsmith & Heard (1961a).*
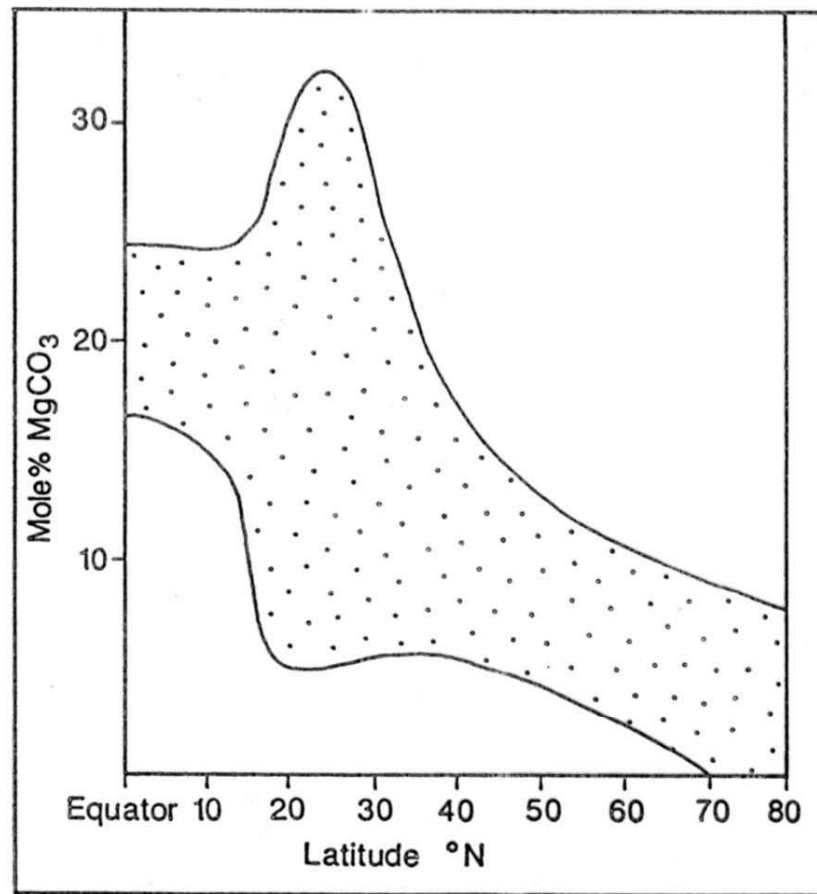
Fig. 6.8 *Range of mole % MgCO₃ in skeletal magnesian calcites plotted against latitude. Data (from Chave, 1954) include red algae and a variety of invertebrate phyla.*

58
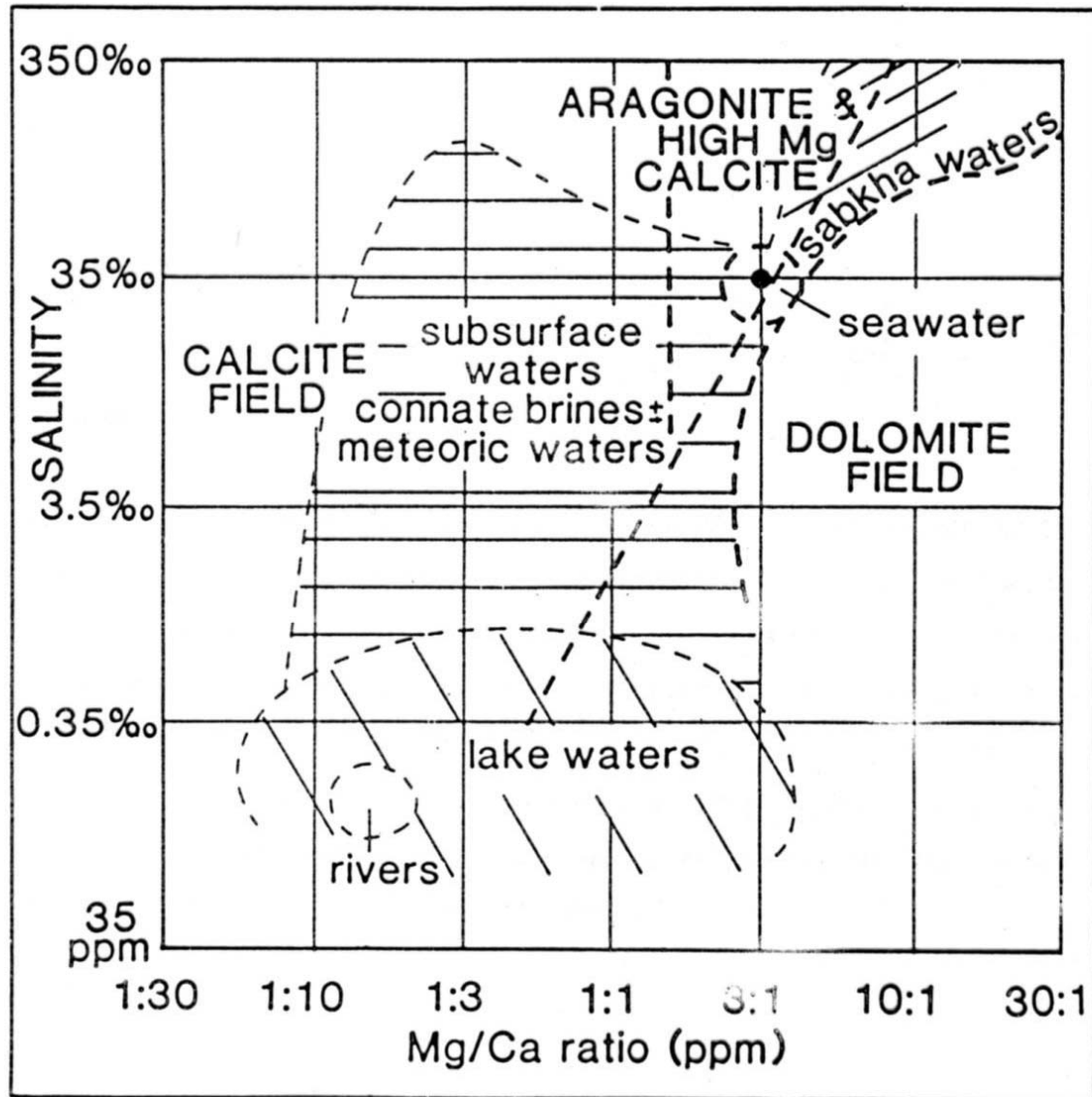
Fig. 8.2 *The precipitational fields of calcite, dolomite and aragonite plus high-Mg calcite in terms of salinity and Mg/Ca ratio of natural waters. After Folk & Land (1975).*

59
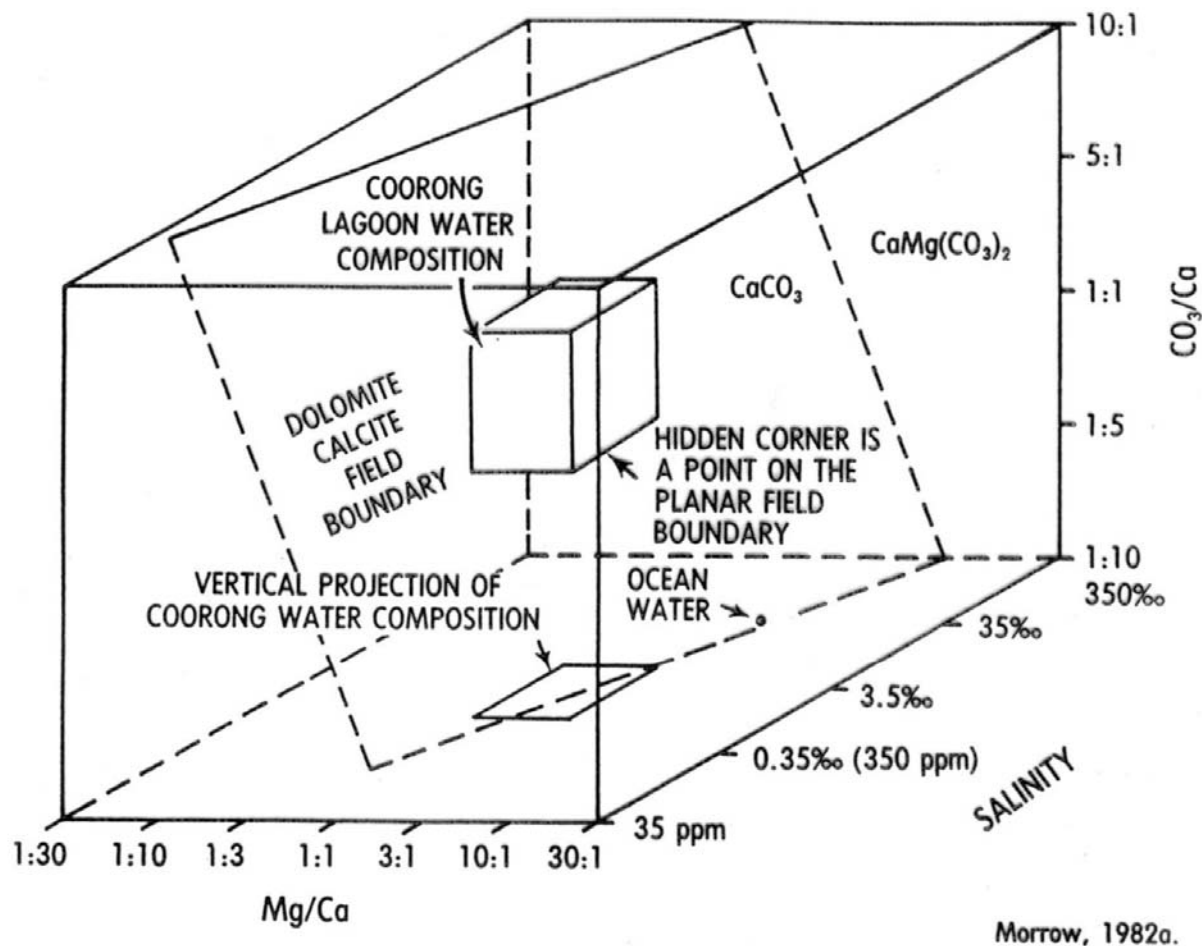
Fig. 6.1. Block diagram showing the effect of variation in the three parameters, the Mg/Ca solution ratio, the salinity, and the CO_3 / Ca ratio. The plane represents the kinetic boundary between dolomite and calcite or aragonite and it includes the hidden corner of the Coorong Lagoon waters as a point on the plane. The basal plane is after Folk and Land (1975). Note that the vertical projection of Coorong Lagoon waters falls largely on the calcite-aragonite side of the stability boundary on the basal plane. A decrease in salinity, an increase in the Mg/Ca ratio or an increase in the CO_3 / Ca ratio favours the precipitation of dolomite. Reprinted with permission of the Geological Association of Canada.

60
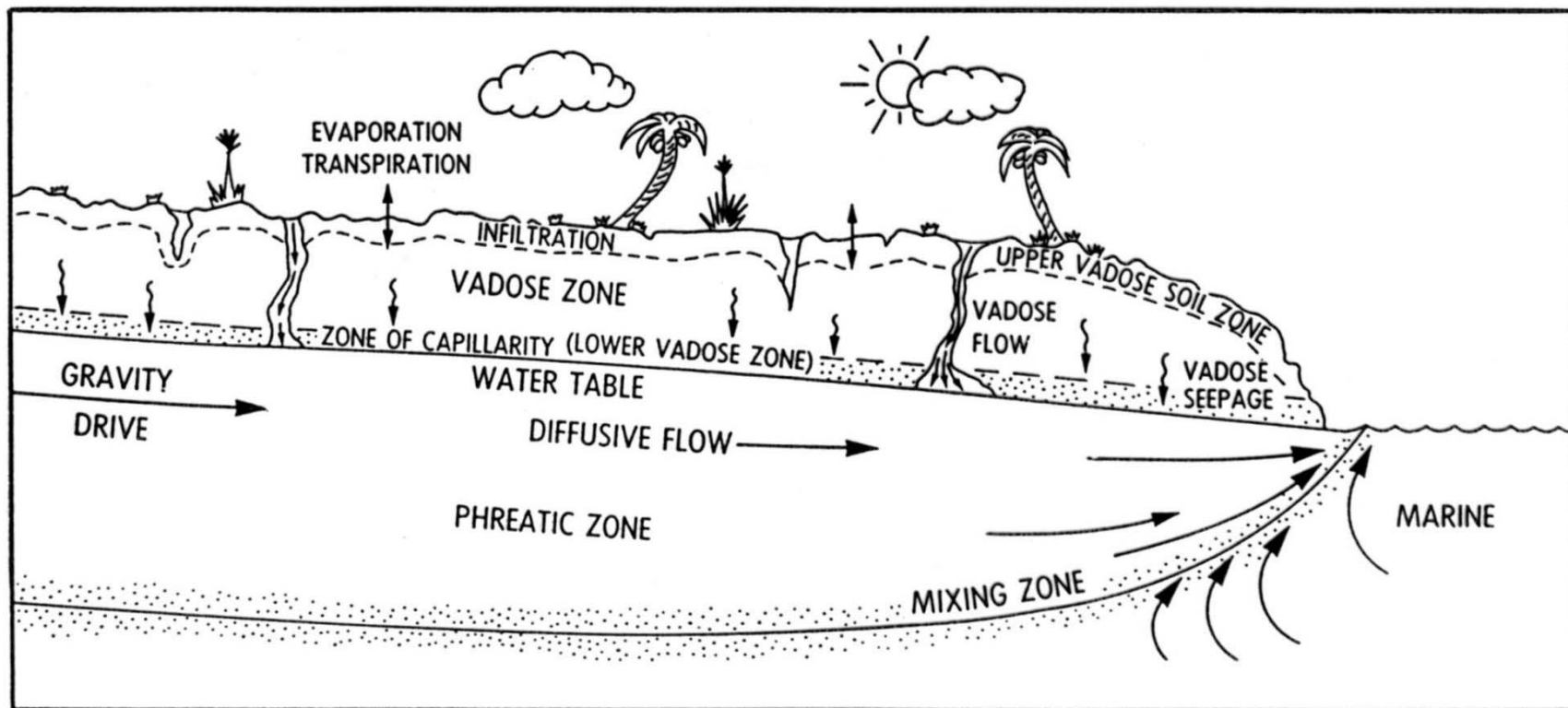
Fig. 6.8. Conceptual model of the major diagenetic environments, and hydrologic conditions present in the meteoric realm.

A Nonplanar: closely packed anhedral crystals with mostly curved, lobate, serrated, or otherwise irregular intercrystalline boundaries.

Xenotopic mosaic

B Planar-e (euhedral): most dolomite crystals are euhedral rhombs.

Idiotopic mosaic.

C Planar-s (subhedral): most dolomite crystals are subhedral to anhedral with straight, compromise boundaries and many crystal-face junctions.

Hypidiotopic mosaic.

Fig. 8.6 *Three common dolomite textures. (A) Non-planar crystals in a xenotopic mosaic. (B) Planar-e crystals (e for euhedral) in an idiotopic mosaic. (C) Planar-s crystals (s for subhedral) in a hypidiotopic mosaic. After Sibley & Gregg (1987).*

62

A   B

C   D

63
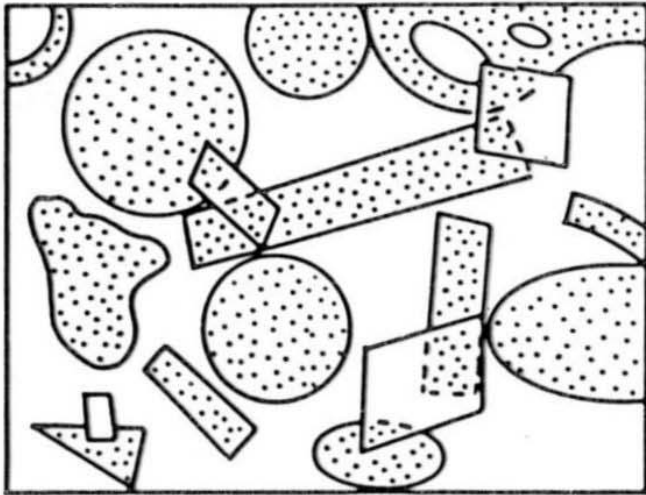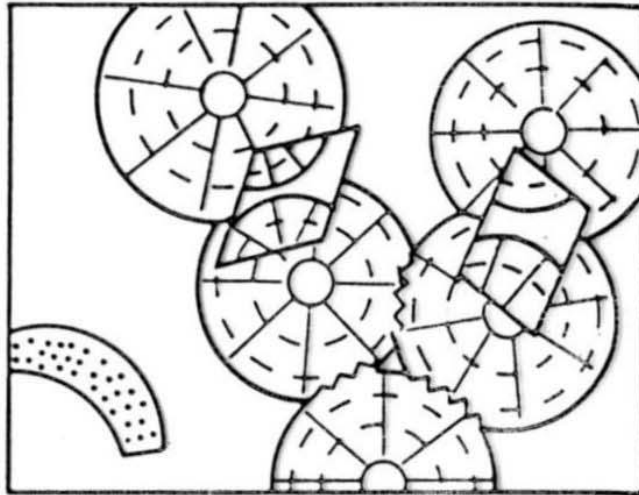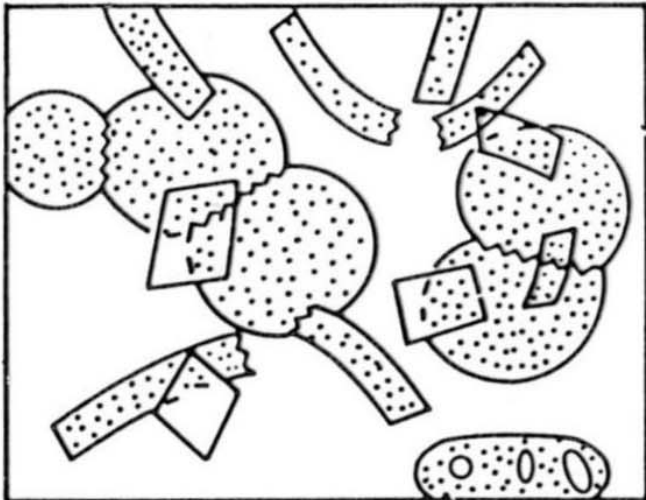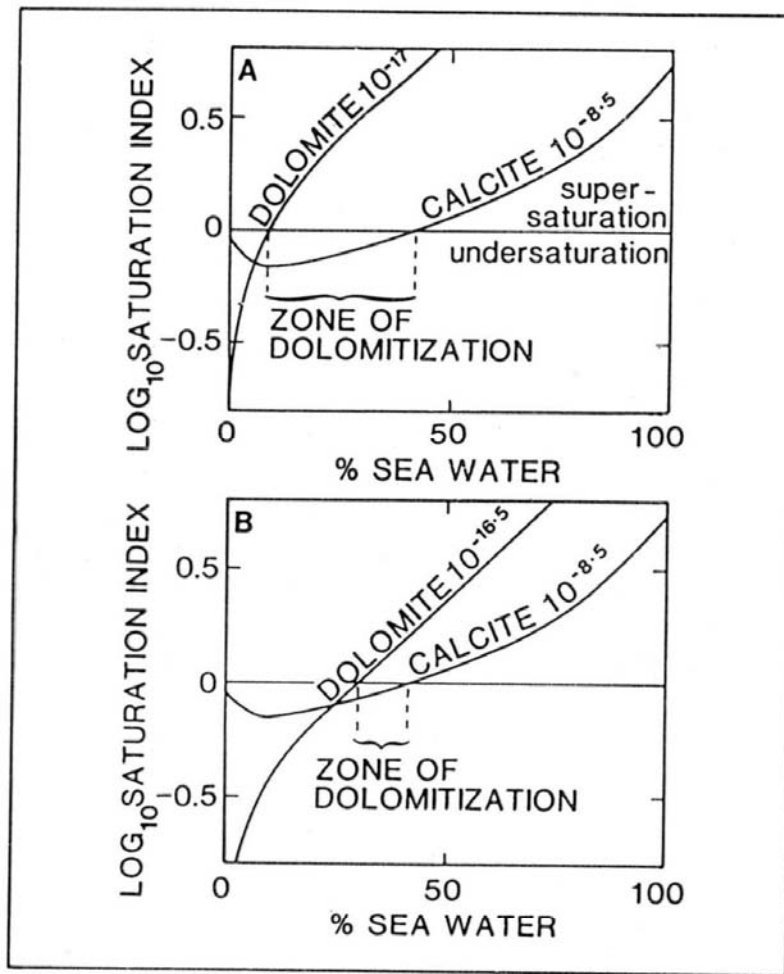
Fig. 8.3 *Mixing-zone dolomitization. Solubility curves for dolomite and calcite in meteoric water with increasing content of seawater. Dolomitization is considered to take place in waters supersaturated with respect to dolomite but undersaturated with respect to calcite. (A) For dolomite with solubility product* $K = 10^{-17}$, *as used by Badiozamani (1973). (B) For disordered dolomite with* $K = 10^{-16.5}$, *as used by Hardie (1987). Note that in (B) the zone of dolomitization is much reduced. After Hardie (1987).*
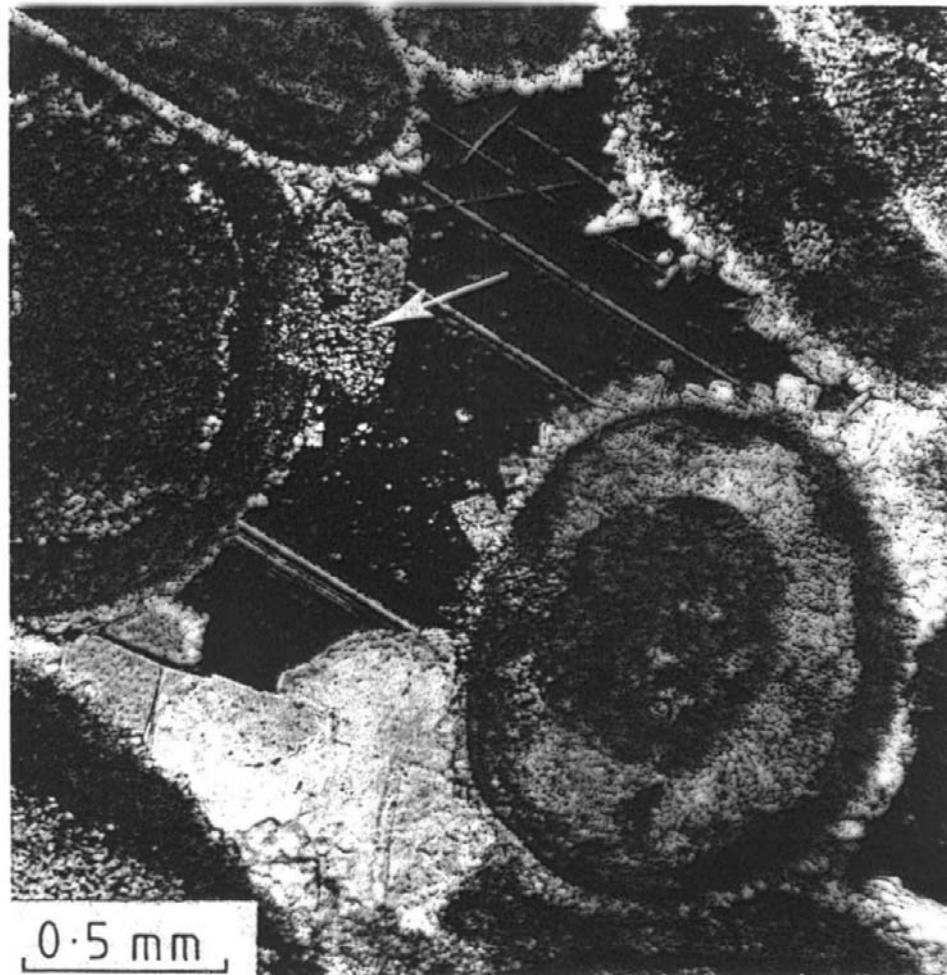
Fig. 4.54 Calcite cement at grain contacts and irregularly around grains. This geometry indicates precipitation in the near-surface, meteoric vadose environment. Later precipitation of large poikilotopic calcite (black, in extinction) took place during burial. Isolated dolomite rhombs (arrowed) were precipitated after the meteoric and before the burial cements. Crossed polars. Lower Carboniferous oolitic grainstone. Glamorgan, Wales.

65

Fig. 8.13 *Pre-compaction dolomite rhomb. Notice that the edge of the ooid is displaced within the rhomb. Gully Oolite, Lower Carboniferous, south Wales.*

250 μm

(a)

67

350 μm

(b)

Q

D

Q

D

D

500 μm

(c)

68
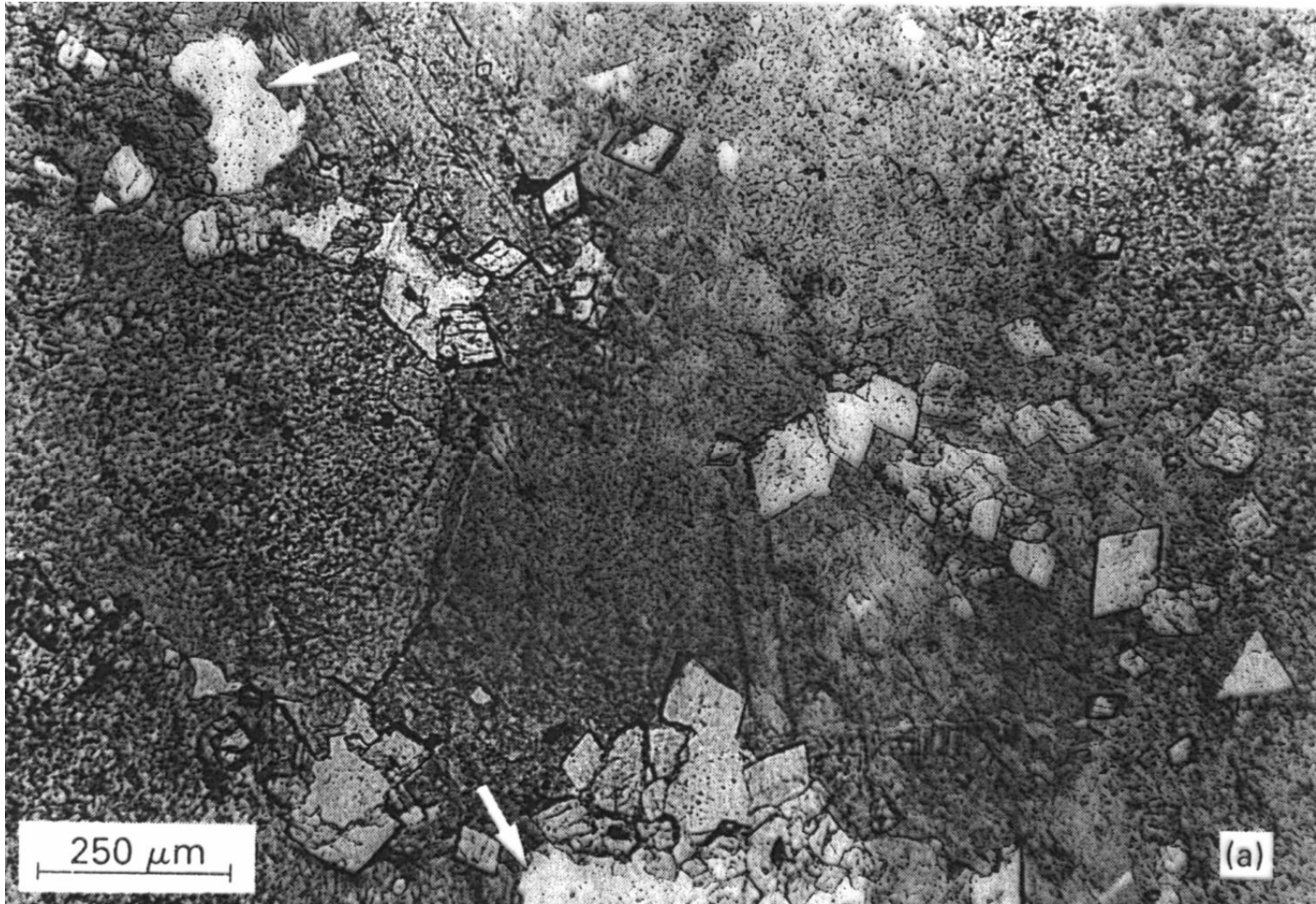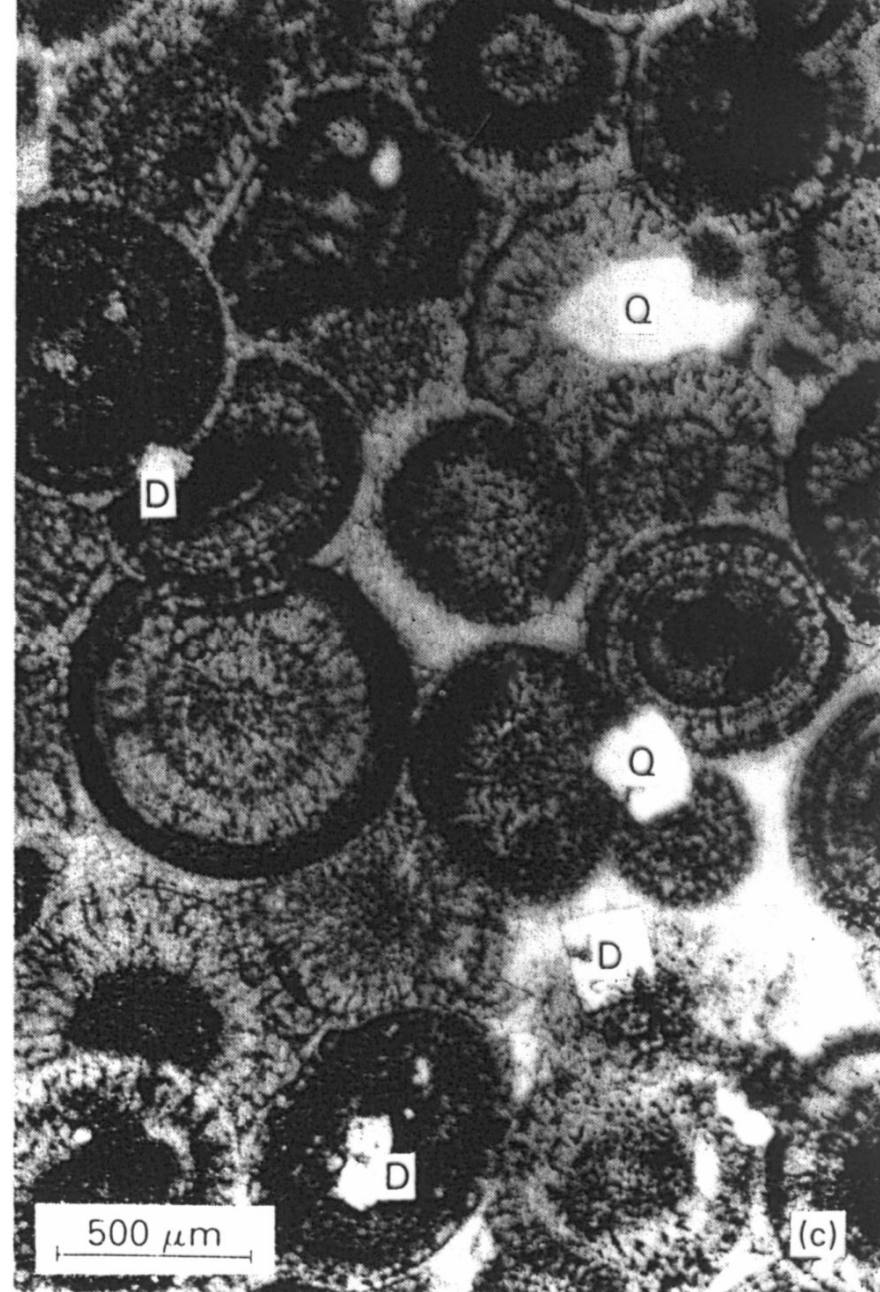
dolomitization models

dolomite paradox: marine water oversaturated with dolomite, but its direct precipitation is inhibited by series of kinetic factors, therefore direct precipitation of A and HMC is more favourable in nature

• **from pore fluids**, Bahamas, Florida, Arab. Gulf, 1-4 mm rhombs, surface crusts; increase of Mg/Ca in pre fluids due to precipitation of A and gypsum-anhydrite, evaporation

• Lake Victoria, **direct precipitation from lake waters**, high Mg/Ca ratio due to weathering of basalts

• **Coorong**, s. Australia, direct precipitation of d., mixing of meteoric Mg rich waters with marine waters in shallow nearshore lakes, penecontemporaneous dolomite

• **lagoons**, periodicaly hypersaline, evaporation

• **intertidal-supratidal**, evaporitic dolomitization, preservation of sed.structures (teepee, birdseyes)

• **shallow subtidal and reef**, infiltration and percolation of lagoonal waters with high Mg/Ca ratio (due to evaporation) back to barrier/reef

• **zone of mixing of meteoric and marine waters**, ratio 2:1 → decrease of calcite saturation, but dolomite saturation; lower salinity, Mg/Ca ratio constant

• **burial**, migration of Mg rich fluids (generated by compaction of pelagic muds) to limestones; sources of Mg: clay minerals, pore fluids, organic matter, also HMC to LMC recrystallization

• subrecent dolomitization in atols and carb. platforms (1200-1400 m depth), cold marine waters percolating the limestones → low temperature, low calcite saturation, but saturated with dolomite; water circulation due to tidal pumping and marine currents → high geothermal gradient …. **Kohoutova konvekce**

• in **anoxic** environments, bacterial reduction of sulphates - kinetic inhibitor of dolomitization, source of Mg partly in organic matter
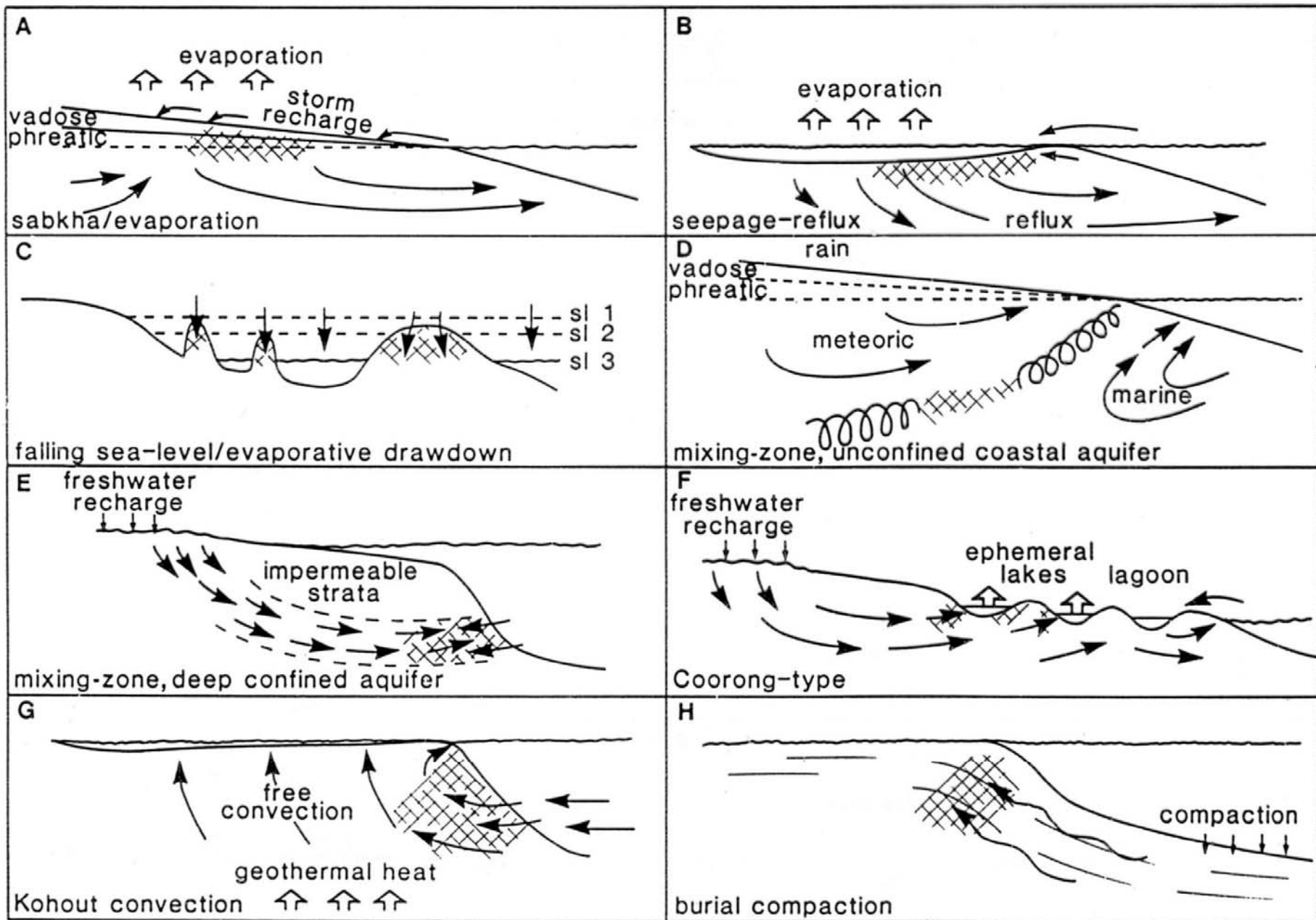
Fig. 8.1 *Models of dolomitization, illustrating the variety of mechanisms for moving dolomitizing fluids through the sediments. In part after Land (1985). Also see Fig. 8.31 for seawater dolomitization models.*
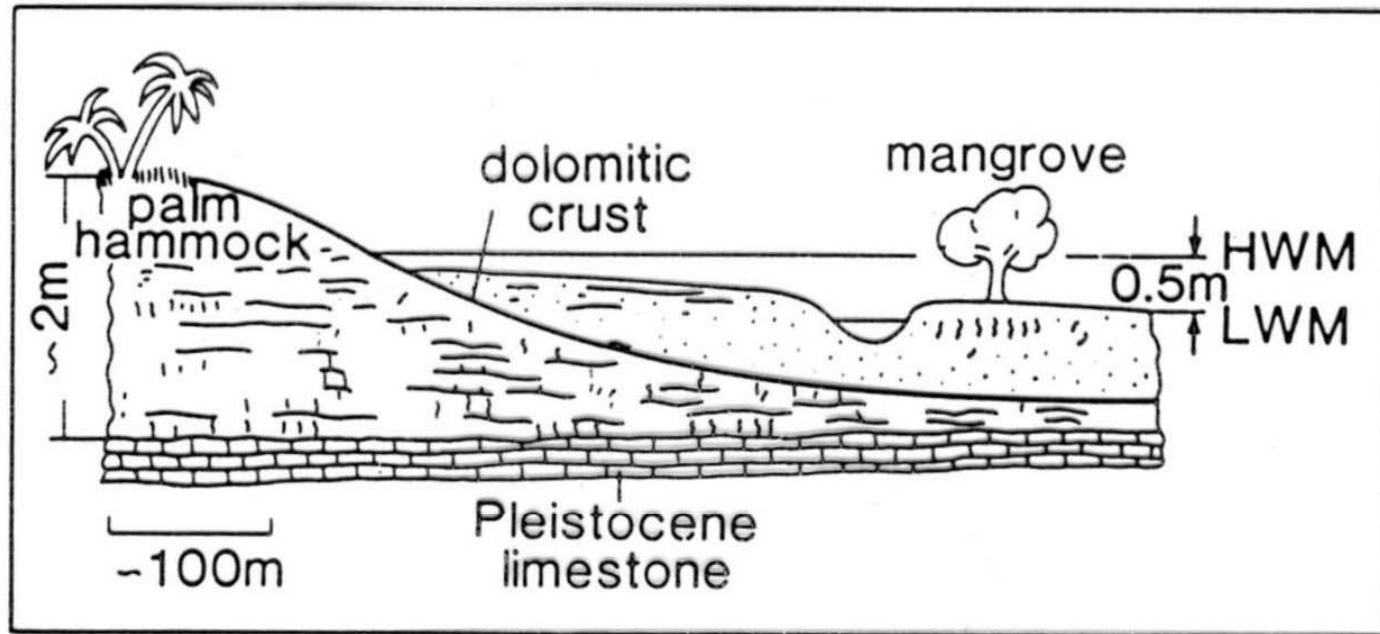
Fig. 8.21 *Schematic cross-section of a palm hammock on the tidal flats of Andros Island, Bahamas, showing dolomitic crust, now forming in the upper intertidal/low supratidal zone, with earlier crust occurring beneath the low intertidal— shallow subtidal sediments. After Shinn et al. (1965).*

Fig. 8.22 *Dolomites of the Coorong region, South Australia. (A) The coastal plain of Quaternary barriers and interdu[ne] [f]lats where ephemeral lakes occur and dolomite is being precipitated. (B) Stratigraphic log of a core from an epheme[ral] [C]oorong lake. After Von der Borch (1976) and Von der Borch & Lock (1979).*

a

PALM HAMMOCK

SAMPLE A 217.1
CONTEMPORARY C¹⁴ AGE

DOLOMITIC CRUST

SAMPLE A 217.2
2200 YEARS OLD C¹⁴ AGE

NORMAL HIGH TIDE

NORMAL LOW TIDE

7'-8'

18"

A

B

PLEISTOCENE ROCK

Vertical scale greatly exaggerated.
Horizontal distance about 1000 yds.

A — Dark gray pelletal mud containing roots, land snails, desiccation laminations, few foraminifera and marine gastropods.

B — Light tan pelletal sediment containing numerous marine gastropods, foraminifera, and red mangrove roots.

b

300'

10% DOLOMITE

25-50% DOLOMITE CRUST

6"

NORMAL HIGH TIDE

CHANNEL

BURROWED INTERTIDAL SEDIMENT

NORMAL LOW TIDE

Shinn and others, 1965, 1969

Fig. 5.7. a. Stratigraphic cross section across the flank of a palm hammock on Andros Island, the Bahamas. Note variation in age along the dolomitic crust. b. Schematic cross section across a tidal channel natural levee on the Andros Island tidal flats. Note that dolomite % is greater in the thin flanks of the levee than in the thicker channel margin part of the levee due to a dilution effect caused by the greater rate of sedimentation along the channel margins. Used with permission of SEPM.

73
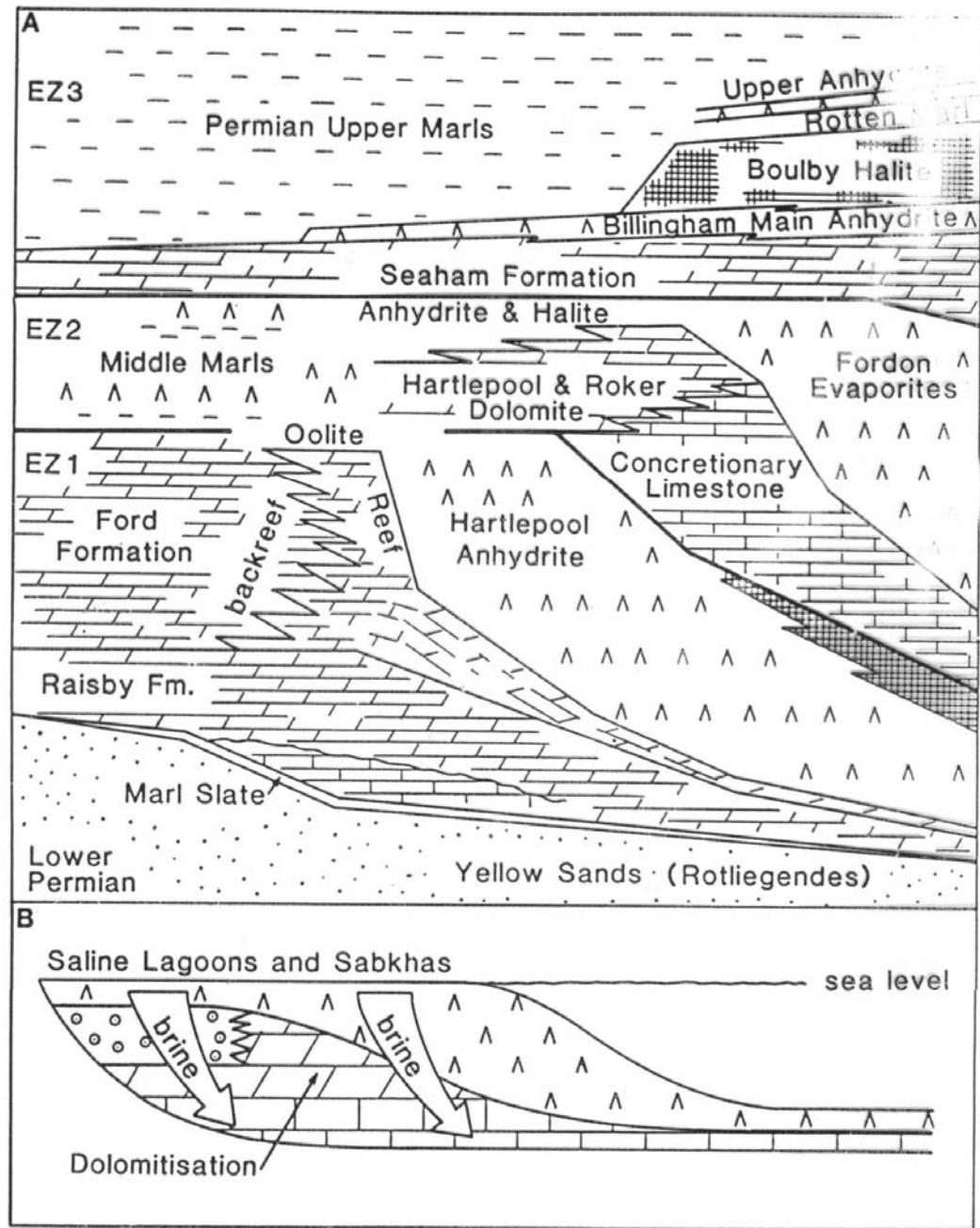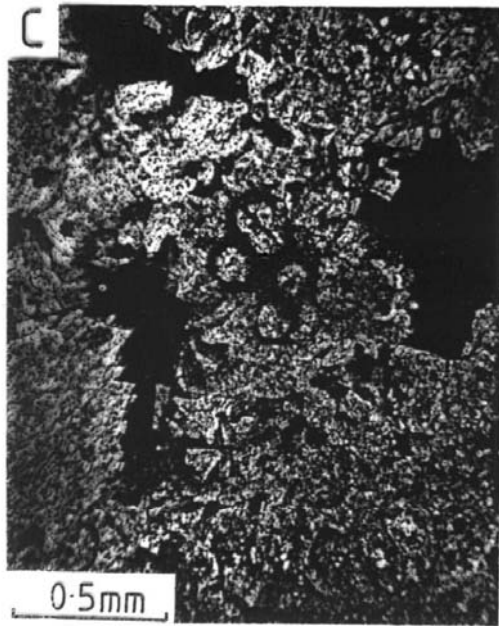
Fig. 8.23 Dolomites of the Upper Permian (Zechstein) of northeast England. (A) Stratigraphy–lithology showing three carbonate–evaporite cycles. The lower part of the Raisby Formation is still limestone; the Concretionary Limestone is mostly a dolomite. (B) Seepage–reflux model for Zechstein dolomitization. After Smith (1981) and Clark (1980). (C) Coarse dolomite, bryozoan in centre and vuggy porosity. Crossed polars.

74
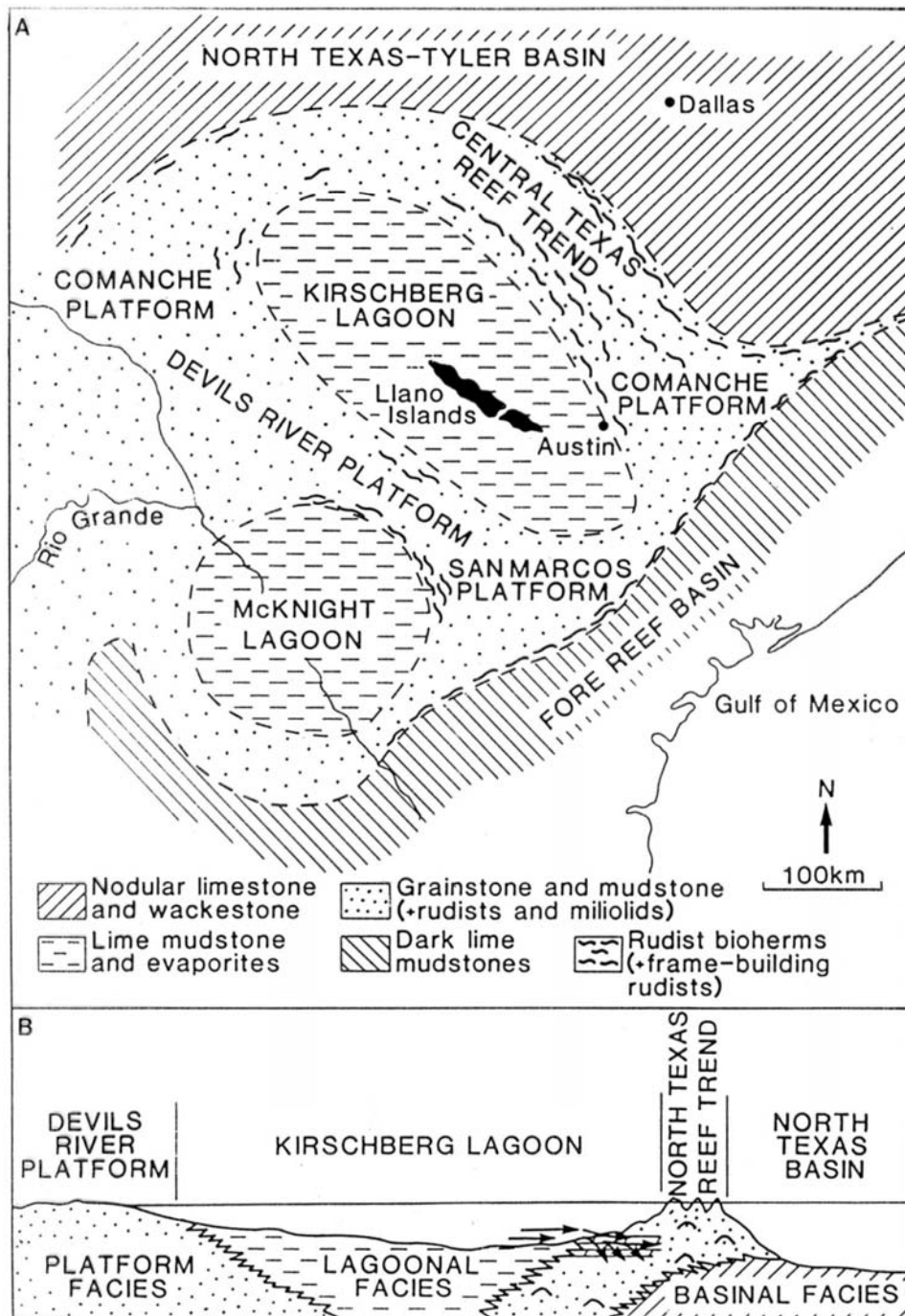
Fig. 8.24 Dolomites of the Lower Cretaceous (Edwards Formation) of Texas. (A) Palaeogeographic map showing shelf-margin reef trends and two onshelf lagoons. (B) Schematic north–south cross-section and seepage–reflux model for dolomitization of the shelf-margin grainstones. After Fisher & Rodda (1969).

75
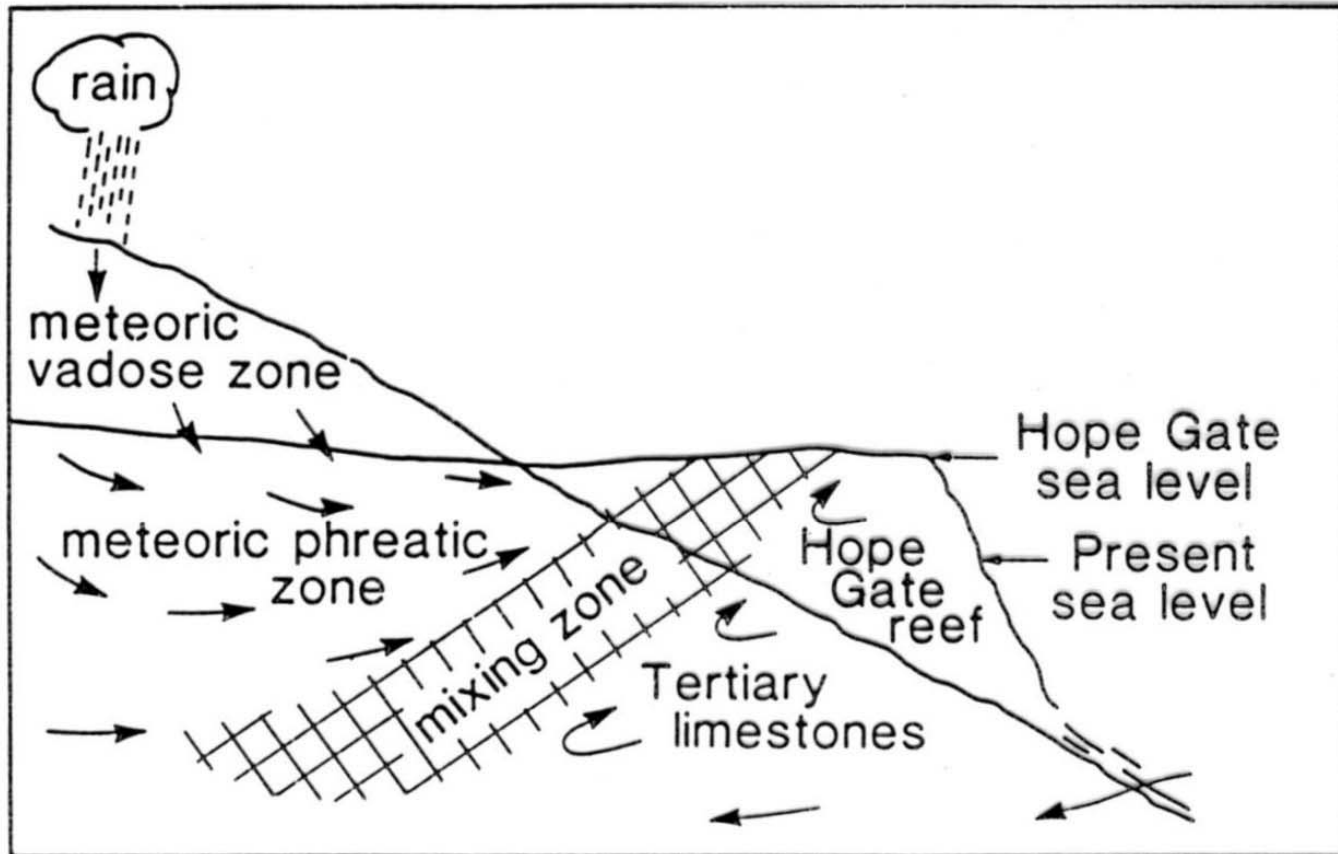
Fig. 8.25 *Mixing-zone model for dolomitization of the Hope Gate Formation of Jamaica. After Land (1973a).*

mixing zone dolomtization

WEST   EAST   EASTERN NEVADA
CENTRAL NEVADA   & UTAH
deeper water basin   shallow water shelf   tidal flat

brackish water

regional offlap

regional onlap

limestone

dolomite

NAMURIAN SSTS clay mineral transformations and organic matter maturation release Fe, Mg, CO_2 and organic acids

shelf carbonates

intense alteration along basin margin

general up-dip migration

intense alteration along margins of sand bodies

P.SST

overpressured mudrocks

expulsion of formation waters aided by dehydration reactions

BOWLAND SHALES

BASEMENT

P.LST

lime mudstones less dolomitized

fault

BASIN MARGIN

Mn rich fluid

fluid migration mostly along permeable horizons i.e. sandstones and calcarenites/breccias

fluid migration

limestone breccia/ conglomerates, calcarenites

calcarenites, lime mudstone, wackestones

lime mudstone-wackestones, terrigenous mudstones
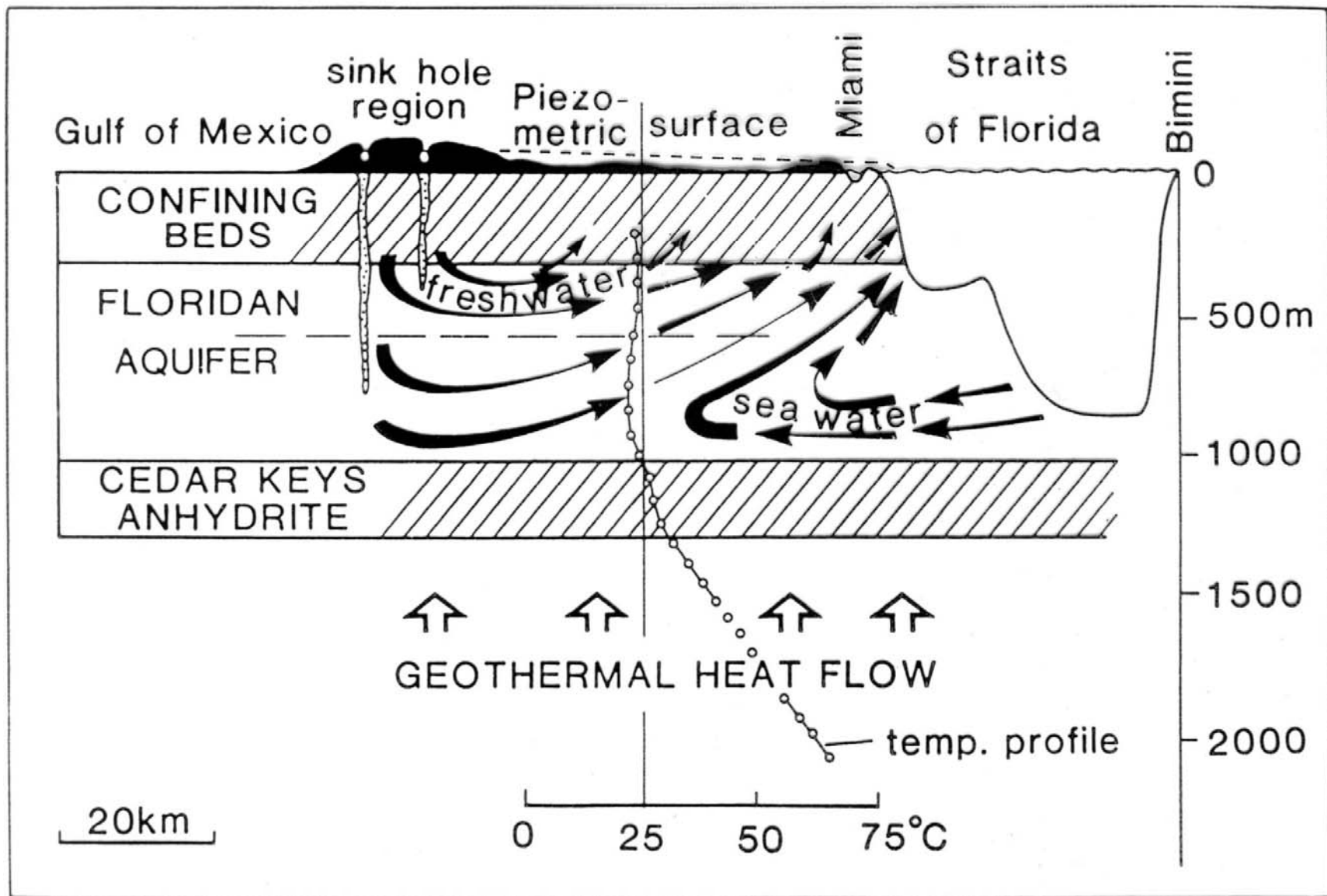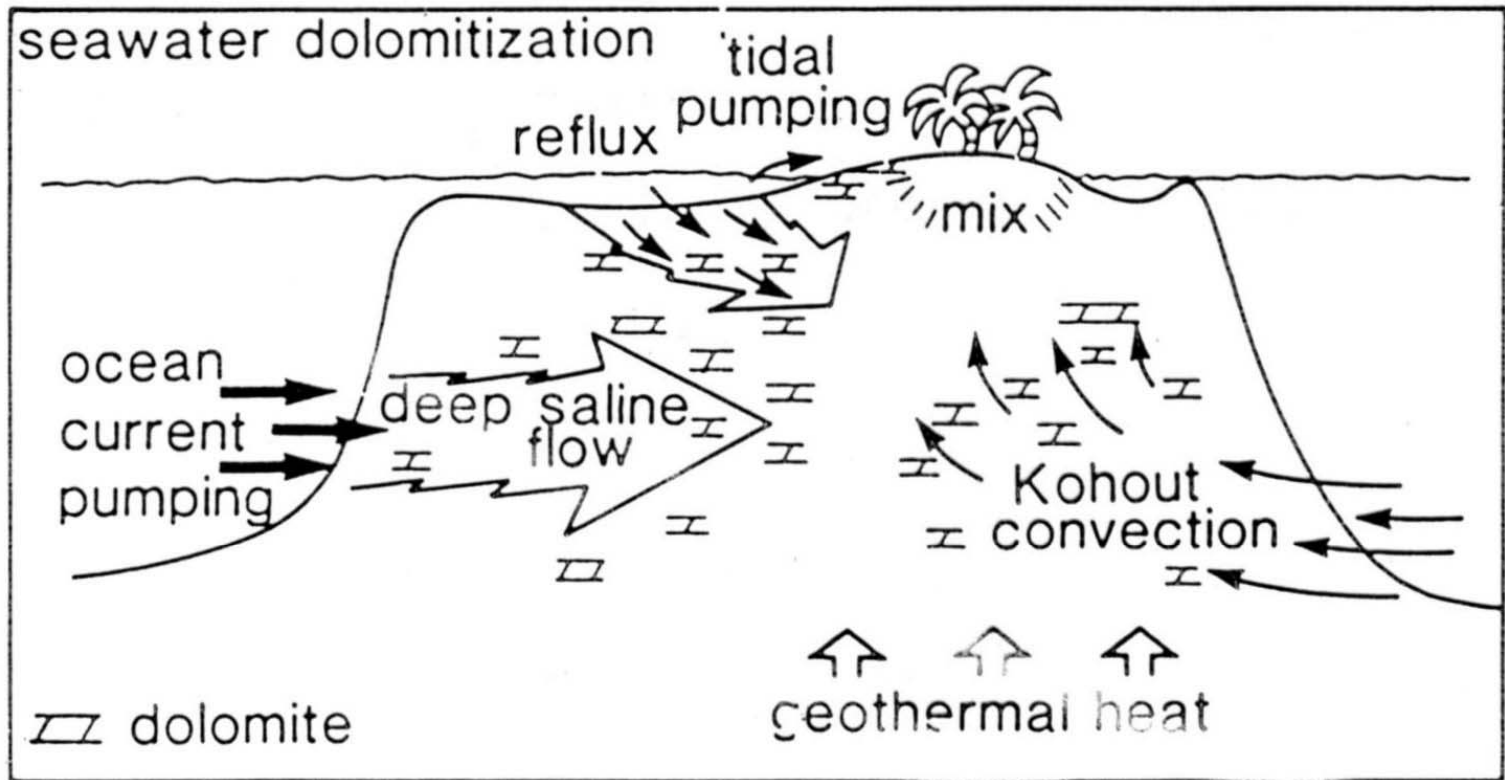
carbonate buildups

dolomite and or secondary porosity

Fig. 8.27 *Burial dolomitization model through mudrock dewatering for Lower Carboniferous sediments, the Pendleside Limestone (P.LST) and Pendleside Sandstone (P.SST), of the Bowland Basin, northwest England. After Gawthorpe (1987).*

78
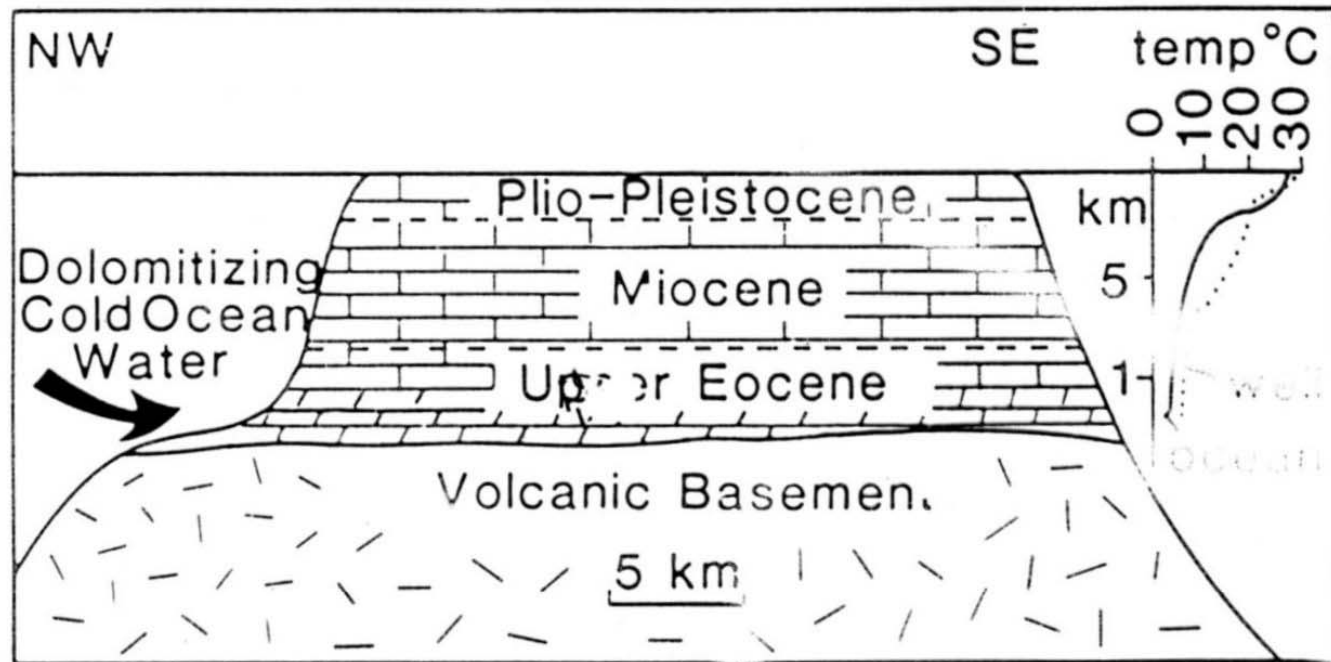
Fig. 8.28 *Model for dolomitization of Eocene limestones of Enewetak Atoll by cold ocean water. The temperature profile of water within the atoll from a deep well is closely parallel to that of the adjacent open ocean, suggesting that ocean water freely circulates through the atoll. There is an increase in temperature near the bottom of the well suggesting that circulating water is removing geothermal heat from Enewetak's volcanic basement. After Saller (1984).*

Gulf of Mexico

sink hole region

Piezo-metric surface

Miami

Straits of Florida

Bimini

CONFINING BEDS

FLORIDAN

AQUIFER

freshwater

sea water

CEDAR KEYS ANHYDRITE

0

500m

1000

1500

2000

GEOTHERMAL HEAT FLOW

temp. profile

20km

0   25   50   75°C

Fig. 4.67 Models for sea-water dolomitization of limestones, all basically different ways of pumping sea water through a carbonate platform. After Tucker & Wright (1990).
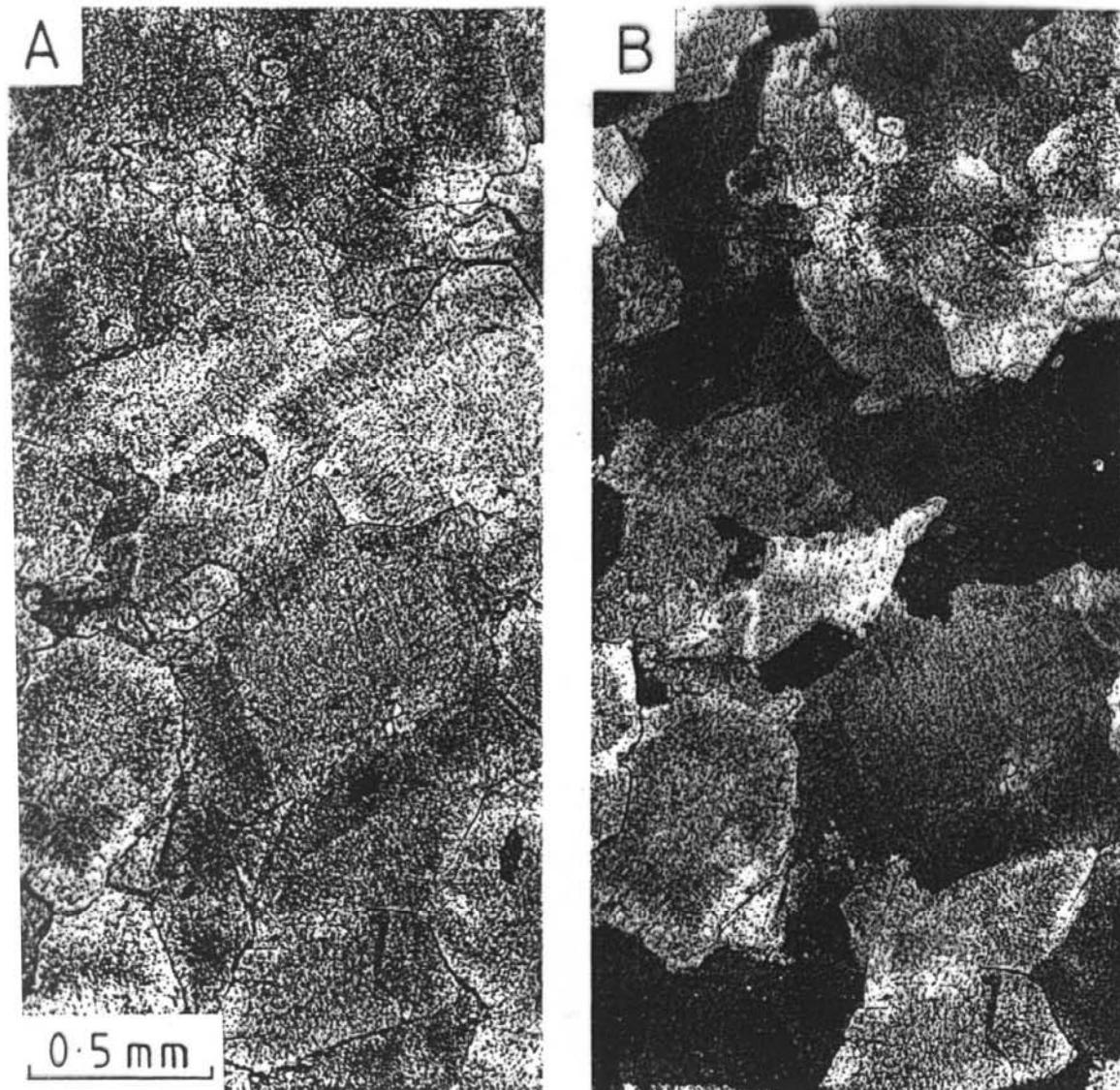
Fig. 4.64 Baroque dolomite; coarse crystals with undulose extinction. A, Plane-polarized light. B, Crossed polars. Lower Carboniferous dolomitized oolite (no relics of structure left). Glamorgan, Wales.
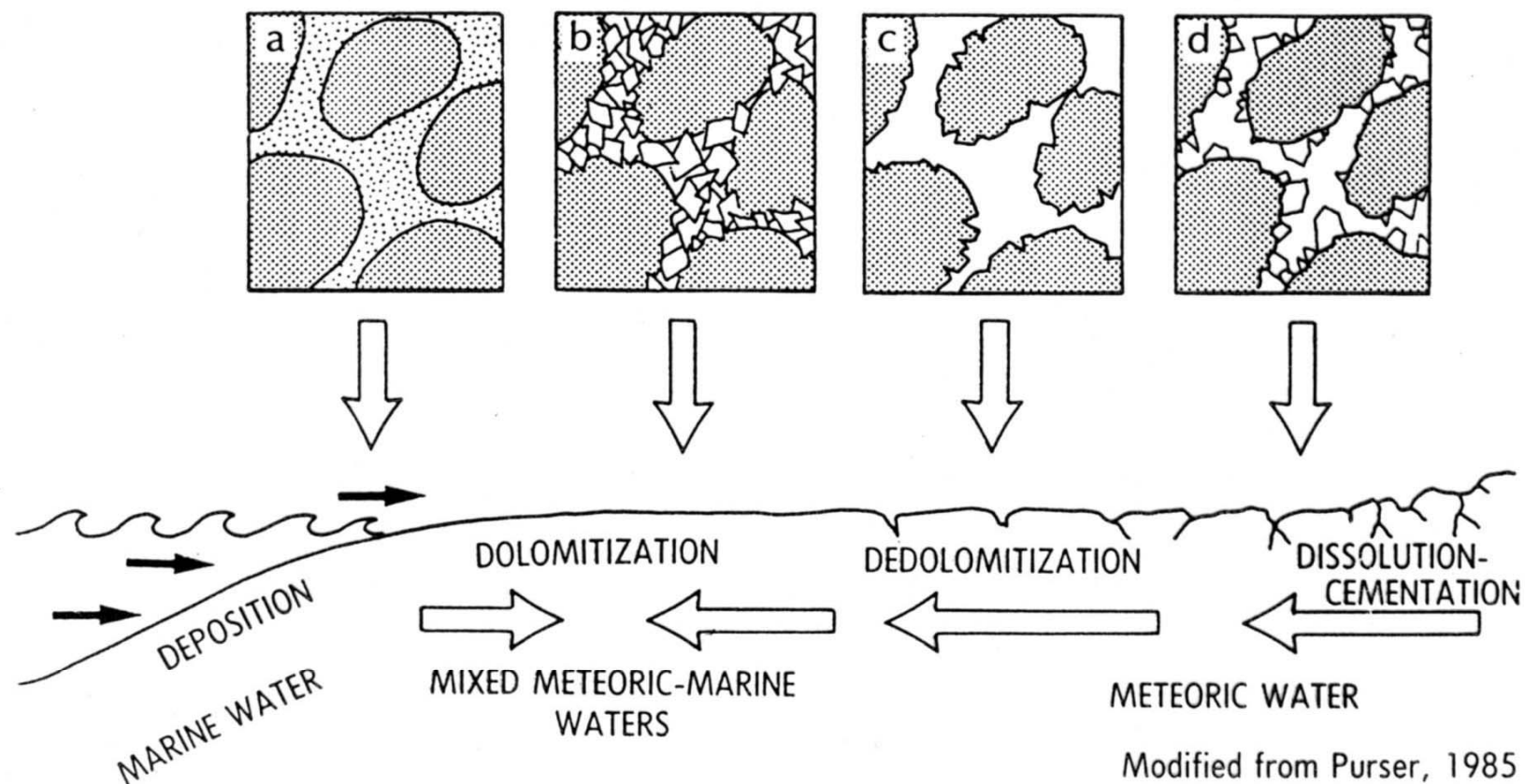
Fig. 2.14. Geologic setting for the dolomitization-dedolomitization of Jurassic ooid packstones from the Paris Basin. Final porosity consists of cement-reduced, dolomite crystal-moldic porosity. Reprinted from Carbonate Petroleum Reservoirs, with permission. Copyright, Springer-Verlag, New York.

porosity
calcite → dolomite, reduction of volume, increase of porosity up to 13%

dedolomitization
dolomite → calcite; contact with meteoric water; surface dissolution of gypsum-anhydrite; burial
identification: pseudomorphs of calcite after dolomite; neomorphic mosaic

silicification of carbonates
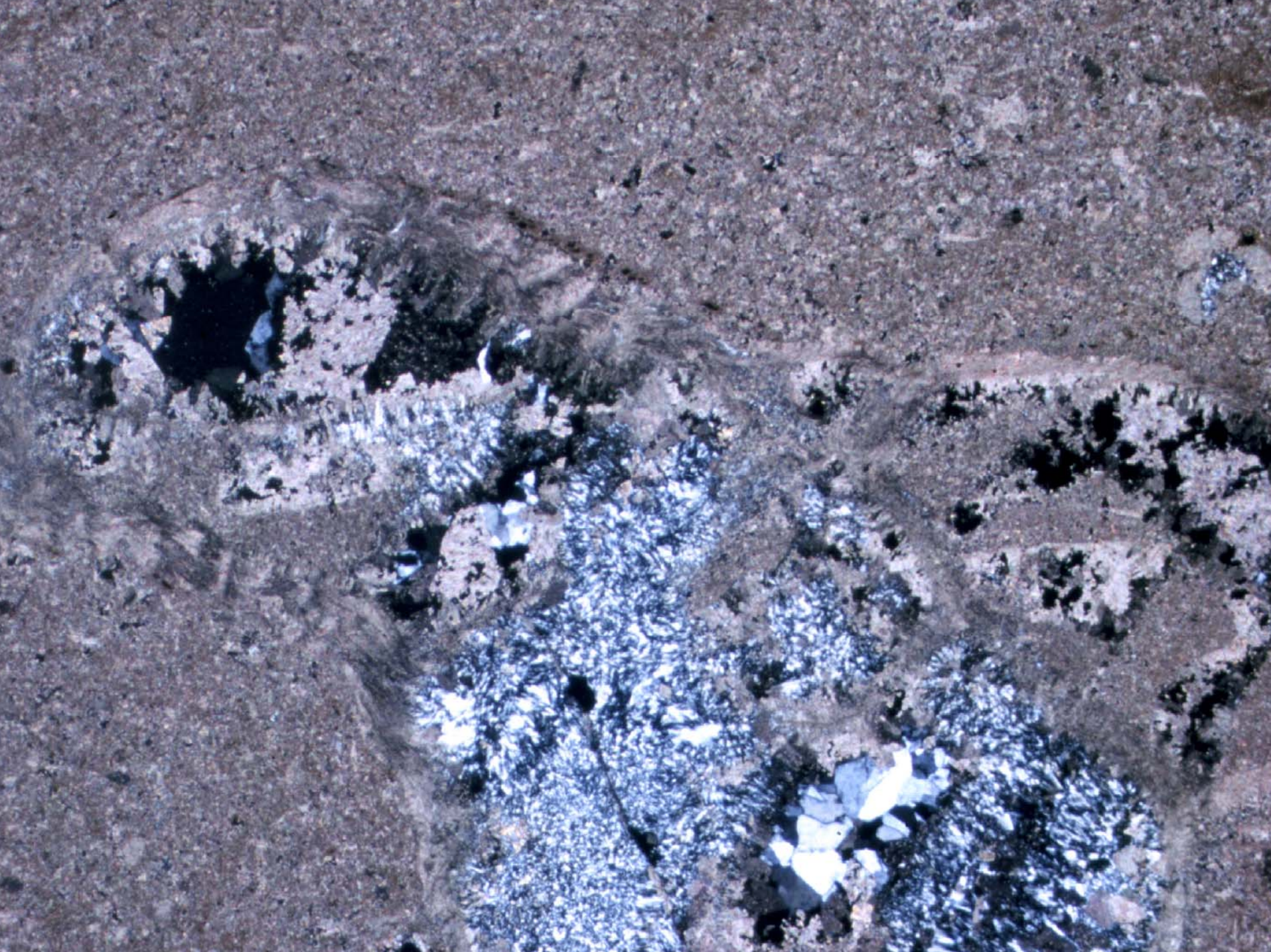early and late; recryst. of bioclasts, node formation, nodular horizons; SiO_2 cement
diagenetic (authigenic) quartz types: 1) euhedral crystals, 2) microquartz, 3) megaquartz, 4) chalcedonic q.
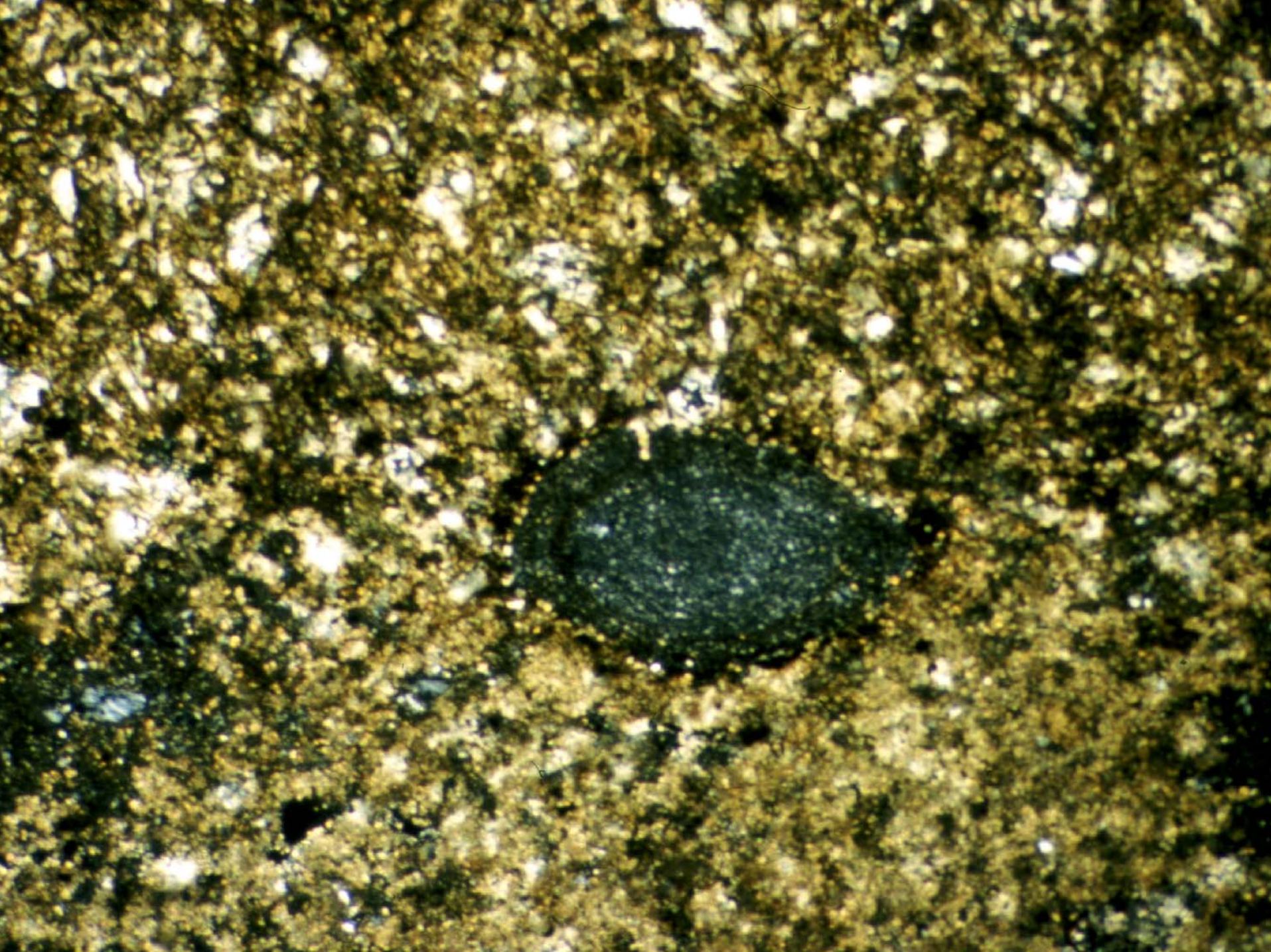source: sponge needles, diatomites, radiolarians, volcanic SiO_2

Reading:

M.E.Tucker: Sedimentary petrology. 3rd ed. Blackwell, 2001.
M.E.Tucker&V.P.Wright: Carbonate Sedimentology. Blackwell, 1994.
C.H.Moore (1989): Carbonate diagenesis and Porosity. Developments in sedimentology 46, Elsevier.
G.Harwood (1988): Principles of sedimentary petrography. In: M.Tucker ed.: Techniques in sedimnetology, Blackwell.